



Design, synthesis and biological evaluation of quinoline-2-carbonitrile-based hydroxamic acids as dual tubulin polymerization and histone deacetylases inhibitors

Camille Hauguel, Sarah Ducellier, Olivier Provot, Nada Ibrahim, Diana Lamaa, Coline Balcerowiak, Boris Letribot, Megane Nascimento, Vincent Blanchard, Laurie Askenatzis, et al.

► To cite this version:

Camille Hauguel, Sarah Ducellier, Olivier Provot, Nada Ibrahim, Diana Lamaa, et al.. Design, synthesis and biological evaluation of quinoline-2-carbonitrile-based hydroxamic acids as dual tubulin polymerization and histone deacetylases inhibitors. *European Journal of Medicinal Chemistry*, 2022, 240, pp.114573. 10.1016/j.ejmech.2022.114573 . hal-03752715

HAL Id: hal-03752715

<https://hal.science/hal-03752715>

Submitted on 23 Nov 2022

HAL is a multi-disciplinary open access archive for the deposit and dissemination of scientific research documents, whether they are published or not. The documents may come from teaching and research institutions in France or abroad, or from public or private research centers.

L'archive ouverte pluridisciplinaire **HAL**, est destinée au dépôt et à la diffusion de documents scientifiques de niveau recherche, publiés ou non, émanant des établissements d'enseignement et de recherche français ou étrangers, des laboratoires publics ou privés.

Design, Synthesis and Biological Evaluation of Quinoline-2-carbonitrile-Based Hydroxamic Acids as Dual Tubulin Polymerization and Histone Deacetylases Inhibitors

Camille Hauguel^a, Sarah Ducellier^b, Olivier Provot^a, Nada Ibrahim^a, Diana Lamaa^a, Coline Balcerowiak^a, Boris Letribot^a, Megane Nascimento^b, Vincent Blanchard^a, Laurie Askenatzis^c, Helene Levaique^c, Jérôme Bignon^c, Francesco Baschieri^d, Cyril Bauvais^e, Guillaume Bollot^e, Dolor Renko^a, Alain Deroussent^f, Bastien Prost^g, Marie-Catherine Laisne^h, Sophie Michallet^h, Laurence Lafanechère^h, Sébastien Papotⁱ, Guillaume Montagnac^d, Christine Tran^a, Mouad Alami^a, Sebastien Apcher^b, Abdallah Hamze^{a*}

^a Université Paris-Saclay, CNRS, BioCIS, 92290 Châtenay-Malabry, France

^b Université Paris-Saclay, Institut Gustave Roussy, Inserm, Immunologie anti-tumorale et immunothérapie des cancers, 94805 Villejuif, France

^c Université Paris-Saclay, CNRS, Institut de Chimie des Substances Naturelles, UPR 2301, 91198 Gif-sur-Yvette, France

^d Université Paris-Saclay, Inserm, Institut Gustave Roussy, Dynamique des cellules tumorales, 94805, Villejuif, France

^e SYNIGHT, 91400 Orsay, France

^f Université Paris-Saclay, CNRS, Institut Gustave Roussy, Aspects métaboliques et systémiques de l'oncogénèse pour de nouvelles approches thérapeutiques, 94805 Villejuif, France

^g Université Paris-Saclay, Inserm, CNRS, Ingénierie et Plateformes au service de l'innovation thérapeutique, 92296, Châtenay-Malabry, France

^h Université Grenoble Alpes, Inserm, CNRS, Institute for Advanced Biosciences, 38000 Grenoble, France

ⁱ Université de Poitiers, CNRS, Institut de Chimie des Milieux et des Matériaux de Poitiers (IC2MP), 86073 Poitiers, France

*Corresponding authors. Tel.: +33 1 46 83 58 47. Fax: +33 1 46 83 58 28. Email: abdallah.hamze@universite-paris-saclay.fr

Abstract

A series of quinoline and quinazoline analogs were designed and synthesized as new tubulin polymerization (TP) and histone deacetylases (HDAC) inhibitors. Compounds **12a** and **12d** showed the best cytotoxicity activities against a panel of human cancer cell lines with an averaged IC₅₀ value of 0.6 and 0.7 nM, respectively. Furthermore, these lead compounds showed good activities against CA-4-resistant colon-carcinoma and multidrug-resistant leukemia cells. In addition, compounds **12a** and **12d** induced HT29 cell cycle arrest in the G2/M phase and produced caspase-induced apoptosis of HT29 cells through mitochondrial dysfunction. Also, **12a** and **12d** inhibited HDAC8, 6, and 11 activities. Furthermore, lead compound **12a** exhibited higher metabolic stability than *iso*CA-4 and was highly potent in suppressing tumor growth in the fibrosarcoma MCA205 tumor model. Collectively, these studies suggest that **12a** represents a new dual inhibitor of TP and HDAC activities, which makes it a suitable candidate for further investigations in clinical development.

Keywords: Cancer, cytotoxicity, tubulin, HDACi, multitargeted compounds

1. Introduction

To avoid off-target effects, most of the currently approved drugs have been designed to target a single biological entity, usually a protein (the so-called “on-target”). However, this model has shown its limits, especially in treating complex diseases like malignant tumors and central nervous system diseases.[1] While drug combination therapies are used as an alternative approach to achieve efficacy, their benefits are often counteracted by adverse drug–drug interactions, unpredictable pharmacokinetics, additive toxicities, and poor patient compliance.[2] Multitarget drugs, where a single drug molecule can interact with several targets simultaneously, lead to new and more effective medications for various complex diseases.[3, 4] They may offer some advantages such as better efficacy, superior treatment compliance, and lower risk of drug–drug interactions.[5] Consequently, in recent years, much attention has been given to discovering multitarget drugs to address the limited efficacy and resistance or toxicity associated with many single-target or combination-based therapies.[6] Multi-targeted drugs share most of the advantages of multi-component drugs but do not have many of their disadvantages, and they also have several distinct advantages of their own. However, they reveal some disadvantages, particularly in terms of their design, increased molecular weight, and sometimes difficult synthesis.

Disruption of microtubules function induces cell cycle arrest in the G₂/M phase and the formation of abnormal mitotic spindles. Therefore, drugs that exert their effect by controlling the microtubule assembly either by hindering tubulin polymerization or by obstructing microtubule disassembly are important in anti-cancer therapy.[7] Various naturally occurring compounds such as paclitaxel, vinblastine, combretastatins, and colchicine exert their effect by modifying the tubulin dynamics. Tubulin polymerization inhibitors (TPIs), like combretastatin A-4 (CA-4), exhibit potent anti-vascular activity in malignant tumors.[8-10] CA-4 phosphate (CA-4P) has received orphan drug status from the US FDA to treat a range of thyroid and ovarian cancers.[11] CA-4 exists in two geometric configurations, *cis*- and *trans*-stilbene, but only the *cis* isomer of CA-4 possesses significant anti-cancer activity. Isomerization of *cis* CA-4 into the less active *trans* isomer is readily observed on storage and *in vivo* during metabolism, accompanied by a dramatic reduction in both anti-tubulin and anti-tumor activities.[12-14] Our group discovered *iso*CA-4,[15-17] a stable non-natural isomer of CA-4 having a 1,1-diarylethylene structure, which has the same biological properties as the natural CA-4. Structure-activity relationships (SAR) on the linker between A- and B-ring[18] showed that the double bond reduction decreased the activity.[19] In contrast, the use of the *N*-Me linker gave an excellent activity.[20-22] Also, we furthermore demonstrated that the traditional 3,4,5-trimethoxyphenyl A-ring of natural CA-4 and *iso*CA-4, which is subject to metabolism reaction (*O*-demethylation), could be replaced successfully by a 2-methylquinazoline **1**,[23] 2-methylquinoline **3**,[24] or quinoline-2-carbonitrile rings **2** and **4**,[25]. The corresponding compounds (**1-4**) showed potent antiproliferative activity.

Histone deacetylases (HDACs) are a family of enzymes that play a crucial role in regulating gene expression by remodeling chromatin structure. They control many cancer-related cellular processes such as cell proliferation, cell migration, cell apoptosis, and angiogenesis. In several cancers, the aberrant expression of HDACs correlates with tumor onset and progression.[26] A clear association between HDAC activity, tumor growth, and cell survival has been well established in a broad spectrum of hematologic and solid tumors,[27, 28] including neuroblastoma, the most common solid tumor in children.[29] HDACs have been identified as attractive molecular targets in cancer therapy for these reasons. Five HDAC inhibitors (HDACi), namely SAHA, romidepsin, belinostat, panobinostat, and

chidamide (approved in China), have been approved to treat hematological malignancies, including refractory cutaneous T cell lymphoma (CTCL).[30] Despite their great success in treating hematological malignancies, most known HDACi failed to show clinical benefits in nearly all types of solid tumors when used as a single agent.[31] Simultaneously inhibiting HDAC and other targets involved in the pathogenesis of solid tumors may address this issue.

Although both TPis and HDACi are limited by insufficient efficacy and tumor resistance,[32, 33] there is strong evidence that simultaneous inhibition of both tubulin polymerization and HDAC can synergistically inhibit tumor growth and improve therapeutic efficacy by limiting the occurrence of resistance.[32, 33] A study has shown an interesting synergic effect of combining the microtubule depolymerizing agent vincristine and vorinostat (HDACi) in leukemia *in vitro* and *in vivo*. [34] In 2018, we found that compound *iso*CA-4HDI, based on the structure of *iso*CA-4 (Fig. 1), was a multi-target-directed ligand of tubulin and HDAC8i.[32] Since then, Yao *et al.* developed 2-methoxyestradiol derivatives as potent dual tubulin/HDAC2 inhibitors.[35] Duan *et al.* designed a series of *cis*-diphenylethene and benzophenone derivatives as tubulin/HDAC7 dual-targeting inhibitors.[36] Also, Chen *et al.* described tubulin/HDAC3 dual inhibitors based on 4-substituted methoxybenzoyl-aryl-thiazoles and entinostat (MS-275).[37] In 2019, regarding antiproliferative activity and metabolic stability, we demonstrated the benefit of switching between the 3,4,5-trimethoxyphenyl A-ring of *iso*CA-4 and quinazoline or quinoline ring.[23, 25] Herein, we report the design, synthesis, and biological evaluation of potent dual TP/HDAC inhibitors.

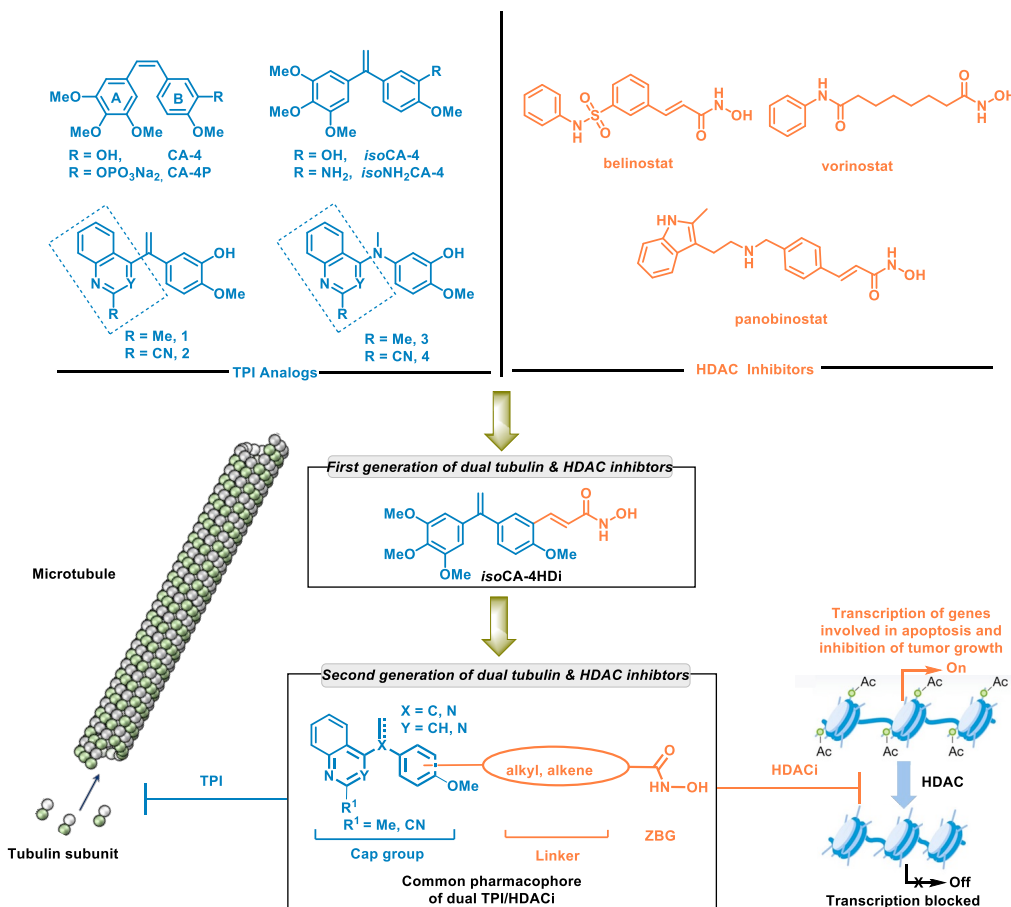


Figure 1. Chemical structures of TPI, HDACi, and target dual compounds.

2. RESULTS AND DISCUSSION

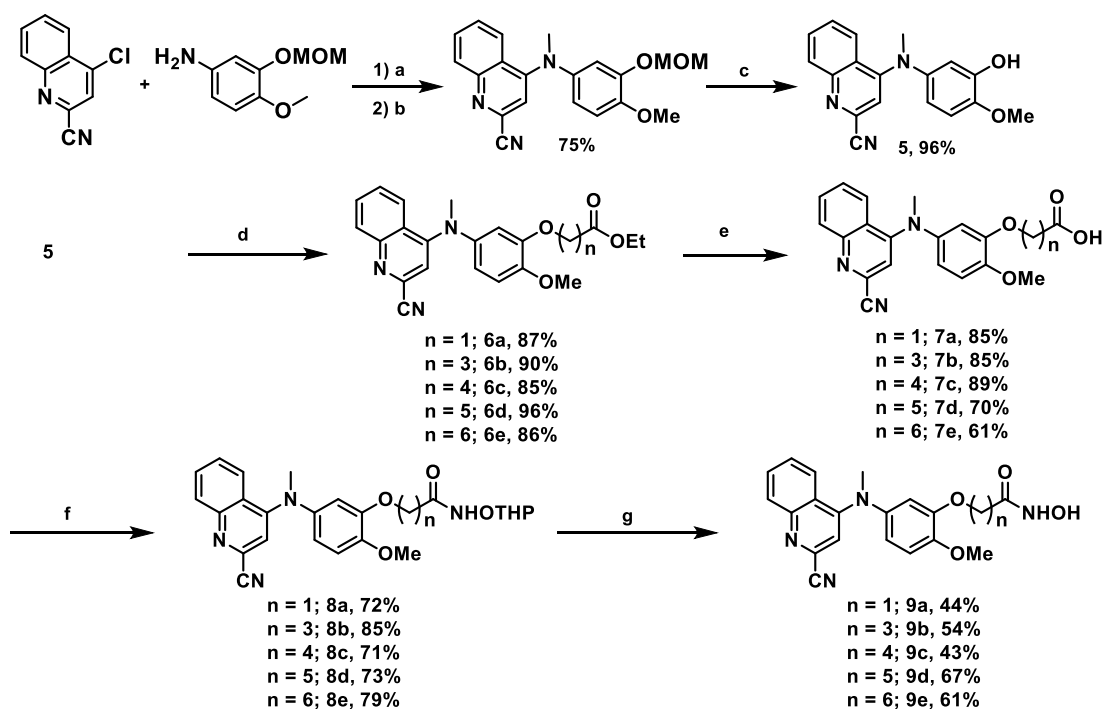
2.1. Chemistry

Chemical synthesis. We outlined the general synthesis of compounds **9a-9e**, **12a-12d**, **13a**, **14a**, **15a**, and **17a** in Schemes 1, 2, and 3. We prepared the key intermediate **5** in three steps: first, we performed a Buchwald-Hartwig cross-coupling reaction between 4-chloroquinoline-2-carbonitrile and 4-methoxy-3-(methoxymethoxy)aniline, then, we methylated the obtained secondary amine in the presence of methyl iodide and sodium hydride, and finally, we realized the deprotection of MOM protective group in acidic media to lead to compound **5**.

We obtained compounds **6a-6e** having different alkyl chains length by reaction between the key intermediate **5** and the corresponding bromoalkyl esters in basic conditions at room temperature (Scheme 1). Then, we converted compounds **6a-e** to their acid derivatives **7a-7e** in the presence of lithium hydroxide. Next, we obtained the hydroxamic acid compounds **9a-9e** in two steps: first, we activated the carboxylic acid function with EDCI/HOBt and TEA, then, we realized the coupling reaction with *O*-(tetrahydro-2*H*-pyran-2-yl)hydroxylamine. In the last step, the THP group was deprotected in acidic media to furnish the final hydroxamic acid compounds **9a-9e**.

In the second series of dual molecules, we modified the linker between the B-ring and the hydroxamate function to an alkene, alkyne, and thioalkyl groups, associated with the change of the R group on A-ring with a nitrile- or a methyl group. The synthesis of derivatives **12**, **13**, **14**, and **15** was performed starting from two key intermediates, **10a** and **10b** (Scheme 2). We prepared compounds **10a** and **10b** by an S_NAr reaction from 4-chloro-2-methylquinoline or 4-chloroquinoline-2-carbonitrile and 3-iodo-4-methoxyaniline. Compounds **12a**, **12b**, and **15a** were obtained by a Heck coupling reaction from **10a** or **10b** and *N*-((tetrahydro-2*H*-pyran-2-yl)oxy)acrylamide or *N*-hydroxypent-4-enamide, followed by deprotection of the THP group in acidic media. To introduce an alkyne function as the linker, we realized a Sonogashira coupling reaction between **10a** and *N*-((tetrahydro-2*H*-pyran-2-yl)oxy)pent-4-ynamide.

Scheme 1. Synthesis of compounds **6**, **7**, **8** and **9^a**



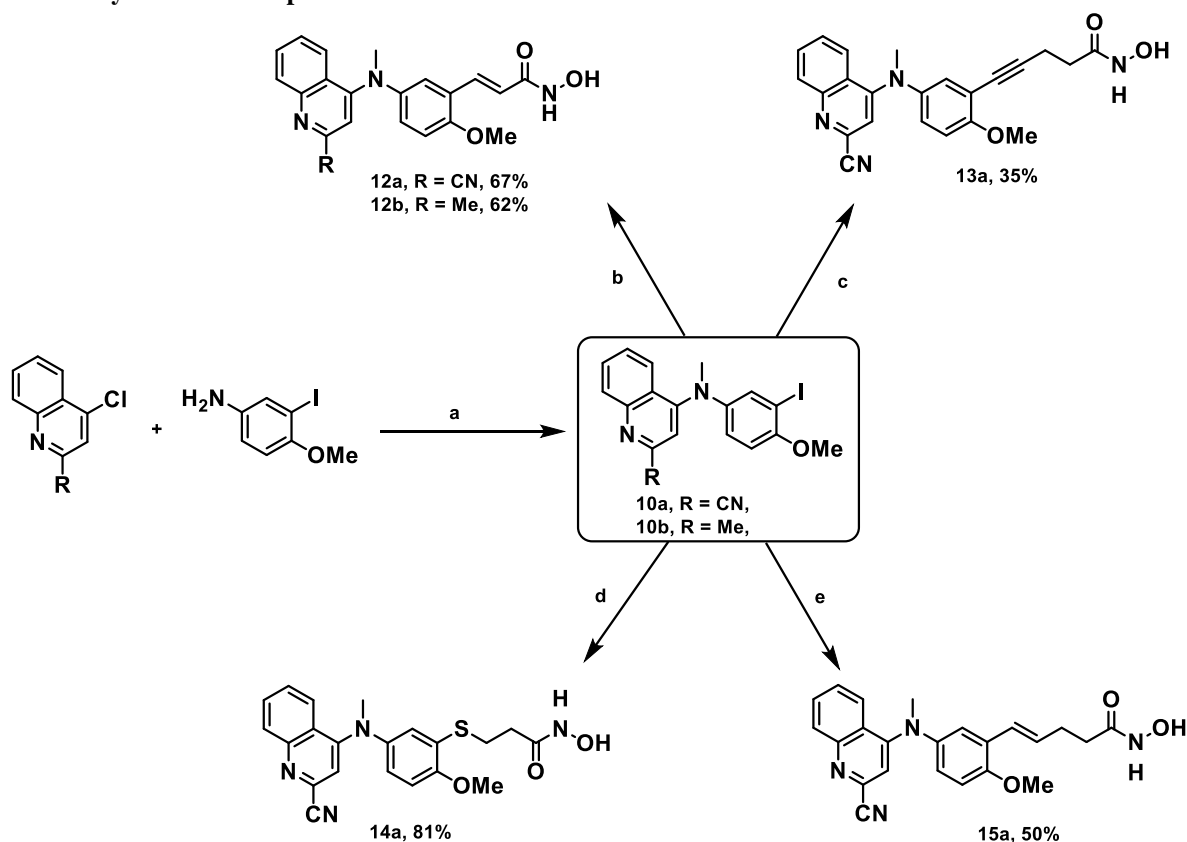
^a Reagents and conditions: (a) Pd₂(dba)₃.CHCl₃, XantPhos, Cs₂CO₃, dioxane, 110 °C; (b) CH₃I, NaH, 0 °C; (c) *p*TSA, MeOH, 60 °C; (d) bromoalkyl ester, K₂CO₃, DMF, rt; (e) LiOH (1M), THF/H₂O, rt; (f) *O*-(tetrahydro-2H-pyran-2-yl)hydroxylamine, EDCI, HOBt, TEA, DCM, rt; (g) HCl (4N), dioxane/MeOH, rt.

We recently reported an efficient method allowing the introduction of glycosyl thiols to various iodo(hetero)aryles,[38] under mild and straightforward conditions using the palladium G3-Xanthphosbiphenyl precatalyst. This method was adapted to our compounds, giving compound **14a** having a thioether bond from 3-mercapto-*N*-((tetrahydro-2H-pyran-2-yl)oxy)propenamide and **10a**.

The third heterocycle that was introduced was a quinazoline as A-ring (Scheme 3). We obtained iodo-derivatives **10c** and **10d** by S_NAr reaction, then Heck coupling with *N*-((tetrahydro-2H-pyran-2-yl)oxy)acrylamide followed by deprotection of the THP group led to hydroxamic acid compounds **12c** and **12d**.

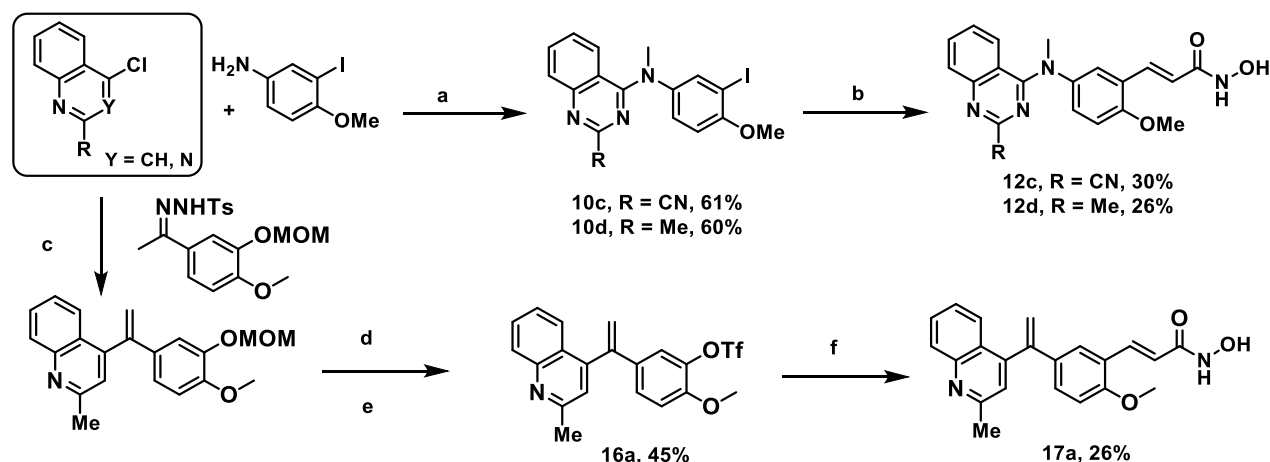
We obtained quinaldine **17a**, having a 1,1-ethylene function instead of the *N*-Me, in two steps: first, we generated triflate intermediate **16a** from the coupling of the corresponding *N*-tosylhydrazone derivative and 4-chloro-2-methylquinazoline,[39, 40] then the Heck coupling between **16a** and ethyl acrylate furnished the corresponding ester, which, in turn, was converted to the hydroxamic acid derivative **17a** by treatment with hydroxylamine.

Scheme 2. Synthesis of compounds 12-15.



^aReagents and conditions: (a) (i) HCl 35% dioxane, 140 °C; (ii) NaH, MeI, DMF; (b) (i) *N*-((tetrahydro-2H-pyran-2-yl)oxy)acrylamide, Pd(OAc)₂, P(*o*-Tolyl)₃, Et₃N, DMF, 100 °C; (ii) HCl in MeOH; (c) (i) *N*-((tetrahydro-2H-pyran-2-yl)oxy)pent-4-ynamide, Pd(PPh₃)₂Cl₂, CuI, Et₃N, DMF rt; (ii) HCl in MeOH; (d) (i) 3-mercapto-*N*-((tetrahydro-2H-pyran-2-yl)oxy)propenamide, PdG3-Xantphos, Et₃N, rt; (ii) HCl in MeOH; (e) (i) *N*-((tetrahydro-2H-pyran-2-yl)oxy)pent-4-enamide, Pd(OAc)₂, P(*o*-Tolyl)₃, Et₃N, DMF, 100°C; (ii) HCl in MeOH;

Scheme 3. Synthesis of compounds 10, 12, and 17.



^aReagents and conditions: (a) (i) HCl 35% dioxane, 140 °C; (ii) NaH, MeI, DMF; (b) (i) *N*-((tetrahydro-2*H*-pyran-2-yl)oxy)acrylamide, P(*o*-Tolyl)₃, Pd(OAc)₂, NEt₃, DMF, 100 °C; (ii) HCl in dioxane; (c) (*E*)-*N'*-(1-(4-methoxy-3-(methoxymethoxy)phenyl)ethylidene)-4-methylbenzenesulfonohydrazide, Pd₂dba₃·CHCl₃, XPhos, LiOtBu, dioxane, 100 °C; (d) PTSA, DCM, 60 °C; (e) Tf₂O, pyridine, 0 °C; (f) (i) ethyl acrylate, PdCl₂(PPh₃)₂, dppp, NaHCO₃, DMF, 150 °C; (ii) NH₂OH, MeOH, rt.

2.2. SAR studies. Antiproliferative Activities of Synthesized Compounds in a Human Colon Carcinoma Cell Line (HCT116).

With a library of 31 heteroaryl-based analogs of *iso*CA-4 in hand, our focus was on evaluating their antiproliferative activity on a human colon-carcinoma cell line (HCT116) in comparison with that of the reference compounds, *iso*CA-4, CA-4 (TPIs),[41] and Trichostatin A (TSA), PCI-34051 (HDACis) (Table 1). We achieved this evaluation using a standard cell viability assay after 72 h of incubation of the cells in the presence of the compounds to be tested. The reported IC₅₀ values are the averages of at least three independent experiments. We attached the ZBG *via* an *O*-alkyl linker to the TPI pharmacophore (Het-NMe-Ar), which serves as the cap group (Table 1). We started our optimization with quinoline-2-carbonitrile as a cap, and we studied the optimal length of the linker between the cap and the ZBG. Different ZBGs were tested, including CO₂Et, COOH, and hydroxamic acid.[42] Based on the linker chain length analysis, we observed that the optimal length regarding cytotoxic activity is one carbon atom (compound **9a**, IC₅₀ = 64.5 nM), followed by three carbon atoms (compound **9b**, IC₅₀ = 381 nM). Among the three tested ZBGs, hydroxamic acid was found to be the most active group, most likely due to its strong binding affinity with the zinc ion of HDAC. While we encountered some problems for synthesizing an *O*-linker with two carbon atoms, we succeeded in preparing compound **14a**, where a sulfur atom replaced the oxygen atom. However, with this chain length, no significant antiproliferative activity was detected even at 1 μM concentration. Compared to the reference's compounds, compound **9a**, the most active compound in this series, showed better antiproliferative activity on HCT116 than PCI-34051, but was still less active than the TSA, *iso*CA-4, and CA-4. Also, the changing of group R to an iodine atom gave a better result than **9a**. This proves that there is room to continue the optimization to improve the activity of the dual compound. In our previous work on SAR of *iso*CA-4,[32, 43] we demonstrated that the iodine atom of *iso*CA-4 could be replaced successfully by an acrylate group.

Moreover, belinostat and panobinostat contain *Csp*²-*Csp*² linkers having hydroxamic acid as ZBG. Accordingly, as shown in Table 2, we focused our work on a linker having *Csp*²-*Csp*² or *Csp*³-*Csp*³ bonds. With *N*-hydroxypent-4-

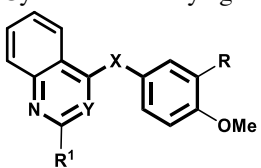
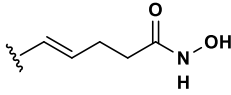
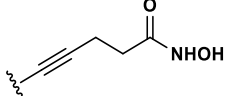
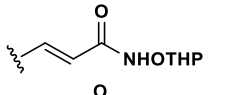
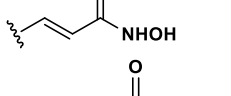
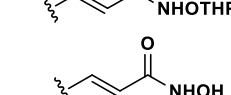
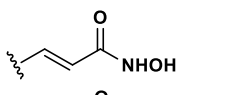
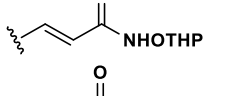
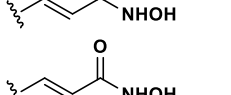
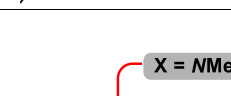

enamide linker, the new chimeric compound **15a** showed better antiproliferative activity than the best analog of *O*-alkyl linker (cf. **9a** and **15a**). A slightly better result was obtained with an alkyne linker (compound **13a**). Shortening the distance between the ZBG and the cap part leads to the best antiproliferative activity (Fig. 2), and compound **12a** was found to exhibit activity in the picomolar range ($IC_{50} = 0.5$ nM). **12a** was 100-fold more active than compound **9a**, and it was 66-fold more active than TSA. We also tested the protected version of compound **12a** with a tetrahydropyranyl ether group (THP). As expected, compound **11a** was less active than **12a**, probably, because it needs more time to be hydrolyzed in the cell to the active hydroxamic acid. This compound can serve as a prodrug backup to enhance the bioavailability of **12a** in case of further oral administration. Next, we turned our attention to the cap part of these dual analogs. In our previous work on the SAR of *iso*-combretastatin-quinolines, we successfully interchanged the nitrile group on the C-2 position of quinolines by a methyl group without losing activity.[24] Therefore, we replaced the nitrile group of compound **12a** with a methyl group. However, we found that compound **12b** was less active than compound **12a**. During our precedent SAR, we demonstrated that the quinazoline ring could replace the traditional 3,4,5-trimethoxyphenyl-A-ring (TMP) of *iso*CA-4. We then used the quinazoline nucleus with nitrile or methyl substituents on the C2-position instead of the quinoline ring. Compound **12c** having 2-cyanoquinazolin-4-yl group afforded a good antiproliferative activity but was still less active than **12a**. Interestingly, using 2-methylquinazolin-4-yl heterocycle (compound **12d**) led to a similar picomolar activity as observed with **12a**. Finally, we switched the *N*-Me function by a C=CH₂. However, in this series, the corresponding compound **17a** showed slightly lower activity than compound **12b**.

Table 1. SAR with *O*-alkyl linker, Cytotoxic Activity against HCT116 Cells^a

compd	R	GI ₅₀ HCT116 (nM) ^b	compd	R	GI ₅₀ HCT116 (nM) ^b
CH238 6a		na ^c	CH247 7d		na ^c
CH241 7a		na ^c	CH252 8d		na ^c
CH245 8a		na ^c	CH254 9d		na ^c
CH249 9a		64.5 ± 1.9	CH244 6e		na ^c
CH225 6b		na ^c	CH248 7e		na ^c
CH227 7b		na ^c	CH251 8e		na ^c
CH228 8b		na ^c	CH254 9e		na ^c
CH236 9b		381 ± 4	VB66 14a		na ^c
CH242 6c		na ^c	10a		24.6 ± 2.8
CH246 7c		na ^c	<i>iso</i> CA4		2.2 ± 0.9
CH250 8c		na ^c	CA4		2.4 ± 0.5
CH255 9c		na ^c	TSA		40 ± 0.7
CH243 6d		na ^c	PCI-34051		2600 ± 1100

^aHCT116 human colon carcinoma cells. ^bCompound concentration required to decrease cell growth by 50%; values represent the average ± SD of three experiments. ^cna = not active at 1 μM.

Table 2. SAR with C-alkene/C-alkyne linker, Cytotoxic Activity against HCT116 Cells^a

					
compd	X	Y	R ¹	R	GI ₅₀ HCT116 (nM)
15a	NMe	CH	CN		34.4 ± 4.0
13a	NMe	CH	CN		25.2 ± 3.2
11a	NMe	CH	CN		4.91 ± 0.84
12a	NMe	CH	CN		0.5 ± 0.002
11b	NMe	CH	Me		30.3 ± 3.4
12b	NMe	CH	Me		6.3 ± 0.7
12c	NMe	N	CN		1.5 ± 0.07
11c	NMe	N	Me		12.5 ± 2.2
12d	NMe	N	Me		0.6 ± 0.003
17a	C=CH ₂	CH	Me		10.1 ± 0.7

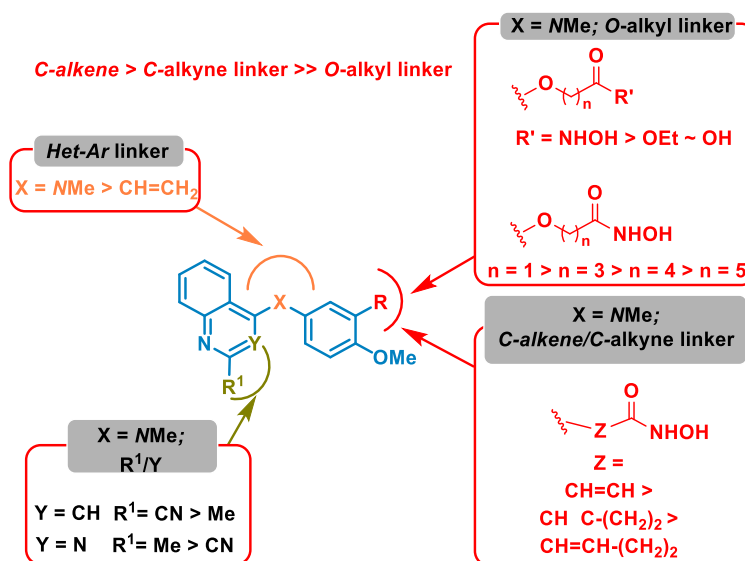


Figure 2. Summary of SARs study of target compounds based on cell viability evaluated on a human colon cancer cell line (HCT116).

2.3. Antiproliferative activities of compounds **12a** and **12d** on various tumor cell lines

Among all tested analogs, compounds **12a** (*isoCYCoQHDi*) and **12d** (*isoCoQHDi*), which showed the best antiproliferative activity on HCT116 cells, were selected for evaluation on nine additional human cancer cell lines and compared with the reference compounds *isoCA4HDi* (First generation of dual tubulin & HDACi), *isoCA-4* and *CA-4* (TPIs), TSA (pan-HDACi) and PCI-34051 (selective HDAC8i). Generally, these new compounds **12a** and **12d** were equipotent, and, whatever the nature of the cancer cell line, they were more active than all the reference compounds.

With average IC₅₀ values of 0.6, 0.7, 2.9, 34, and 102 nM for **12a**, **12d**, *isoCA4-HDi*, *isoCA4*, and **TSA**, respectively, compounds **12a** and **12d** appeared to be the most active compounds in the series (for *CA-4*, and PCI-34051 the average of IC₅₀ values were >1000 nM, respectively).

We evaluated the effect of our lead compounds on multidrug-resistant (MDR) leukemia cells. We used parental K562 cells and MDR1-overexpressing K562R cells in this study. Our results revealed that compound **12a** showed high antiproliferative activity on the K562R cell line, with an IC₅₀ value in the sub-nanomolar range; thus, it was 45-, 160-, and 3900-fold more active than the reference compounds, *CA-4*, **TSA**, and PCI-34051, respectively. These results demonstrated that this compound is not a substrate for P-glycoprotein (Pgp). We also observed the same trend in favor of compounds **12a** and **12d** on A549 and MCF7 cell lines, where again, the reference compounds were ineffective. On the other hand, the colon-carcinoma cells HT-29 were resistant to *CA-4* because of the overexpression of a multidrug-resistance protein (MRP-1).[44] Given the excellent antiproliferative activity of compounds **12a** and **12d**, we tested their activity on this resistant HT-29 cell line and compared it with the four reference compounds. As depicted in Table 3, compounds **12a** and **12d** were still active against this resistant cell line, with sub-nanomolar IC₅₀ values of 0.6 and 0.7 nM, respectively. In contrast *isoCA-4*, **TSA**, and especially *CA-4* and PCI-34051 were inactive on HT-29 resistant cells, with IC₅₀ values of 275 nM (*isoCA-4*), 55 nM (**TSA**), > 10000 nM for (*CA-4* and PCI-34051). Cross-resistance observed for *isoCA-4* and *CA-4* can be explained by the structural resemblance between these two isomers, which can be a substrate of MRP-1.

In contrast, the new structures of **12a** and **12d** (absence of the 3,4,5-trimethoxyphenyl ring) allow escaping the detoxifying actions of these proteins overexpressed in HT-29 cells.

Table 3. Activities of compounds **12a** and **12d** and references compounds against various tumor cell lines (IC₅₀ nM)^b

tumor type											
comp d	Stomac h	leukemia		pancreas	ovarian	lung	breast		colon		
	NCI- N87	K562	K562R	MiaPaca2	SKOV3	A549	MCF7	MDA MB231	HCT 116	HT-29	average (IC ₅₀)
12a	0.1 ± 0.01	0.35 ± 0.01	0.56 ± 0.02	0.94 ± 0.04	0.60 ± 0.17	0.84 ± 0.11	0.78 ± 0.02	0.7 ± 0.15	0.6 ± 0.02	0.62 ± 0.05	0.6
12d	0.17 ± 0.03	0.38 ± 0.03	1.63 ± 0.6	1.1 ± 0.07	0.3 ± 0.07	0.51 ± 0.07	0.8 ± 0.04	0.55 ± 0.02	0.7 ± 0.03	0.66 ± 0.15	0.7
<i>iso</i> CA	3.2	1.6	1.4	6	4	2	2.2	4.6	1.5	2.0	2.9
4-HDi	± 0.1	± 0.05	± 0.1	± 0.2	± 0.1	± 0.5	± 0.1	± 0.23	± 0.5	± 0.25	
<i>iso</i> CA	14	5.2	3	10	5	12	8	4	2.5	275	34
4	± 1.2	± 0.2	± 0.15	± 1.2	± 1.8	± 0.1	± 0.4	± 0.2	± 0.9	± 22	
CA4	11	5.5	25.0	8	6	200	172	3	2.9	> 10000	>1000
	± 1.2	± 0.2	± 0.2	± 2	± 2	± 5	± 5	± 0.1	± 0.5		
TSA	58	260	90	200 ± 15	100	80	54	91	35	55	102
	± 6.1	± 7.2	± 0.5		± 21	± 5	± 4.2	± 6.1	± 1.2	± 2.9	
PCI- 34051	1500	2010	2200	> 20000	nd	2000	2980	nd	2600	> 10000	> 1000
	± 250	± 650	± 1270			± 450	± 1050		± 1100		

^aLegend  = Dual compounds;  TPI compounds;  HDACi compounds; ^bCompound concentration required to decrease cell growth by 50%; For values represent the average ± SD of three experiments, see SI.

2.4. Effect of compounds **12a** and **12d** on the cell cycle arrest

Microtubules and microfilaments are essential for cell division, and their disruption can induce G₂/M arrest and apoptosis. To investigate whether the cytotoxicity of compounds **12a** and **12d** was due to the cell cycle arrest, we examined, after 24 h of treatment, their effects on HT-29 cell cycle progression using propidium iodide (PI) staining by flow cytometry analysis. As shown in Fig. 3, **12a** and **12d** dose-dependently arrested HT-29 cells in the G₂/M phase. The two lead compounds caused a significant G₂/M arrest at a low dose starting from 1 nM. At the highest concentration of 5 nM, more than 95% of the cells were arrested in G₂/M. The effects of **12a** and **12d** observed on cell-cycle progression correlated well with their antiproliferative and anti-tubulin activities (see *infra*).

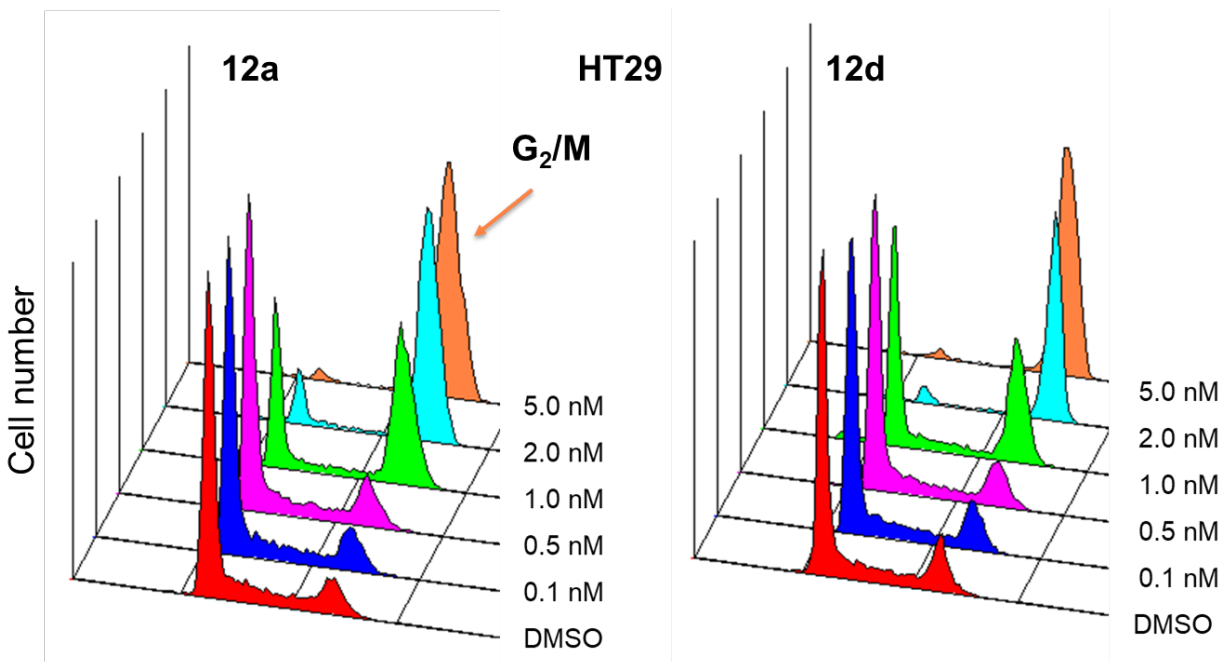


Figure 3. Effects of compounds **12a** and **12d** on the cell cycle distribution in HT-29 cell lines at 0.1, 0.5, 1, and 2 nM, as determined by flow cytometry analysis (DMSO control in red). DNA content was assessed *via* propidium iodide staining.

2.5. Effect of 12a and 12d on mitochondrial dysfunction in HT-29 cells

Mitochondria play critical roles in cellular metabolism, homeostasis, and stress responses by generating ATP for energy and regulating cell death.[45] Mitochondrial dysfunctions are usually caused by depolarization which is the early hallmark of toxicity mediated through caspase-induced apoptosis.[46] The carbocyanine dye JC-1 has been generally considered a reliable and sensitive fluorescent probe for detecting differences in maintaining the mitochondrial membrane potential ($\Delta\psi_m$) due to its dual emission characteristics. At low concentrations, JC-1 exists mainly in a monomeric form which emits green fluorescence, while at high concentrations, this molecule forms aggregates, which emit orange-red fluorescence. Due to the disrupted mitochondrial membrane in apoptotic cells JC-1 accumulates in its monomer form in the cytoplasm, where it generates a green fluorescence.[47] As shown in Fig. 4, compounds **12a** and **12d** induced mitochondrial dysfunction, which was detected using the above described fluorescence-based mitochondrion-specific voltage-dependent dye, JC-1. Treated cells emitted mostly green fluorescence, whereas viable cells emitted orange-red fluorescence. Thus, our results showed that **12a** and **12d** induced mitochondrial dysfunctions at a low concentration of 2 nM. Our study provides convincing evidence indicating that compounds **12a** and **12d** caused caspase-induced apoptosis of HT-29 cells through mitochondrial dysfunction.

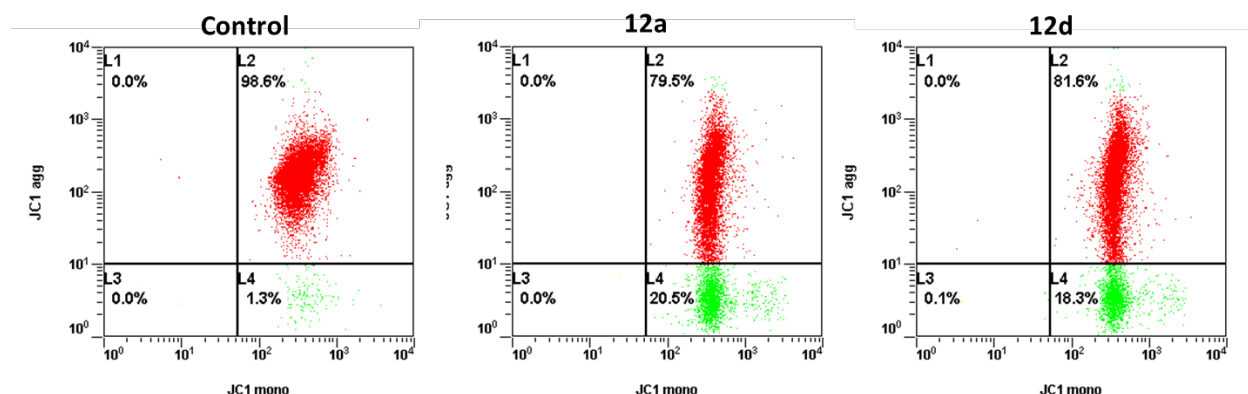


Figure 4. **12a** and **12d** induced mitochondrial dysfunctions in HT-29 colorectal colon cancer cells. Cells were incubated with **12a** or **12d** at concentrations of 2 nM for 48 h at 37 °C. The portion of mitochondria dysfunction was measured using the JC1 assay.

2.6. Effect of 12a and 12d on HDAC inhibition

Newt, we tested compounds **12a** and **12d** *in vitro* for HDACs inhibitory effect (1 to 11) on lysine deacetylation on the platform Cerep/Eurofins (Fig. 5). Each recombinant HDAC was incubated with its fluorogenic acetylated substrate in the presence or absence of the tested compound, and acetylation was further measured by fluorometry.[48] Reference compounds include TSA for HDAC1-10 and Scriptaid for HDAC11. At 1 μ M concentration, **12a** and **12d** were able to inhibit HDAC8 (HDAC class I) strongly and partially HDAC6 (class IIb) and HDAC11 (class IV), and no inhibition was noticed for class IIa.

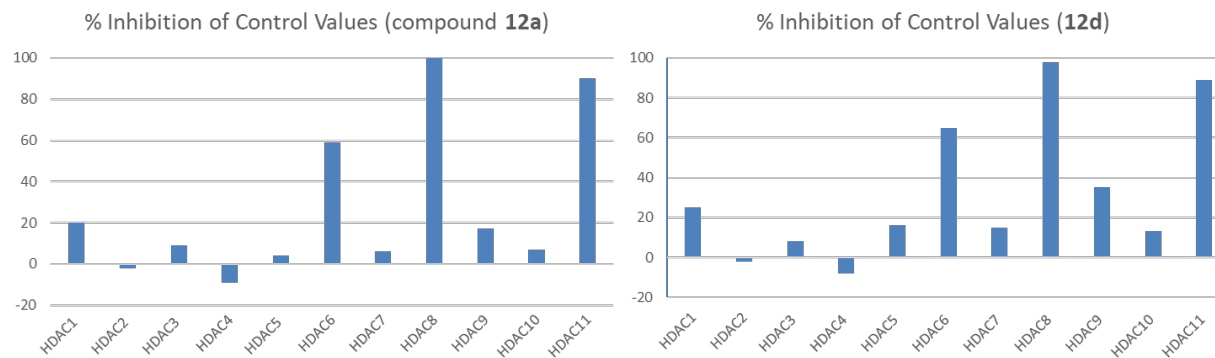


Figure 5. Inhibition profile and isoform selectivity of **12a** and **12d** against HDAC isoforms 1–11. Selected compounds were used at 10^{-6} M.

Following these results, we determined the IC_{50} *in vitro* of these two compounds on HDAC6, 8, and 11 (Table 4) in the presence of reference compounds, TSA, PCI-34051, and Scriptaid. Compounds **12a** and **12d** were found selective for HDAC8 with IC_{50} = 150 nM, and IC_{50} = 280 nM respectively. Quinaldine derivative **12a** was found about 7-fold less active for HDAC6 and 13-fold less active for HDAC11. The reference compound TSA has better activity against HDAC6. No activity of HDACi was observed with *iso*CA4 and **10a**, which have the pharmacophore of TPI but without the linker having the hydroxamic acid group. Compared to *iso*CA-4-HDi, compounds **12a** and **12d** were found to be more active on the three HDACs (6, 8, and 11).

Table 4. *In vitro* inhibition of recombinant HDACs 6, 8, and 11 for selected compounds.

Compound	IC ₅₀ (nM)		
	HDAC6	HDAC8	HDAC11
<i>iso</i> CA4-HDi	15000 ± 1300	340 ± 26	10000 ± 850
12a	1000 ± 30	150 ± 10	1900 ± 100
12d	2000 ± 45	280 ± 15	3200 ± 100
10a	Na ^c	Na ^c	Na ^c
TSA	20 ± 1.4	790 ± 20	Nt ^a
PCI-34051 ^b	3100 ± 30	12 ± 2.2	Nt ^a
Scriptaid	Nt ^a	Nt ^a	5200 ± 100
<i>iso</i> CA-4	Na ^c	Na ^c	Na ^c

^aNt = not tested. ^bPCI-34051 (CAS number = 950762-95-5). ^cNa = not active.

Phosphorylation of H2AX (γ -H2AX) is an evolutionarily conserved response to DNA double-strand breaks.[49, 50] HDAC inhibitors have been shown to prolong the duration of γ -H2AX in irradiated melanoma[51] and prostate[52] cell lines. In both these two articles, it was suggested that HDACi radiosensitize human tumor cells by affecting their ability to repair the DNA damage induced by ionizing radiation and that γ -H2AX phosphorylation can be used as a predictive marker of radioresponse.[51] Therefore, we examined whether compound **12a**, which inhibits HDAC activities, can modulate the γ H2AX level (Fig. 6). Compared to mock-treated cells, HT-29 cells treated with compound **12a** resulted in γ H2AX induction.

Interestingly, an increase in **12a** concentration led to a dose-dependent increase in γ H2AX. The increase of γ H2AX level following treatment with **12a** indicates that HDAC inhibition disrupts the DNA repair process. This mechanism potentially sensitizes HT-29 cells to the cytotoxic effects of the anti-tubulin effect of **12a**.

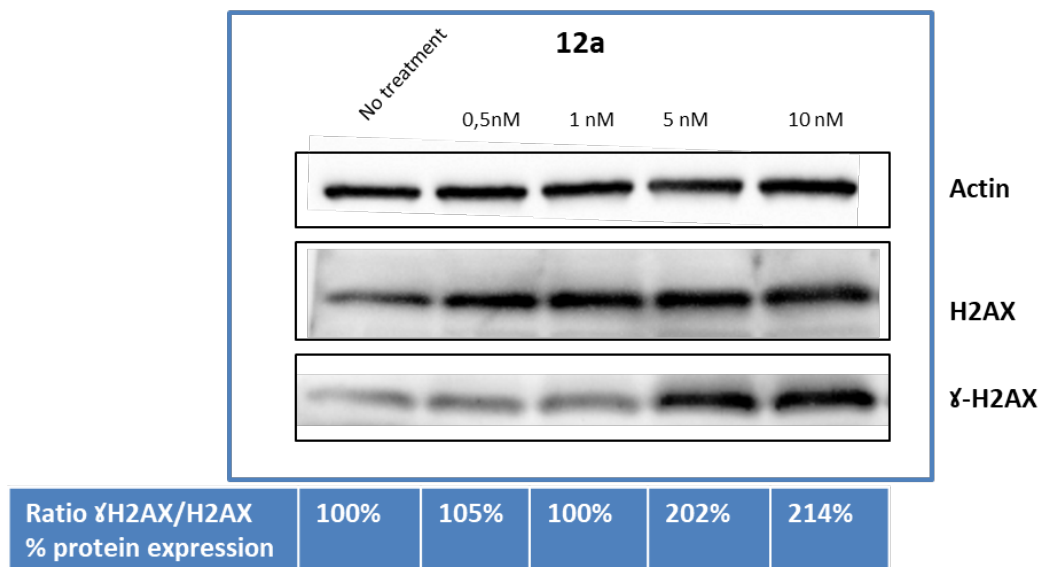


Figure 6. γH2AX induction after colon carcinoma cells (HT-29) treatment with compound **12a**. HT-29 cells were mock-treated or treated with **12a** at the indicated doses. After 24 h, phosphorylated H2AX (γH2AX) and actin were measured by Western blot.

In addition to *in vitro* studies, the HT-29 colon carcinoma cell line treated with **12a** and the reference compound PCI-34051, an HDAC8 specific inhibitor, and the cell lysates were analyzed by Western blot (Fig. 7). Compared to mock-treated cells, cells treated with **12a** displayed a strong increase in acetylation of SMC3, a well-known HDAC8 substrate. The increase in **12a** concentration led to a dose-dependent increase in acetylated SMC3.

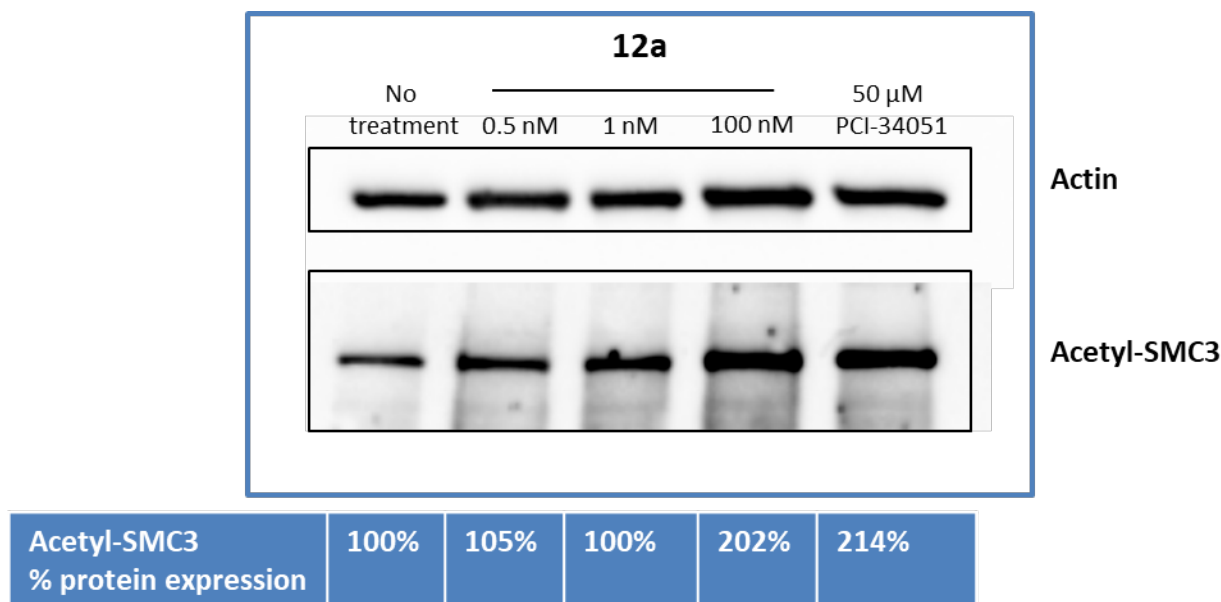


Figure 7. Compound **12a** was able to inhibit HDAC8 activity on SMC3 protein. HT-29 colon carcinoma cells were treated with **12a**, or PCI-34051 (50 μM), and cell lysates obtained after 30 min were analyzed by Western blot.

Finally, we analyzed the HT-29 colon carcinoma cell line treated with **12a** by Western blot. However, at 0.5, 1, and 10 nM no significant increase of the acetylated tubulin was observed.

2.7. Effect on microtubules

We first analyzed the effect of **12a** on *in vitro* tubulin polymerization (Fig. 8) by monitoring absorbance at 350 nm. Tubulin (40 μ M) was incubated with different concentrations of **12a**, as indicated, in the presence of 1 mM GTP, and the formation of microtubules was induced by raising the temperature to 37 °C. In these experimental conditions, we found that compound **12a** was able to inhibit tubulin polymerization in a dose-dependent manner, with a maximal effect achieved for a 10 μ M concentration.

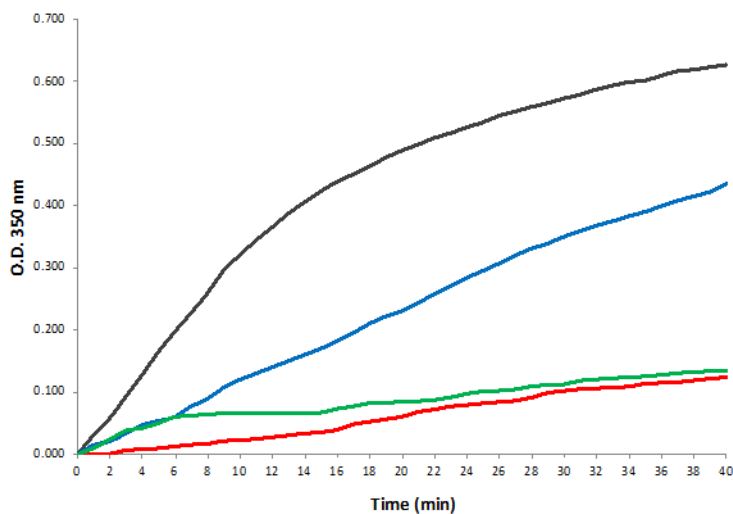


Figure 8. Effect of **12a** on tubulin polymerization. Compound **12a** was added at different concentrations to 40 μ M tubulin, and its effect on tubulin kinetics assembly was monitored. Black: DMSO, control; blue: 5 μ M; green: 10 μ M; red: 15 μ M. Representative curves of two independent experiments.

We then analyzed the effect of **12a** on cell microtubules, using both tubulin immunofluorescence (Fig. 9) and a recently described sensitive cell-based assay,[53, 54] which quantifies the amount of microtubules present in cells (Fig. 11), allowing quantitative comparisons. As shown in Fig. 9, **12a** depolymerizes the cell microtubule network, indicating that it can penetrate into cells and target microtubules as equally as the compound CA-4.

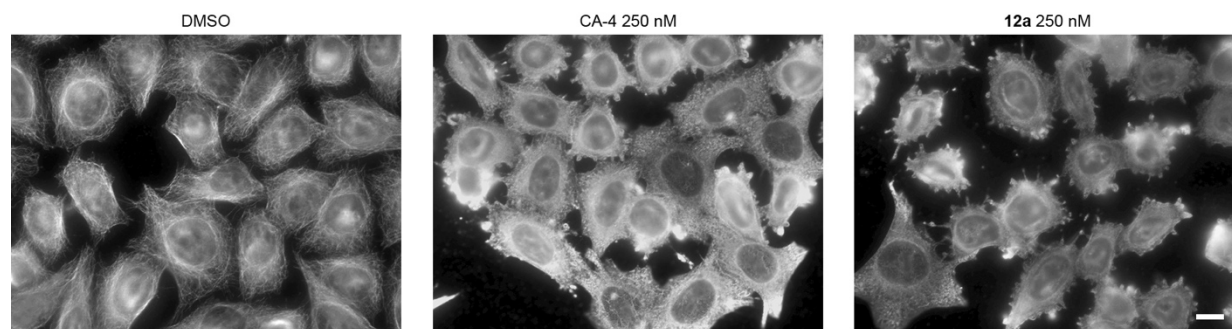


Figure 9. Effect of **12a** and CA-4 on cell microtubule network. HeLa cells were treated for 30 min with DMSO (control) or CA-4 and **12a**, at 250 nM for 30 min. Cells were then fixed and processed for immunofluorescence, as indicated in the methods section. Bar= 10 μ m.

We then tested if this effect was cell-specific. For that, HeLa Cells treated for 30 min with **12a** at 125 nM displayed a significantly less dense microtubule network and, in some cases, an almost complete loss of microtubules. The effect was even more pronounced when **12a** was used at 250 nM. This effect is not cell-specific since it is also observed on other cancer cell lines such as the MDA-MB-231 breast cancer cells. These observations suggest that **12a** interferes with tubulin polymerization (Fig. 10, upper panel).

To verify this hypothesis, we performed a microtubules polymerization assay in HeLa cells. Briefly, cells were incubated on ice for 45 min to allow for microtubules depolymerization. Cells were then shifted back to the permissive temperature of 37°C and fixed at the early phases of microtubules repolymerization. Microtubules start to grow as asters from microtubules organizing centers (MTOCs) such as the centrosome. Treatment with **12a** at 125 nM reduced of approximately 4-folds the number of cells with asters. Additionally, the few asters observed in **12a** treated cells were less developed than asters in DMSO treated cells, indicating a severe defect in tubulin polymerization (Fig. 10, lower panel).

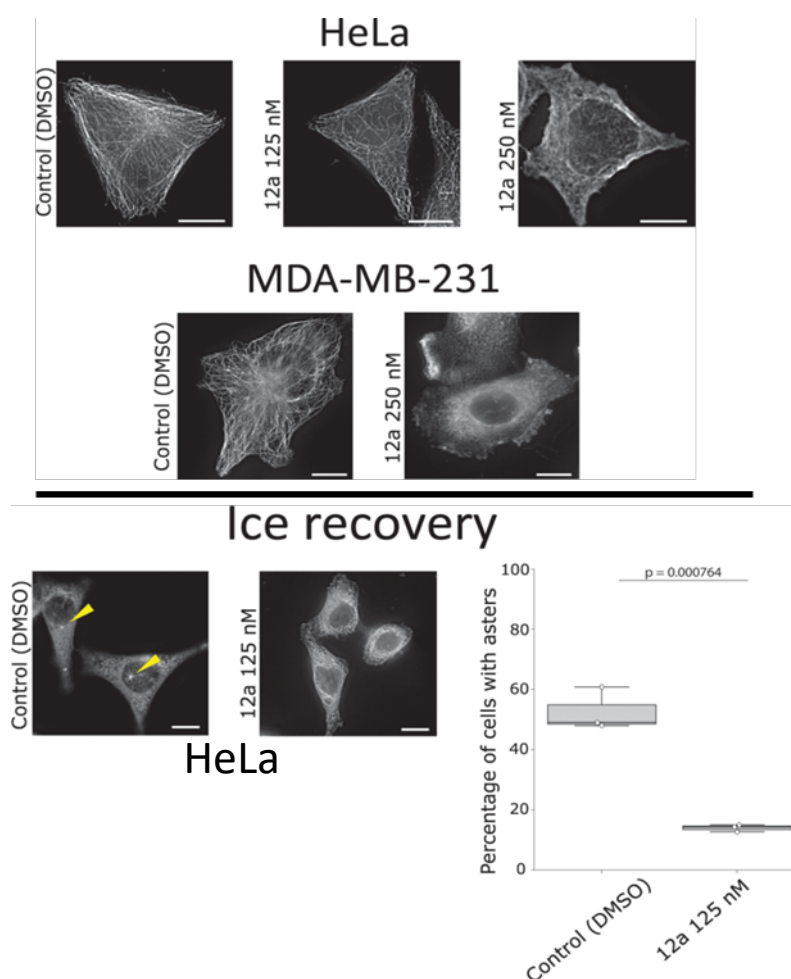


Figure 10. Upper panel) HeLa cells or MDA-MB-231 cells seeded on glass coverslips were treated with DMSO or **12a** at the indicated concentrations for 30 min. Cells were then fixed and immunostained for alpha-tubulin. Scale bars: 10 μm. **Lower panel)** HeLa cells seeded on glass coverslips were incubated on ice for 45 min to depolymerize microtubules. DMSO or **12a** were then added at the indicated concentrations and cells were put at 37°C for 10 min

to allow for microtubules repolymerization (yellow arrowheads point to microtubule asters). The percentage of cells displaying microtubule asters was calculated in each condition in three independent experiments and data are shown on the graph. The p value (0.000764) was obtained with Student's T-test. Scale bars: 10 μm .

We then quantitatively compared the depolymerizing effect of **12a** to CA-4 and *iso*CA4. As shown in Fig. 11, after 30 min of incubation, we observed that **12a** induced dose-dependent depolymerization of the microtubule network, with maximal depolymerization observed for a 250 nM concentration. In this assay, compound **12a** (IC_{50} = 20 nM) was found less potent than CA-4 and *iso*CA4 (IC_{50} of 3 nM and 6 nM, respectively).

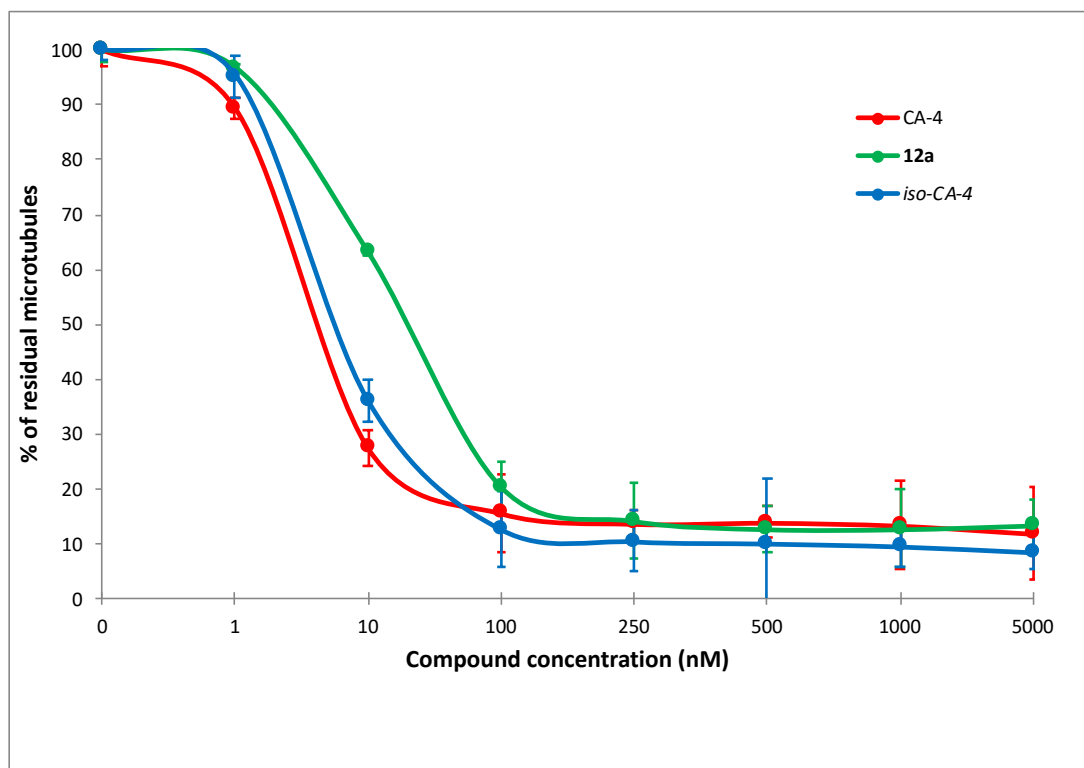


Figure 11. Comparative analysis of the effect of **12a**, CA-4, and *iso*CA-4 on microtubule dynamics in HeLa cells. Different doses of the compounds were applied to HeLa cells in microplates, and the amount of residual microtubules was assessed after 30 min, using a luminescent assay described in the material and methods section. Results are expressed as mean \pm SEM of their independent experiments.

2.8. Molecular Docking into tubulin

To understand the structural basis for the observed effect of **12a**, we undertook docking simulations using the protein preparation wizard from the Schrödinger suite. The colchicine binding site of tubulin is composed of α - and β -chain. The molecular docking gave a perfect overlay for *iso*CA4-HDi[32] and **12a** compounds (Fig. 12). The benzene moiety of **12a** establishes a CH/ π interaction with the side chain of Asn β 258 residue. Another CH/ π interaction is observed between the quinoline ring of **12a** and the side chain of Ala β 316. A hydrogen bond occurs by the proximity between the CO backbone of Asn β 349 and the NH hydroxamic acid of **12a**. An additional hydrogen bond is identified between the CO backbone of Ala- α -180 and the OH hydroxamic acid of **12a**.

2.9. Molecular Docking into HDAC8

The CO function of hydroxamic acid of **12a** (as well as *iso*CA4-HDi[32]) coordinates the zinc atom in the catalytic site of HDAC8. A classical hydrogen bond interaction occurs between the NH moiety of **12a** of the hydroxamic acid group and the CO backbone of Gly151 (Fig. 12). Benzene moiety establishes π/π -stacking interactions with the aromatic ring of Phe152 residue. A CH/ π interaction between the OMe function of **12a** and the side chain of the aromatic ring of Phe208 has been detected. A type of CH/CH interaction was observed between the NMe function of **12a** and the side chain of Met274.

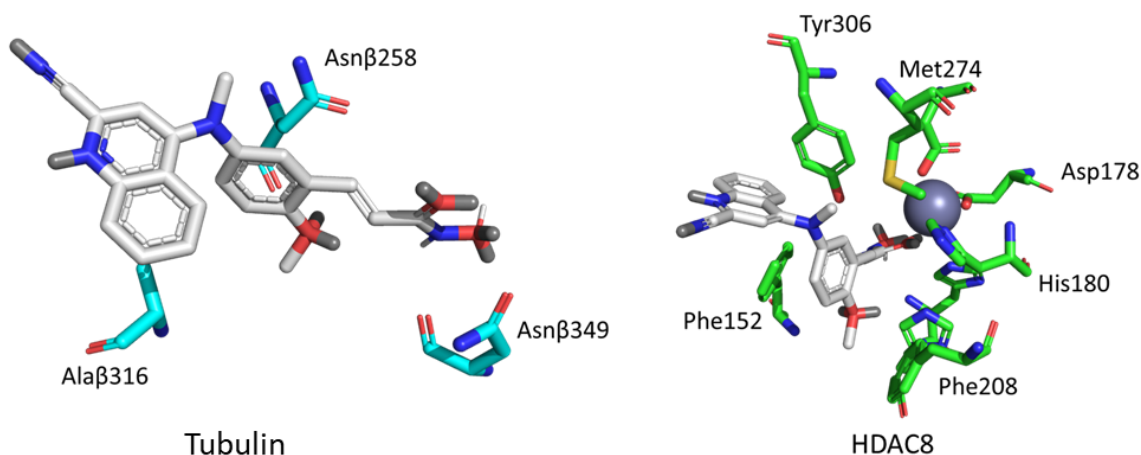


Figure 12. Left: putative binding mode of compounds **12a** in the colchicine binding site of tubulin (code PDB: 6H9B). Right: Putative binding mode of compounds **12a** in the binding site of HDAC8 (code PDB: 2V5X).

2.8. Physicochemical properties

Appropriate physicochemical parameters are the key to the druggability of a candidate compound. To this end, physicochemical properties of **12a** and **12d** were assessed in parallel with the reference compounds *iso*CA-4 and *iso*CA4-HDi. As a result, compounds **12a** and **12d** have been shown to conform to Lipinski's rule of five (Table 5).

Additionally, **12a** and **12d** have shown an improved aqueous solubility compared to *iso*CA-4, indicating that the presence of the hydroxamic acid moiety fosters water solubility. Therefore, our findings showed that combining the 2-cyanoquinazolin-4-yl group and a linker with a hydroxamic acid group improved aqueous solubility with better anti-proliferative activity than *iso*CA-4.

Table 5. Water solubility and physicochemical properties of compounds **12a**, **12d** and *isoCA-4*

Cmpd.	MW ^a	HBA ^b	HBD ^c	cLogP ^d	tPSA ^e	Water solubility (µg/ml) ^f
<i>isoCA-4</i>	316.35	5	1	2.86	57.16	11.62
12a	374.40	7	2	2.87	98.48	68.7
12d	364.40	7	2	2.77	87.58	65.0
<i>isoCA4-HDi</i>	385.42	7	2	2.84	86.26	69.20
RO5 (violations)^g	0	0	0	0	0	

^aMW: molecular weight; ^bHBA: hydrogen-bond acceptor atoms. ^cHBD: hydrogen-bond donor atoms. ^dclogP: calculated logarithm of the octanol-water partition coefficient. ^etPSA: topological polar surface area, calculated using <http://www.molinspiration.com/cgi-bin/properties>. ^fWater solubility. ^gRO5: Lipinski's rule of five.

2.9. Metabolic stability

The metabolic stability was expressed by the intrinsic clearance CL_{int}, which was calculated from the *in vitro* half-life time (t_{1/2}). Propafenone (PPF) was shown as a reference compound with a medium CL_{int} to ensure the integrity of the metabolic experiment. The t_{1/2} values of the studied compounds were found higher in the following ascending order, **12d** < *isoCA-4* < *isoCA4-HDi* < **12a**, in agreement with the descending order for CL_{int} with both rat and human microsomes (Table 6). Despite an improved aqueous solubility, the hydroxamic acid on the B-ring of *isoCA4-HDi*, could not decrease its CL_{int} significantly compared to *isoCA-4*. Thus, among new analogs, with the lowest CL_{int}, compound **12a** showed better metabolic stability than *isoCA-4* and *isoCA4-HDi*, through its quinoline-2-carbonitrile-based and hydroxamic acid structure.

Table 6. Metabolic stability of **12a**, **12d** vs. *isoCA4-HDi*, *isoCA-4*, and PPF.

Compound	RLM		HLM	
	t _{1/2} (h)	CL _{int} ^a	t _{1/2} (h)	CL _{int} ^a
12a	6.60	1.75	32	0.36
12d	3.53	3.27	9	1.28
<i>isoCA4-HDi</i>	4.42	2.57	14	0.83
<i>isoCA-4</i>	4.24	2.73	12	0.96
PPF^b	1.95	5.92	2.5	4.62

^a The *in vitro* metabolic stability was expressed by the intrinsic clearance CL_{int} (given in $\mu\text{L}/\text{min}/\text{mg}$ protein) using rat liver microsomes (RLM) and human liver microsomes (HLM). ^b Propafenone was used as a control to validate the accuracy of the test system.

2.10. *In vivo* antitumor activity

Based on the high antiproliferative activity seen *in vitro*, excellent metabolic stability, and good physicochemical properties, compound **12a** was selected to evaluate the *in vivo* antitumor efficacy. To test our molecules *in vivo*, without having to use PDX models, we decided to test them on an allogeneic sarcoma model in C57BL/6 mice that we routinely use in our laboratory, the MCA205 fibrosarcoma cell line. Therefore, before looking at the effect of compound **12a** on tumor growth *in vivo*, we evaluated the *in vitro* antiproliferative activity of compound **12a** against MCA205 cells (Fig. 13). The compound **12a** shows an interesting activity with an $\text{IC}_{50} = 2.78 \pm 0.4$ nM (Fig. 13).

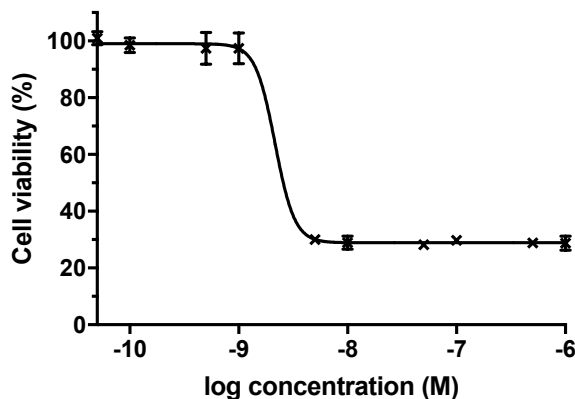


Figure 13. Effect of **12a** on the viability of MCA205 cells.

To go further, it was necessary to check the compound's toxicity at different doses intraperitoneally before looking at the effect of compound **12a** on tumor growth. Supplementary Fig. S1 shows that injecting the compound **12a** in an intraperitoneal route does not affect the tumor growth at a very low dose concentration. In contrast, the compound becomes toxic to mice at the highest concentration.

Different injection routes are used to treat cancer, from oral to intravenous to intratumorally ways. In fact, there are currently over 25 clinical trials using the intratumoral route to inject various treatments (www.ClinicalTrials.gov). Intratumoral injection consists of injecting immunomodulatory molecules or immune checkpoints inhibitors directly into the tumor site, which can act directly on the tumor cells while intensely decreasing the cytotoxic effect of these different treatments.[55] It has been reported that the toxicity of intravenously injected immunotherapy is related to the dose injected.[56] Systemic administration requires the use of a large amount of the immunomodulatory agent to induce an antitumor response, which is accompanied by high toxicity. In contrast, local administration at the tumor level will require a much lower dose to induce an equal or better response than systemic administration, and this with limited side effects due to the limited diffusion of the immunomodulatory agent. To overcome the toxicity observed intraperitoneally, we decided to inject compound **12a** in an intratumorally way. To this end, MCA205 WT cells were subcutaneously inoculated into C57BL/6 mice as previously described.[57] From day 7 post cell inoculation and three times a week for two weeks, each group of mice was intratumorally treated with 0.1 mg/kg, 0.25 mg/kg or 0.50 mg/kg of compound **12a** (Fig. 14a). At 0.25 mg/kg and 0.50 mg/kg dose, a significant decrease in MCA205 tumor growth over time was observed after treatment with **12a** compared to the control group (Fig. 14b). No toxicity was observed at the doses used. More specifically, we observed a 70% decrease in MCA205 fibrosarcoma growth (Fig. 14c) upon treatment with **12a**. However, when 0.1 mg/kg of compound **12a** was injected intratumorally, no significant decrease in MCA205 WT tumor growth over time was observed. Furthermore, **12a** treatment extends overall survival with about 60% of mice bearing MCA205 tumors that experience complete tumor regression upon treatment with 0.5mg/kg of **12a** and 40% of mice that experience complete tumor regression upon treatment with 0.25mg/kg of **12a** (Fig. 14e) when no overall survival was observed when mice were treated with 0.1 mg/kg of compound **12a**. In parallel, the mouse body weight in each group was monitored during and after the treatment. The gradual increase in body weight among all of the experimental groups treated or not with the compound **12a** was consistent with that observed with the control group, which represents the gradual growth of tumor-bearing mice body weight (Fig. 14d), demonstrating no side effects of **12a** on treated tumor-bearing mice.

Overall, the results demonstrate that **12a** has a strong anticancer activity *in vivo* at low doses and can extend the overall survival of treated mice that experience complete tumor regression when injected intratumorally.

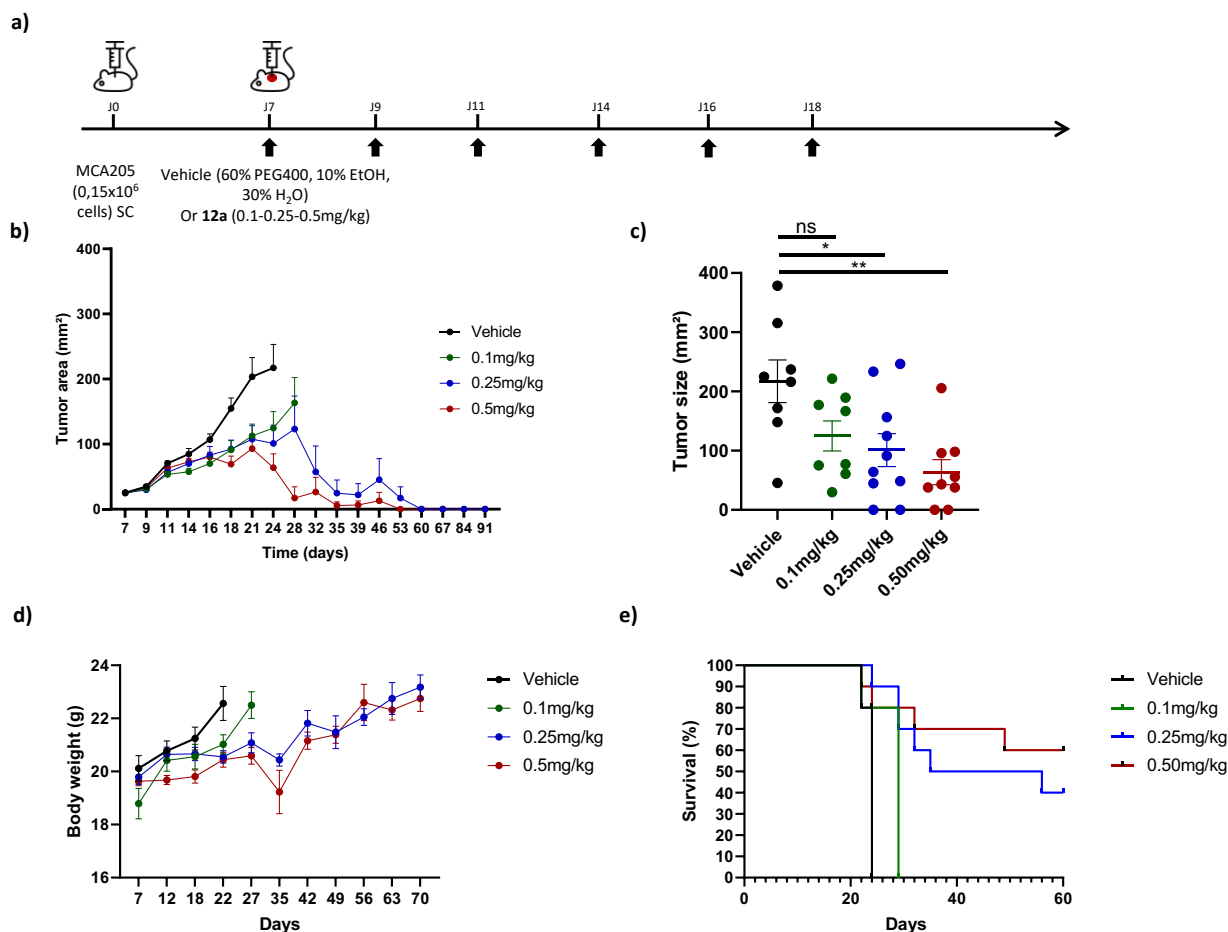


Figure 14. Inhibitory effect of **12a** on the allograft model. (a) MCA205 tumor cells were injected subcutaneously in the right flank of 7 weeks old C57BL/6 mice. At day 7 post-inoculation, mice were treated intra-tumorally with **12a** (0.1 mg/kg; 0.25 mg/kg or 0.5 mg/kg) diluted in PEG vehicle three times a week for two weeks. (b) Tumours size have been monitored before every injection from day 7 to day 21 and twice a week from day 21 to day 91. (c) shows tumour size at day 24 post tumour inoculation. (d) shows body weight monitored twice a week during the treatment phase and once a week during the survival. (e) shows the percentage of survival in the control and treated group. 40% of treated mice were tumor-free when treated at 0.25 mg/kg, and 60% of treated mice were tumor-free when treated with 0.5 mg/kg. Results are expressed as mean \pm SEM, n=10 per group. Significance were performed using a mixed-effects analysis and multiple comparisons between control and treated groups (* p < 0,05; **** p < 0,0001). A non-parametric Kruskal-Wallis test was performed in (c).

3. Conclusion

Structure-activity relationship (SAR) studies have been done on the different heterocyclic substitutions on the quinoline or quinazoline moieties, as well as both on the linker of the cap part (C=CH₂ vs. NMe), or the linker between the cap and the ZBG. Among studied compounds, we identified novel dual TPI and HDACsi with improved antiproliferative activity and enzymatic activity against HDACs 6, 8, and 11. We selected compounds **12a** and **12d** as advanced leads compounds and evaluated their antiproliferative activity against ten different cancer cell lines. Compared to the first generation of dual tubulin/HDACi (*iso*CA4HDi) and other reference compounds *iso*CA-4, TSA, and PCI-34051, the antiproliferative activity of compounds **12a** and **12d** were found superior, with an IC₅₀ value in the subnanomolar range. In addition, the metabolic study showed that compound **12a** (second generation) was more stable than *iso*CA4HDi (first generation).

Interestingly, these two lead compounds demonstrated high antiproliferative activity in Pgp-overexpressing multidrug-resistant leukemia cells (K562-R) and multidrug- and CA-4-resistant HT-29 cells; this result is of clinical significance given that the expression of Pgp is frequently associated with clinical resistance to chemotherapy. Compounds **12a** and **12d** induced arrest of the cell cycle in the G₂/M phase at a low concentration of 2 nM and triggered apoptosis of HT-29 cells through mitochondrial dysfunction. In addition, **12a** and **12d** inhibited HDAC8, 6, and 11 with better efficacy than *iso*CA-4HDi. Furthermore, compound **12a** increased the level of γ H2AX, indicating that HDAC inhibition disrupts the DNA repair process. Compound **12a** exhibits a higher *in vitro* metabolic stability than *iso*CA-4HDi and *iso*CA-4. Notably, the most active compound, **12a**, efficiently inhibited tubulin polymerization both *in vitro*, on pure tubulin, and in cells, with an IC₅₀ in the nM range, by targeting the colchicine-binding site of tubulin. Finally, **12a** was highly effective in suppressing tumor growth in the fibrosarcoma MCA205 tumor model. Taken together, these results suggest that quinaldine derivative **12a** represents a new promising class of dual TPI and HDACi deserving further investigations.

4. Experimental Section

4.1. Chemistry. General considerations

The compounds were all identified by ¹H-NMR, ¹³C-NMR, IR, and HRMS. Melting points (mp) were recorded on a Büchi B-450 apparatus and were uncorrected. NMR spectra were performed on a Bruker AMX 200 (¹H, 200 MHz; ¹³C, 50 MHz; ¹⁹F, 88 MHz), Bruker AVANCE 300 or Bruker AVANCE 400 (¹H, 300 MHz or 400 MHz; ¹³C, 75 MHz or 100 MHz). Solvent peaks were used as reference values, with CDCl₃ at 7.26 ppm for ¹H NMR and 77.16 ppm for ¹³C NMR, with (CD₃)₂SO at 2.50 ppm for ¹H NMR and 39.52 ppm for ¹³C NMR. Chemical shifts δ are given in ppm, and the following abbreviations are used: singlet (s), doublet (d), doublet of doublet (dd), triplet (t), quadruplet (q), and multiplet (m). Infrared spectra (IR) were measured on a Bruker Vector 22 spectrophotometer and were recorded in film (film, cm⁻¹). High-resolution mass spectra (HRMS) were recorded on a MicrotofQ Bruker Daltonics. The purity of the final compounds was determined to be $\geq 95\%$ using high-pressure liquid chromatography-mass spectrometry (HPLC-MS) on a Waters Alliance 2695 (HPLC) and LCT Premier, ESI-TOF mass spectrometer with an XBridge C18 column (2.1 \times 150 mm, 3.5 μ m) eluting at 0.25 mL/min with water + 0.1 % formic acid/MeCN + 0.1 % formic acid, gradient 95/5 to 0/100 in 20 min. Reaction courses and product mixtures were monitored by TLC on silica gel (precoated F254 Merck plates), and compounds were visualized under a UVP Mineralight UVGL-58 lamp (254 nm) and with phosphomolybdic acid/heating, or vanillin/heating.

4.2. Procedure for the synthesis of starting materials

4.2.1. 4-chloroquinoline-2-carbonitrile.[24] A solution of 2,4-dichloroquinoline (3 g, 15.1 mmol) in 33 mL DMF was introduced in a sealed tube dried and flushed with argon. Zinc cyanide (907 mg, 7.7 mmol) and Pd(PPh₃)₄ (1.75 g, 1.51 mmol) were added to the solution. The medium was heated to 120 °C for 1 hour. The solution became clear, and then a precipitate appeared. The medium was diluted with 120 mL of a saturated solution of NH₄Cl and extracted with ethyl acetate three times. The organic phase was dried with MgSO₄ and evaporated under a vacuum. Flash chromatography on silica gel (100% cyclohexane to 9/1 mixture of cyclohexane/ethyl acetate) afforded 4-chloro-2-cyanoquinoline (2.4 g, yield 85%). White solid. mp 109-111 °C. ¹H NMR (300 MHz, CDCl₃) δ : 8.30 (dd, *J* = 8.2, 1.4 Hz, 1H), 8.20 (dd, *J* = 8.2, 1.4 Hz, 1H), 7.91 (t, *J* = 6.9 Hz, 1H), 7.83 (d, *J* = 7.3 Hz, 1H), 7.79 (s, 1H). ¹³C NMR (75

MHz, CDCl₃) δ 148.9, 144.3, 133.4, 132.2, 130.7 (2C), 127.3, 124.4, 123.4, 116.8. HRMS (ESI⁺) calcd for C₁₀H₆N₂Cl [M + H]⁺ 189.0220, found 189.0217.

4.2.2. 4-((4-methoxy-3-(methoxymethoxy)phenyl)amino)quinoline-2-carbonitrile. A mixture of 4-chloroquinoline-2-carbonitrile (515mg, 2.75mmol), 4-methoxy-3-(methoxymethoxy)aniline (500 mg, 2.75 mmol), Pd₂(dba)₃.CHCl₃ (56 mg, 2 mol%), XantPhos (78 mg, 5 mol%), and cesium carbonate (1.25 g, 3.85 mmol) in 1,4-dioxane (10 mL) was heated at 110 °C in a sealed tube under argon for 2 hours. The reaction mixture was filtered, the filtrate was concentrated in vacuum. Flash chromatography on silica gel (EtOAc/Cyclohexane 0% to 30%) afforded the desired product (yield 84%). Yellow powder, mp: 167 – 169 °C. IR (film): 3359, 2954, 2933, 1558, 1529, 1251, 1232, 997, 763 cm⁻¹. ¹H NMR (200 MHz, CDCl₃) δ 8.07 (d, *J* = 8.6 Hz, 1H), 7.91 (d, *J* = 7.7 Hz, 1H), 7.78 (t, *J* = 7.7 Hz, 1H), 7.61 (t, *J* = 7.2 Hz, 1H), 7.12 (s, 1H), 6.98 (m, 3H), 6.80 (s, 1H), 5.25 (s, 2H), 3.95 (s, 3H), 3.53 (s, 3H). ¹³C NMR (75 MHz, CDCl₃) δ 150.1 (C), 148.9 (C), 148.7 (C), 147.6 (C), 134.5 (C), 131.1 (C), 130.9 (CH), 130.8 (CH), 127.7 (CH), 119.5 (CH), 119.1 (CN), 119.0 (CH), 118.3 (CH), 114.0 (CH), 112.8 (CH), 104.0 (CH), 95.7 (CH₂), 56.5 (CH₃), 56.4 (CH₃). HRMS (ESI⁺) (M + H)⁺: *m/z* calcd C₁₉H₁₈N₃O₃ 336.1343, found 336.1345.

4.2.3. 4-((4-methoxy-3-(methoxymethoxy)phenyl)(methyl)amino)quinoline-2-carbonitrile. 4-((4-methoxy-3-(methoxymethoxy)phenyl)amino)quinoline-2-carbonitrile (500 mg, 1.5 mmol) was dissolved in DMF (5mL) and cooled at 0 °C with an ice bath. NaH (120 mg, 3.0 mmol) was added by portion, and the reaction was stirred at 0 °C for 30 min. Methyl iodide (130 μ L, 2.3 mmol) was added drop by drop and the reaction was stirred at 0 °C for 1 hour. Deionized water was added slowly, and the mixture was extracted with EtOAc. The organic layer was dried with MgSO₄, filtered, and concentrated in a vacuum. Flash chromatography on silica gel (EtOAc/Cyclohexane 0% to 30%) afforded the desired compound (yield 89%). Orange powder, mp: 118 – 120 °C. IR (film): 2956, 1569, 1498, 1238, 989, 766 cm⁻¹. ¹H NMR (300 MHz, CDCl₃) δ 8.02 (d, *J* = 8.8 Hz, 1H), 7.61 (t, *J* = 7.7 Hz, 1H), 7.55 (d, *J* = 8.8 Hz, 1H), 7.27 (t, *J* = 7.7 Hz, 1H), 7.19 (s, 1H), 6.90 (d, *J* = 2.6 Hz, 1H), 6.80 (d, *J* = 8.7 Hz, 1H), 6.61 (dd, *J* = 8.7, 2.6 Hz, 1H), 5.11 (s, 2H), 3.86 (s, 3H), 3.47 (s, 3H), 3.41 (s, 3H). ¹³C NMR (75 MHz, CDCl₃) δ 154.5 (C), 150.0 (C), 147.5 (C), 143.2 (C), 134.3 (C), 130.6 (CH), 130.2 (CH), 127.0 (CH), 125.5 (CH), 123.2 (C), 118.2 (C), 117.4 (CH), 116.2 (CN), 113.0 (CH), 112.6 (CH), 111.9 (CH), 95.7 (CH₂), 56.3 (CH₃), 56.3 (CH₃), 43.7 (CH₃). HRMS (ESI⁺) (M + H)⁺: *m/z* calcd for C₂₀H₂₀N₃O₃ 350.1499, found 350.1507.

4.2.4. 4-((3-hydroxy-4-methoxyphenyl)(methyl)amino)quinoline-2-carbonitrile (5). 4-((4-methoxy-3-(methoxymethoxy)phenyl)(methyl)amino)quinoline-2-carbonitrile (450 mg, 1.3 mmol), was dissolved in MeOH (30 mL) and heated at 60 °C. PTSA monohydrate (735 mg, 3.9 mmol) was added and the reaction was stirred at 60 °C for 1 hour. Methanol was evaporated, deionized water was added (15 mL) followed by an extraction with EtOAc. The organic layer was dried with MgSO₄, filtered, and concentrated in a vacuum. Flash chromatography on silica gel (EtOAc/Cyclohexane 20/80) afforded **5** (yield 96%). Orange powder, mp: 233 – 235 °C. IR (film): 1570, 1500, 1244, 764 cm⁻¹. ¹H NMR (300 MHz, DMSO-*d*₆) δ 9.10 (s, 1H), 7.95 (d, *J* = 8.4 Hz, 1H), 7.67 (t, *J* = 7.6 Hz, 1H), 7.52 (s, 1H), 7.50 (s, 1H), 7.35 (t, *J* = 7.6 Hz, 1H), 6.86 (d, *J* = 8.4 Hz, 1H), 6.52 (s, 1H), 6.49 (d, *J* = 2.7 Hz, 1H), 3.74 (s, 3H), 3.41 (s, 3H). ¹³C NMR (75 MHz, DMSO-*d*₆) δ 153.9 (C), 149.0 (C), 147.3 (C), 145.2 (C), 143.2 (C), 133.5 (C), 130.1 (CH), 129.7 (CH), 126.8 (CH), 125.2 (CH), 122.4 (C), 118.0 (C), 114.5 (CH), 113.0 (CH), 111.5 (CH), 111.4 (CH), 55.7 (CH₃), 43.7 (CH₃). HRMS (ESI⁺) (M + H)⁺: *m/z* calcd for C₁₈H₁₆N₃O₂ 306.1237, found 306.1243.

4.3. General Procedure for the Synthesis of Compounds 6a-6e (Method A).

Compound **5** (1 equiv), anhydrous potassium carbonate (2 equiv), and the corresponding bromo acid ethyl esters (1.1 equiv) were dissolved in anhydrous DMF (1 mL/0.1 mmol). The reaction mixture was stirred at room temperature overnight. Water was added, and the mixture was extracted with ethyl acetate. The organic layer was dried with MgSO_4 , filtered, and concentrated in a vacuum. The crude was purified by column chromatography on silica gel.

4.3.1. Ethyl 2-(5-((2-cyanoquinolin-4-yl)(methyl)amino)-2-methoxyphenoxy) acetate (6a). Compound **6a** was prepared according to method A from **5** (0.46 mmol) and ethyl 2-bromoacetate (0.50 mmol). Purification by column chromatography on silica gel (EtOAc/cyclohexane, 0/10 to 3/7) afforded **6a** (yield 87%). Yellow solid, mp: 134 – 136 °C. IR (film): 1730, 1570, 1501, 1258, 1238, 1178, 1027, 734 cm^{-1} . ^1H NMR (300 MHz, CDCl_3) δ 8.09 (d, J = 8.5 Hz, 1H), 7.69 (td, J = 7.6, 6.8, 1.3 Hz, 1H), 7.60 (d, J = 8.6 Hz, 1H), 7.39 – 7.32 (m, 2H), 6.89 (d, J = 8.5 Hz, 1H), 6.72 (d, J = 2.5 Hz, 1H), 6.68 (q, J = 2.5 Hz, 1H), 4.64 (s, 2H), 4.21 (q, J = 7.1 Hz, 2H), 3.94 (s, 3H), 3.52 (s, 3H), 1.29 (t, J = 7.1 Hz, 3H). ^{13}C NMR (75 MHz, CDCl_3) δ 168.6 (C), 154.4 (C), 149.9 (C), 148.3 (C), 147.5 (C), 143.1 (C), 134.3 (C), 130.5 (CH), 130.2 (CH), 127.2 (CH), 125.3 (CH), 123.1 (C), 118.1 (C), 117.6 (CH), 113.1 (CH), 111.9 (CH), 111.4 (CH), 66.8 (CH_2), 61.4 (CH_2), 56.3 (CH_3), 43.8 (CH_3), 14.3 (CH_3). HRMS (ESI⁺) ($\text{M} + \text{H}$)⁺: m/z calcd for $\text{C}_{22}\text{H}_{22}\text{N}_3\text{O}_4$ 392.1610, found 392.1608.

4.3.2. Ethyl 4-(5-((2-cyanoquinolin-4-yl)(methyl)amino)-2-methoxyphenoxy)butanoate (6b). Compound **6b** was prepared according to method A from **5** (0.42 mmol) and ethyl 4-bromobutanoate (0.46 mmol). Purification by column chromatography on silica gel (EtOAc/cyclohexane, 0/10 to 3/7) afforded **6b** (yield 90%). Yellow solid, mp: 130 – 132 °C. IR (film): 1753, 1568, 1498, 1432, 1238, 1196, 1026, 765 cm^{-1} . ^1H NMR (300 MHz, CDCl_3) δ 8.01 (d, J = 8.5 Hz, 1H), 7.67 – 7.48 (m, 2H), 7.31 – 7.23 (m, 1H), 7.18 (s, 1H), 6.78 (d, J = 8.6 Hz, 1H), 6.63 (d, J = 2.6 Hz, 1H), 6.57 (dd, J = 8.5, 2.6 Hz, 1H), 4.12 (q, J = 7.2 Hz, 2H), 3.91 (t, J = 6.4 Hz, 2H), 3.84 (s, 3H), 3.47 (s, 3H), 2.45 (t, J = 7.2 Hz, 2H), 2.04 (p, J = 7.1 Hz, 2H), 1.24 (t, J = 7.1 Hz, 3H). ^{13}C NMR (75 MHz, CDCl_3) δ 173.1 (CO), 154.5 (C), 149.9 (C), 149.4 (C), 147.4 (C), 143.4 (C), 134.3 (C), 130.5 (CH), 130.2 (CH), 127.1 (CH), 125.5 (CH), 123.1 (C), 118.2 (C), 116.3 (CH), 112.7 (CH), 111.5 (CH), 110.0 (CH), 68.2 (CH_2), 60.6 (CH_2), 56.3 (CH_3), 43.9 (CH_3), 30.7 (CH_2), 24.4 (CH_2), 14.4 (CH_3). HRMS (ESI⁺) ($\text{M} + \text{H}$)⁺: m/z calcd for $\text{C}_{24}\text{H}_{26}\text{N}_3\text{O}_4$ 420.1923, found 420.1920.

4.3.3. Ethyl 5-(5-((2-cyanoquinolin-4-yl)(methyl)amino)-2-methoxyphenoxy)pentanoate (6c). Compound **6c** was prepared according to method A from **5** (0.43 mmol) and ethyl 5-bromopentanoate (0.47 mmol). Purification by column chromatography on silica gel (EtOAc/cyclohexane, 0/10 to 3/7) afforded **6c** (yield 85%). Yellow solid, mp: 94 – 96 °C. IR (film): 1727, 1568, 1499, 1235, 1175, 1021, 764 cm^{-1} . ^1H NMR (300 MHz, CDCl_3) δ 8.01 (d, J = 8.5 Hz, 1H), 7.61 (m, 1H), 7.55 (d, J = 8.7 Hz, 1H), 7.27 (m, 1H), 7.18 (s, 1H), 6.80 (d, J = 8.4 Hz, 1H), 6.65 – 6.55 (m, 2H), 4.12 (q, J = 7.1 Hz, 2H), 3.87 (m, 5H), 3.48 (s, 3H), 2.34 (t, J = 7.1 Hz, 2H), 1.84 – 1.74 (m, 4H), 1.25 (t, J = 7.1 Hz, 3H). ^{13}C NMR (75 MHz, CDCl_3) δ 173.3 (CO), 154.3 (C), 149.8 (C), 149.4 (C), 147.3 (C), 143.2 (C), 134.2 (C), 130.4 (CH), 130.0 (CH), 126.9 (CH), 125.4 (CH), 122.9 (C), 118.1 (C), 116.2 (CH), 112.6 (CH), 111.4 (CH), 109.8 (CH), 68.7 (CH_2), 60.3 (CH_2), 56.3 (CH_3), 43.8 (CH_3), 33.9 (CH_2), 28.5 (CH_2), 21.5 (CH_2), 14.3 (CH_3). HRMS (ESI⁺) ($\text{M} + \text{H}$)⁺: m/z calcd for $\text{C}_{25}\text{H}_{28}\text{N}_3\text{O}_4$ 434.2080, found 434.2083.

4.3.4. Ethyl 6-(5-((2-cyanoquinolin-4-yl)(methyl)amino)-2-methoxyphenoxy)hexanoate (6d). Compound **6d** was prepared according to method A from **5** (0.43 mmol) and ethyl 6-bromohexanoate (0.47 mmol). Purification by column chromatography on silica gel (EtOAc/cyclohexane, 0/10 to 3/7) afforded **6d** (yield 96%). Yellow solid, mp: 78 – 80 °C. IR (film): 2938, 1729, 1569, 1500, 1237, 1027, 767 cm^{-1} . ^1H NMR (300 MHz, CDCl_3) δ 8.00 (d, J = 8.5 Hz, 1H),

7.64 – 7.57 (m, 1H), 7.55 (d, J = 8.7 Hz, 1H), 7.31 – 7.22 (m, 1H), 7.19 (s, 1H), 6.81 (d, J = 8.4 Hz, 1H), 6.65 – 6.55 (m, 2H), 4.13 (q, J = 7.2 Hz, 2H), 3.87 (m, 5H), 3.49 (s, 3H), 2.31 (t, J = 7.2 Hz, 2H), 1.77 (q, J = 7.1 Hz, 2H), 1.66 (q, J = 7.7 Hz, 2H), 1.48 (m, 2H), 1.26 (t, J = 7.1 Hz, 3H). ^{13}C NMR (75 MHz, CDCl_3) δ 173.4 (CO), 154.3 (C), 149.7 (C), 149.4 (C), 147.2 (C), 143.1 (C), 134.1 (C), 130.3 (CH), 129.9 (CH), 126.8 (CH), 125.4 (CH), 122.8 (C), 118.1 (C), 116.1 (CH), 112.5 (CH), 111.2 (CH), 109.7 (CH), 68.9 (CH_2), 60.2 (CH_2), 56.2 (CH_3), 43.7 (CH_3), 34.1 (CH_2), 28.7 (CH_2), 25.5 (CH_2), 24.6 (CH_2), 14.2 (CH_3). HRMS (ESI⁺) ($\text{M} + \text{H}$)⁺: m/z calcd for $\text{C}_{26}\text{H}_{30}\text{N}_3\text{O}_4$ 448.2236, found 448.2240.

4.3.4. Ethyl 7-(5-((2-cyanoquinolin-4-yl)(methyl)amino)-2-methoxyphenoxy)heptanoate (6e). Compound **6e** was prepared according to method A from **5** (0.43 mmol) and ethyl 7-bromoheptanoate (0.47 mmol). Purification by column chromatography on silica gel (EtOAc/cyclohexane, 0/10 to 3/7) afforded **6e** (yield 86%). Orange oil. IR (film): 2938, 1790, 1570, 1501, 1238, 1024, 767 cm^{-1} . ^1H NMR (300 MHz, CDCl_3) δ 8.00 (d, J = 8.5 Hz, 1H), 7.64 – 7.58 (m, 1H), 7.56 (d, J = 9.7 Hz, 1H), 7.31 – 7.23 (m, 1H), 7.19 (s, 1H), 6.81 (d, J = 8.5 Hz, 1H), 6.66 – 6.56 (m, 2H), 4.14 (q, J = 7.1 Hz, 2H), 3.87 (m, 5H), 3.49 (s, 3H), 2.30 (t, J = 7.4 Hz, 2H), 1.75 (q, J = 6.7 Hz, 2H), 1.64 (q, J = 7.4 Hz, 2H), 1.44 – 1.32 (m, 4H), 1.26 (t, J = 7.4 Hz, 3H). ^{13}C NMR (75 MHz, CDCl_3) δ 173.5 (CO), 154.2 (C), 149.7 (C), 149.4 (C), 147.2 (C), 143.1 (C), 134.0 (C), 130.2 (CH), 129.9 (CH), 126.7 (CH), 125.3 (CH), 122.8 (C), 118.0 (C), 116.0 (CH), 112.5 (CH), 111.1 (CH), 109.7 (CH), 69.0 (CH_2), 60.1 (CH_2), 56.2 (CH_3), 43.7 (CH_3), 34.1 (CH_2), 28.7 (CH_2), 25.5 (CH_2), 24.7 (CH_2), 14.2 (CH_3). HRMS (ESI⁺) ($\text{M} + \text{H}$)⁺: m/z calcd for $\text{C}_{27}\text{H}_{32}\text{N}_3\text{O}_4$ 462.2393, found 462.2397.

4.4. General Procedure for the Synthesis of Compounds 7a-7e (Method B). **6a-6e** (1 equiv) were dissolved in a mixture of water, and THF (1:2) and 1M aqueous lithium hydroxide (1 equiv) was added. The mixture was stirred at room temperature for 4 h. Then, THF was removed by evaporation, and the pH value was adjusted to 4-5. The mixture was extracted with ethyl acetate. The organic layer was dried with MgSO_4 , filtered, and concentrated in a vacuum. The crude was purified by column chromatography on silica gel.

4.4.1. 2-(5-((2-cyanoquinolin-4-yl)(methyl)amino)-2-methoxyphenoxy)acetic acid (7a). Compound **7a** was prepared according to method B from **6a** (0.35 mmol) and 1N lithium hydroxide solution (0.35 mmol). Purification by column chromatography on silica gel (DCM/MeOH, 97/3) afforded **7a** (yield 85%). Yellow solid, mp: 215 – 217 °C. IR (film): 1709, 1570, 1502, 1238, 1024, 765 cm^{-1} . ^1H NMR (300 MHz, $\text{DMSO}-d_6$) δ 7.94 (d, J = 8.5 Hz, 1H), 7.71 – 7.62 (m, 1H), 7.50 (s, 1H), 7.48 (d, J = 8.7 Hz, 1H), 7.38 – 7.28 (m, 1H), 6.87 (d, J = 2.5 Hz, 1H), 6.84 (d, J = 8.7 Hz, 1H), 6.47 (dd, J = 8.7, 2.5 Hz, 1H), 4.58 (s, 2H), 3.74 (s, 3H), 3.42 (s, 3H). ^{13}C NMR (75 MHz, $\text{DMSO}-d_6$) δ 170.0 (CO), 153.9 (C), 149.0 (C), 148.1 (C), 146.4 (C), 142.9 (C), 133.5 (C), 130.0 (CH), 129.7 (CH), 126.8 (CH), 125.1 (CH), 122.3 (C), 118.0 (C), 116.3 (CH), 112.7 (CH), 111.4 (CH), 110.3 (CH), 65.5 (CH_2), 55.7 (CH_3), 43.5 (CH_3). HRMS (ESI⁺) ($\text{M} + \text{H}$)⁺: m/z calcd for $\text{C}_{20}\text{H}_{18}\text{N}_3\text{O}_4$ 364.1297, found 364.1307.

4.4.2. 4-(5-((2-cyanoquinolin-4-yl)(methyl)amino)-2-methoxyphenoxy) butanoic acid (7b). Compound **7b** was prepared according to method B from **6b** (0.38 mmol) and 1N lithium hydroxide solution (0.38 mmol). Purification by column chromatography on silica gel (DCM/MeOH, 97/3) afforded **7b** (yield 85%). Yellow solid, mp: 161 – 163 °C. IR (film): 3379, 1732, 1570, 1502, 1239, 1027, 766 cm^{-1} . ^1H NMR (300 MHz, CDCl_3) δ 8.01 (d, J = 8.2 Hz, 1H), 7.63 – 7.55 (m, 1H), 7.52 (d, J = 8.7 Hz, 1H), 7.29 – 7.21 (m, 1H), 7.18 (s, 1H), 6.79 (d, J = 8.4 Hz, 1H), 6.66 – 6.55 (m, 2H), 3.93 (t, J = 6.7 Hz, 2H), 3.84 (s, 3H), 3.47 (s, 3H), 2.52 (t, J = 6.7 Hz, 2H), 2.02 (p, J = 6.7 Hz, 2H). ^{13}C

NMR (75 MHz, CDCl₃) δ 177.7 (CO), 154.5 (C), 149.8 (C), 149.2 (C), 147.4 (C), 143.3 (C), 134.2 (C), 130.3 (CH), 130.2 (CH), 127.0 (CH), 125.5 (CH), 123.0 (C), 118.1 (C), 116.4 (CH), 112.7 (CH), 111.6 (CH), 110.1 (CH), 68.0 (CH₂), 56.3 (CH₃), 43.9 (CH₃), 30.3 (CH₂), 24.1 (CH₂). HRMS (ESI⁺) (M + H)⁺: m/z calcd for C₂₂H₂₂N₃O₄ 392.1610, found 392.1609.

4.4.3. 5-(5-((2-cyanoquinolin-4-yl)(methyl)amino)-2-methoxyphenoxy) pentanoic acid (**7c**). Compound **7c** was prepared according to method B from **6c** (0.32 mmol) and 1N lithium hydroxide solution (0.32 mmol). Purification by column chromatography on silica gel (DCM/MeOH, 97/3) afforded **7c** (yield 89%). Yellow solid, mp: 120 – 122 °C. IR (film): 1708, 1570, 1502, 1238, 1024, 767 cm⁻¹. ¹H NMR (300 MHz, CDCl₃) δ 8.03 (d, J = 7.9 Hz, 1H), 7.67 – 7.55 (m, 1H), 7.54 (d, J = 8.7 Hz, 1H), 7.33 – 7.20 (m, 1H), 7.18 (s, 1H), 6.81 (d, J = 8.3 Hz, 1H), 6.66 – 6.55 (m, 2H), 3.90 (m, 2H), 3.86 (s, 3H), 3.49 (s, 3H), 2.48 – 2.37 (m, 2H), 1.85 – 1.77 (m, 4H). ¹³C NMR (75 MHz, CDCl₃) δ 178.5 (CO), 154.4 (C), 149.6 (C), 149.4 (C), 147.3 (C), 143.1 (C), 134.0 (C), 130.1 (CH), 130.1 (CH), 126.9 (CH), 125.4 (CH), 122.8 (C), 117.9 (C), 116.3 (CH), 112.6 (CH), 111.2 (CH), 109.9 (CH), 68.7 (CH₂), 56.3 (CH₃), 43.8 (CH₃), 33.6 (CH₂), 28.3 (CH₂), 21.4 (CH₂). HRMS (ESI⁺) (M + H)⁺: m/z calcd for C₂₃H₂₄N₃O₄ 406.1767, found 406.1765.

4.4.4. 6-(5-((2-cyanoquinolin-4-yl)(methyl)amino)-2-methoxyphenoxy) hexanoic acid (**7d**). Compound **7d** was prepared according to method B from **6d** (0.41 mmol) and 1N lithium hydroxide solution (0.41 mmol). Purification by column chromatography on silica gel (DCM/MeOH, 97/3) afforded **7d** (yield 70%). Orange solid, mp: 192 – 194 °C. IR (film): 3341, 1709, 1570, 1502, 1238, 1022, 766 cm⁻¹. ¹H NMR (300 MHz, DMSO-*d*₆) δ 7.94 (d, J = 8.5 Hz, 1H), 7.71 – 7.61 (m, 1H), 7.52 (s, 1H), 7.47 (d, J = 8.7 Hz, 1H), 7.38 – 7.28 (m, 1H), 6.88 – 6.80 (m, 2H), 6.51 (dd, J = 8.5, 2.5 Hz, 1H), 3.84 (t, J = 6.4 Hz, 2H), 3.72 (s, 3H), 3.45 (s, 3H), 2.19 (t, J = 7.3 Hz, 2H), 1.71 – 1.52 (m, 2H), 1.54 – 1.42 (m, 2H), 1.41 – 1.28 (m, 2H). ¹³C NMR (75 MHz, DMSO-*d*₆) δ 174.3 (CO), 153.9 (C), 149.0 (C), 148.9 (C), 146.6 (C), 143.1 (C), 133.5 (C), 130.0 (CH), 129.7 (CH), 126.7 (CH), 125.1 (CH), 122.2 (C), 118.0 (C), 115.8 (CH), 112.6 (CH), 111.4 (CH), 109.9 (CH), 68.1 (CH₂), 55.7 (CH₃), 43.6 (CH₃), 33.6 (CH₂), 28.2 (CH₂), 25.0 (CH₂), 24.2 (CH₂). HRMS (ESI⁺) (M + H)⁺: m/z calcd for C₂₄H₂₆N₃O₄ 420.1923, found 420.1920.

4.4.5. 6-(5-((2-cyanoquinolin-4-yl)(methyl)amino)-2-methoxyphenoxy) hexanoic acid (**7e**). Compound **7e** was prepared according to method B from **6e** (0.41 mmol) and 1N lithium hydroxide solution (0.41 mmol). Purification by column chromatography on silica gel (DCM/MeOH, 97/3) afforded **7e** (yield 61%). Orange solid, mp: 125 – 127 °C. IR (film): 1707, 1570, 1502, 1238, 1023, 767 cm⁻¹. ¹H NMR (300 MHz, CDCl₃) δ 8.03 (d, J = 7.9 Hz, 1H), 7.66 – 7.58 (m, 1H), 7.55 (d, J = 8.7 Hz, 1H), 7.31 – 7.23 (m, 1H), 7.19 (s, 1H), 6.81 (d, J = 8.4 Hz, 1H), 6.60 (m, 2H), 3.86 (m, 5H), 3.49 (s, 3H), 2.37 (t, J = 7.4 Hz, 2H), 1.81 – 1.57 (m, 4H), 1.52 – 1.31 (m, 4H). ¹³C NMR (75 MHz, CDCl₃) δ 179.1 (CO), 154.4 (C), 149.7 (C), 149.5 (C), 147.3 (C), 143.1 (C), 134.0 (C), 130.1 (2CH), 126.9 (CH), 125.5 (CH), 122.8 (C), 118.0 (C), 116.1 (CH), 112.6 (CH), 111.2 (CH), 109.8 (CH), 69.1 (CH₂), 56.3 (CH₃), 43.8 (CH₃), 34.0 (CH₂), 28.8 (2CH₂), 25.6 (CH₂), 24.6 (CH₂). HRMS (ESI⁺) (M + H)⁺: m/z calcd for C₂₅H₂₈N₃O₄ 434.2080, found 434.2077.

4.5. General Procedure for the Synthesis of Compounds **8a-8e** (Method C). **7a-7e** (1 equiv) and NH₂OTHP (1.1 equiv) were dissolved in dry DCM at 0 °C. HOBt (1.5 equiv) was added in one portion, followed by EDCI (2.0 equiv) and TEA (2 equiv). The reaction mixture was stirred at room temperature for 2 h, then washed with water for 3 times. The crude was purified by column chromatography on silica gel.

4.5.1. 2-(5-((2-cyanoquinolin-4-yl)(methyl)amino)-2-methoxyphenoxy)-N-((tetrahydro-2H-pyran-2-yl)oxy)acetamide (**8a**). Compound **8a** was prepared according to method C from **7a** (0.34 mmol) and NH₂OTHP (0.37 mmol), HOBt (0.50 mmol), EDCI (0.68 mmol) and TEA (0.68 mmol). Purification by column chromatography on silica gel (EtOAc/cyclohexane, 6/4) afforded **8a** (yield 72%). Yellow solid, mp: 183 – 185 °C. IR (film): 2941, 1570, 1501, 1239, 1023 cm⁻¹. ¹H NMR (300 MHz, CDCl₃) δ 9.63 (s, 1H), 8.04 (d, *J* = 8.6 Hz, 1H), 7.67 – 7.59 (m, 1H), 7.53 (d, *J* = 8.6 Hz, 1H), 7.34 – 7.27 (m, 1H), 7.21 (s, 1H), 6.81 (d, *J* = 8.7 Hz, 1H), 6.68 (d, *J* = 2.5 Hz, 1H), 6.63 (dd, *J* = 8.7, 2.5 Hz, 1H), 4.96 (s, 1H), 4.51 (s, 2H), 3.99 (t, *J* = 10.2 Hz, 1H), 3.86 (s, 3H), 3.63 (d, *J* = 12.2 Hz, 1H), 3.45 (s, 3H), 1.92 – 1.76 (m, 3H), 1.71 – 1.54 (m, 3H). ¹³C NMR (75 MHz, CDCl₃) δ 165.0 (CO), 154.4 (C), 150.0 (C), 148.2 (C), 147.4 (C), 143.5 (C), 134.4 (C), 130.7 (CH), 130.4 (CH), 127.4 (CH), 125.1 (CH), 123.3 (C), 118.3 (CH), 118.0 (C), 113.1 (CH), 112.6 (CH), 102.8 (2CH), 70.3 (CH₂), 62.6 (CH₂), 56.3 (CH₃), 43.6 (CH₃), 28.1 (CH₂), 25.1 (CH₂), 18.6 (CH₂). HRMS (ESI⁺) (M + H)⁺: *m/z* calcd for C₂₅H₂₇N₄O₅ 463.1981, found 463.1978.

4.5.2. 4-(5-((2-cyanoquinolin-4-yl)(methyl)amino)-2-methoxyphenoxy)-N-((tetrahydro-2H-pyran-2-yl)oxy)butanamide (**8b**). Compound **8b** was prepared according to method C from **7b** (0.26 mmol) and NH₂OTHP (0.29 mmol), HOBt (0.39 mmol), EDCI (0.52 mmol) and TEA (0.52 mmol). Purification by column chromatography on silica gel (EtOAc/cyclohexane, 0/10 to 3/7) afforded **8b** (yield 85%). Orange solid, mp: 79 – 81 °C. IR (film): 2947, 1695, 1570, 1500, 1239, 1024, 767 cm⁻¹. ¹H NMR (300 MHz, CDCl₃) δ 8.79 (s, 1H), 8.01 (d, *J* = 8.5 Hz, 1H), 7.66 – 7.57 (m, 1H), 7.54 (d, *J* = 8.7 Hz, 1H), 7.31 – 7.22 (m, 1H), 7.18 (s, 1H), 6.77 (d, *J* = 8.6 Hz, 1H), 6.66 (d, *J* = 2.4 Hz, 1H), 6.55 (dd, *J* = 8.6, 2.4 Hz, 1H), 4.91 (s, 1H), 3.94 (t, *J* = 6.1 Hz, 2H), 3.85 (s, 3H), 3.56 (d, *J* = 11.5 Hz, 1H), 3.46 (s, 3H), 2.34 (s, 1H), 2.11 – 2.05 (m, 2H), 1.87 – 1.72 (m, 4H), 1.66 – 1.51 (m, 4H). ¹³C NMR (75 MHz, CDCl₃) δ 170.0 (CO), 154.3 (C), 149.7 (C), 149.0 (C), 147.1 (C), 143.2 (C), 134.1 (C), 130.3 (CH), 130.0 (CH), 126.9 (CH), 125.2 (CH), 122.9 (C), 118.0 (C), 116.3 (CH), 112.4 (CH), 111.5 (CH), 110.1 (CH), 102.4 (CH), 68.0 (2CH₂), 62.5 (CH₂), 56.1 (CH₃), 43.6 (CH₃), 28.0 (CH₂), 24.9 (2CH₂), 18.6 (CH₂). HRMS (ESI⁺) (M + H)⁺: *m/z* calcd for C₂₇H₃₁N₄O₅ 491.2294, found 491.2293.

4.5.3. 5-(5-((2-cyanoquinolin-4-yl)(methyl)amino)-2-methoxy phenoxy)-N-((tetrahydro-2H-pyran-2-yl)oxy)pentanamide (**8c**). Compound **8c** was prepared according to method C from **7c** (0.31 mmol) and NH₂OTHP (0.34 mmol), HOBt (0.47 mmol), EDCI (0.62 mmol) and TEA (0.62 mmol). Purification by column chromatography on silica gel (DCM/MeOH, 97/3) afforded **8c** (yield 71%). Orange solid, mp: 70 – 72 °C. IR (film): 2948, 1663, 1569, 1500, 1236, 1020, 765, 732 cm⁻¹. ¹H NMR (300 MHz, CDCl₃) δ 9.43 (s, 1H), 8.01 (d, *J* = 8.5 Hz, 1H), 7.69 – 7.49 (m, 2H), 7.37 – 7.23 (m, 1H), 7.19 (s, 1H), 6.80 (d, *J* = 8.5 Hz, 1H), 6.67 – 6.50 (m, 2H), 5.01 (s, 1H), 4.04 – 3.84 (m, 5H), 3.65 – 3.55 (m, 1H), 3.49 (s, 3H), 2.30 (s, 2H), 1.91 – 1.54 (m, 11H). ¹³C NMR (75 MHz, CDCl₃) δ 170.6 (CO), 154.4 (C), 149.8 (C), 149.3 (C), 146.7 (C), 143.3 (C), 134.2 (C), 130.4 (CH), 130.1 (CH), 127.0 (CH), 125.4 (CH), 123.0 (C), 118.1 (C), 115.9 (CH), 112.1 (CH), 111.6 (CH), 108.8 (CH), 102.4 (CH), 69.7 (CH₂), 62.5 (2CH₂), 56.1 (CH₃), 43.8 (CH₃), 28.2 (2CH₂), 25.1 (2CH₂), 18.7 (CH₂). HRMS (ESI⁺) (M + H)⁺: *m/z* calcd for C₂₈H₃₃N₄O₅ 505.2451, found 505.2448.

4.5.4. 6-(5-((2-cyanoquinolin-4-yl)(methyl)amino)-2-methoxy phenoxy)-N-((tetrahydro-2H-pyran-2-yl)oxy)hexanamide (**8d**). Compound **8d** was prepared according to method C from **7d** (0.19 mmol) and NH₂OTHP (0.21 mmol), HOBt (0.29 mmol), EDCI (0.38 mmol) and TEA (0.38 mmol). Purification by column chromatography on silica gel (DCM/MeOH, 97/3) afforded **8d** (yield 73%). Orange solid, mp: 74 – 76 °C. IR (film): 2944, 1662, 1570,

1501, 1238, 1022, 767 cm^{-1} . ^1H NMR (300 MHz, CDCl_3) δ 8.73 (s, 1H), 8.02 (d, J = 8.5 Hz, 1H), 7.68 – 7.57 (m, 1H), 7.54 (d, J = 8.7 Hz, 1H), 7.32 – 7.22 (m, 1H), 7.19 (s, 1H), 6.79 (d, J = 9.2 Hz, 1H), 6.62 – 6.54 (m, 2H), 4.94 (s, 1H), 3.98 – 3.80 (m, 5H), 3.68 – 3.54 (m, 1H), 3.48 (s, 3H), 2.26 – 1.36 (m, 15H). ^{13}C NMR (75 MHz, CDCl_3) δ 154.4 (C), 149.8 (C), 149.4 (C), 147.2 (C), 143.2 (2C), 134.2 (C), 130.1 (CH), 130.2 (CH), 127.0 (CH), 125.4 (CH), 123.0 (C), 118.1 (C), 116.1 (CH), 112.6 (CH), 111.4 (CH), 109.7 (CH), 102.6 (CH), 68.9 (2CH₂), 62.6 (CH₂), 56.3 (CH₃), 43.8 (CH₃), 28.7 (CH₂), 28.1 (CH₂), 25.6 (CH₂), 25.1 (2CH₂), 18.7 (CH₂). HRMS (ESI⁺) ($M + H$)⁺: m/z calcd for $\text{C}_{29}\text{H}_{35}\text{N}_4\text{O}_5$ 519.2607, found 519.2608.

4.5.5 7-(5-((2-cyanoquinolin-4-yl)(methyl)amino)-2-methoxy phenoxy)-*N*-((tetrahydro-2H-pyran-2-yl)oxy)heptanamide (**8e**). Compound **8e** was prepared according to method C from **7e** (0.18 mmol) and NH_2OTHP (0.20 mmol), HOBT (0.27 mmol), EDCI (0.36 mmol) and TEA (0.36 mmol). Purification by column chromatography on silica gel (DCM/MeOH, 97/3) afforded **8e** (yield 79%). Orange solid, mp: 67 – 69 °C. IR (film): 2940, 1662, 1570, 1501, 1238, 1022, 767 cm^{-1} . ^1H NMR (300 MHz, CDCl_3) δ 8.82 (s, 1H), 8.01 (d, J = 8.5 Hz, 1H), 7.59 (dd, J = 16.8, 8.1 Hz, 2H), 7.33 – 7.21 (m, 1H), 7.18 (s, 1H), 6.80 (d, J = 9.0 Hz, 1H), 6.64 – 6.53 (m, 2H), 4.95 (s, 1H), 4.03 – 3.78 (m, 5H), 3.70 – 3.55 (m, 1H), 3.48 (s, 3H), 2.13 (s, 2H), 1.88 – 1.32 (m, 15H). ^{13}C NMR (75 MHz, CDCl_3) δ 154.5 (C), 149.7 (C), 149.5 (C), 147.3 (C), 143.2 (2C), 134.1 (C), 130.3 (CH), 130.2 (CH), 127.0 (CH), 125.5 (CH), 122.9 (C), 118.1 (C), 116.1 (CH), 112.6 (CH), 111.4 (CH), 109.7 (CH), 102.6 (CH), 69.0 (2CH₂), 62.7 (CH₂), 56.3 (CH₃), 43.9 (CH₃), 28.8 (2CH₂), 28.2 (CH₂), 25.6 (CH₂), 25.1 (2CH₂), 18.7 (CH₂). HRMS (ESI⁺) ($M + H$)⁺: m/z calcd for $\text{C}_{30}\text{H}_{37}\text{N}_4\text{O}_5$ 533.2764, found 533.2760.

4.6. General Procedure for the Synthesis of Compounds **9a-9e** (Method D). **8a-8e** (1 equiv) were dissolved in a mixture of dioxane and methanol (1:1). 4N HCl in dioxane solution (1.2 equiv) was added, and the mixture was stirred for 1 h. The solvents were removed by evaporation. The crude was purified by preparative HPLC.

4.6.1. 2-(5-((2-cyanoquinolin-4-yl)(methyl)amino)-2-methoxyphenoxy)-*N*-hydroxyacetamide (**9a**). Compound **9a** was prepared according to method D from **8a** (0.13 mmol) and HCl 4N in dioxane (0.16 mmol). Purification by preparative HPLC (ACN/Water, 1/9 to 10/0 in 10 min) afforded **9a** (yield 44%). Yellow solid, mp: 157 – 159 °C. IR (film): 1652, 1569, 1501, 1237, 1022, 766 cm^{-1} . ^1H NMR (300 MHz, CDCl_3) δ 9.63 (s, 1H), 8.03 (d, J = 8.4 Hz, 1H), 7.62 (t, J = 7.4 Hz, 1H), 7.52 (d, J = 8.5 Hz, 1H), 7.34 – 7.27 (m, 1H), 7.21 (s, 1H), 6.82 (d, J = 8.4 Hz, 1H), 6.69 – 6.66 (m, 1H), 6.64 (s, 1H), 4.49 (s, 2H), 3.86 (s, 3H), 3.45 (s, 3H). ^{13}C NMR (75 MHz, CDCl_3) δ 165.7 (CO), 154.4 (C), 149.9 (C), 147.9 (C), 147.2 (C), 143.5 (C), 134.3 (C), 130.6 (CH), 130.4 (CH), 127.5 (CH), 125.1 (CH), 123.3 (C), 118.2 (CH), 118.0 (C), 113.1 (CH), 112.6 (CH), 112.1 (CH), 69.4 (CH₂), 56.3 (CH₃), 43.6 (CH₃). HRMS (ESI⁺) ($M + H$)⁺: m/z calcd for $\text{C}_{20}\text{H}_{19}\text{N}_4\text{O}_4$ 379.1406, found 379.1405.

4.6.2. 4-(5-((2-cyanoquinolin-4-yl)(methyl)amino)-2-methoxyphenoxy)-*N*-hydroxybutanamide (**9b**). Compound **9b** was prepared according to method D from **8b** (0.12 mmol) and HCl 4N in dioxane (0.15 mmol). Purification by preparative HPLC (ACN/Water, 1/9 to 10/0 in 10 min) afforded **9b** (yield 54%). Yellow solid, mp: 132 – 134 °C. IR (film): 1672, 1569, 1498, 1237, 1023, 765, 731 cm^{-1} . ^1H NMR (300 MHz, CDCl_3) δ 9.59 (s, 1H), 8.00 (d, J = 8.0 Hz, 1H), 7.60 (t, J = 6.7 Hz, 1H), 7.52 (d, J = 8.5 Hz, 1H), 7.27 (t, J = 7.4 Hz, 1H), 7.18 (s, 1H), 6.79 (d, J = 8.5 Hz, 1H), 6.65 – 6.52 (m, 2H), 3.87 (s, 5H), 3.46 (s, 3H), 2.39 (s, 2H), 2.03 (s, 2H). ^{13}C NMR (75 MHz, CDCl_3) δ 170.8 (CO), 154.5 (C), 149.9 (C), 148.8 (C), 146.8 (C), 143.4 (C), 134.3 (C), 130.5 (CH), 130.3 (CH), 127.2 (CH), 125.4 (CH),

123.1 (C), 118.1 (C), 116.5 (CH), 112.4 (CH), 111.9 (CH), 109.5 (CH), 68.4 (CH₂), 56.3 (CH₃), 43.8 (CH₃), 30.4 (CH₂), 24.5 (CH₂). HRMS (ESI⁺) (M + H)⁺: *m/z* calcd for C₂₂H₂₃N₄O₄ 407.1917, found 407.1720.

4.6.3. 5-(5-((2-cyanoquinolin-4-yl)(methyl)amino)-2-methoxyphenoxy)-N-hydroxypentanamide (**9c**). Compound **9c** was prepared according to method D from **8c** (0.21 mmol) and HCl 4N in dioxane (0.25 mmol). Purification by preparative HPLC afforded **9c** (yield 43%). Yellow solid, mp: 164 – 166 °C. IR (film): 1654, 1570, 1502, 1237, 1022, 767 cm⁻¹. ¹H NMR (300 MHz, DMSO-*d*₆) δ 10.33 (s, 1H), 8.66 (s, 1H), 7.94 (d, *J* = 8.4 Hz, 1H), 7.66 (t, *J* = 7.6 Hz, 1H), 7.52 (s, 1H), 7.48 (d, *J* = 8.4 Hz, 1H), 7.38 – 7.28 (m, 1H), 6.86 (d, *J* = 2.4 Hz, 1H), 6.82 (s, 1H), 6.49 (dd, *J* = 8.4, 2.4 Hz, 1H), 3.85 (t, *J* = 5.0 Hz, 2H), 3.73 (s, 3H), 3.45 (s, 3H), 1.99 (t, *J* = 5.5 Hz, 2H), 1.63 – 1.56 (m, 4H). ¹³C NMR (75 MHz, DMSO-*d*₆) δ 168.9 (CO), 153.9 (C), 149.0 (C), 148.9 (C), 146.5 (C), 143.1 (C), 133.5 (C), 130.0 (CH), 129.7 (CH), 126.8 (CH), 125.1 (CH), 122.2 (C), 118.1 (C), 115.9 (CH), 112.5 (CH), 111.4 (CH), 109.8 (CH), 67.9 (CH₂), 55.7 (CH₃), 43.6 (CH₃), 31.9 (CH₂), 28.1 (CH₂), 21.8 (CH₂). HRMS (ESI⁺) (M + H)⁺: *m/z* calcd for C₂₃H₂₅N₄O₄ 421.1876, found 421.1872.

4.6.4. 6-(5-((2-cyanoquinolin-4-yl)(methyl)amino)-2-methoxyphenoxy)-N-hydroxyhexanamide (**9d**). Compound **9d** was prepared according to method D from **8d** (0.11 mmol) and HCl 4N in dioxane (0.13 mmol). Purification by preparative HPLC (ACN/Water, 1/9 to 10/0 in 10 min) afforded **9d** (yield 67%). Yellow solid, mp: 139 – 141 °C. IR (film): 3250, 1647, 1569, 1501, 1236, 1021, 766 cm⁻¹. ¹H NMR (300 MHz, DMSO-*d*₆) δ 10.31 (s, 1H), 8.66 (s, 1H), 7.94 (d, *J* = 8.4 Hz, 1H), 7.66 (t, *J* = 7.1 Hz, 1H), 7.52 (s, 1H), 7.47 (d, *J* = 8.6 Hz, 1H), 7.41 – 7.27 (m, 1H), 6.89 – 6.76 (m, 2H), 6.51 (dd, *J* = 8.6, 2.3 Hz, 1H), 3.83 (t, *J* = 6.3 Hz, 2H), 3.72 (s, 3H), 3.45 (s, 3H), 1.94 (t, *J* = 7.2 Hz, 2H), 1.65 – 1.44 (m, 4H), 1.37 – 1.25 (m, 2H). ¹³C NMR (75 MHz, DMSO-*d*₆) δ 168.9 (CO), 153.9 (C), 149.0 (C), 148.9 (C), 146.5 (C), 143.1 (C), 133.5 (C), 130.0 (CH), 129.7 (CH), 126.7 (CH), 125.1 (CH), 122.2 (C), 118.1 (C), 115.8 (CH), 112.6 (CH), 111.4 (CH), 109.8 (CH), 68.2 (CH₂), 55.7 (CH₃), 43.6 (CH₃), 32.2 (CH₂), 28.3 (CH₂), 25.1 (CH₂), 24.8 (CH₂). HRMS (ESI⁺) (M + H)⁺: *m/z* calcd for C₂₄H₂₇N₄O₄ 435.2032, found 435.2030.

4.6.5. 7-(5-((2-cyanoquinolin-4-yl)(methyl)amino)-2-methoxyphenoxy)-N-hydroxyheptanamide (**9e**). Compound **9e** was prepared according to method D from **8e** (0.13 mmol) and HCl 4N in dioxane (0.16 mmol). Purification by preparative HPLC (ACN/Water, 1/9 to 10/0 in 10 min) afforded **9e** (yield 61%). Yellow solid, mp: 111 – 113 °C. IR (film): 1570, 1502, 1238, 1022 cm⁻¹. ¹H NMR (300 MHz, CDCl₃) δ 9.01 (s, 1H), 8.05 (d, *J* = 7.8 Hz, 1H), 7.68 – 7.60 (m, 1H), 7.56 (d, *J* = 8.3 Hz, 1H), 7.33 – 7.27 (m, 1H), 7.21 (s, 1H), 6.84 (d, *J* = 8.5 Hz, 1H), 6.66 (d, *J* = 8.5 Hz, 1H), 6.52 (s, 1H), 3.99 – 3.74 (m, 5H), 3.50 (s, 3H), 2.17 (s, 2H), 1.64 (s, 4H), 1.31 (s, 4H). ¹³C NMR (75 MHz, CDCl₃) δ 171.3 (CO), 154.6 (C), 149.8 (C), 149.3 (C), 147.2 (C), 143.2 (C), 134.1 (C), 130.3 (CH), 130.3 (CH), 127.1 (CH), 125.5 (CH), 123.0 (C), 118.1 (C), 116.0 (CH), 112.7 (CH), 111.5 (CH), 109.7 (CH), 68.9 (2CH₂), 56.4 (CH₃), 43.8 (CH₃), 28.6 (2CH₂), 25.4 (CH₂), 25.2 (CH₂). HRMS (ESI⁺) (M + H)⁺: *m/z* calcd for C₂₅H₂₉N₄O₄ 449.2189, found 449.2190.

4.7.1. 4-(3-iodo-4-methoxyphenyl)aminoquinoline-2-carbonitrile. A solution of 4-chloro-2-cyanoquinoline (500 mg, 2.65 mmol) in 1,4-dioxane (20 mL) was introduced in a dried sealed tube flushed with argon. Then 3-iodo-4-methoxyaniline (660 mg, 2.65 mmol) was added along with a concentrated HCl (30 μL). The reaction was stirred at 140 °C overnight. The completion was monitored by TLC (1/1 cyclohexane/ethyl acetate). The medium was diluted with a solution of NaOH (0.5 M) until pH = 7 – 8. Then it was extracted by ethyl acetate, three times. The organic phase was dried with MgSO₄ and evaporated under a vacuum. Flash chromatography on silica gel (100% cyclohexane

to 60/40 mixture of cyclohexane/ethyl acetate) afforded 4-(3-iodo-4-methoxyphenyl)amino)quinoline-2-carbonitrile (570 mg, yield 54%). White solid. ^1H NMR (300 MHz, MeOD) δ : 8.34 (d, J = 8.5 Hz, 1H), 7.96 (d, J = 8.6 Hz, 1H), 7.87 – 7.80 (m, 2H), 7.72 – 7.65 (m, 1H), 7.45 (dd, J = 8.6, 2.4 Hz, 1H), 7.12 (d, J = 8.8 Hz, 1H), 6.90 (s, 1H), 3.96 (s, 3H).

4.7.2. 4-((3-iodo-4-methoxyphenyl)(methyl)amino)quinoline-2-carbonitrile (10a). A solution of 4-(3-iodo-4-methoxyphenyl)amino)quinoline-2-carbonitrile (570 mg, 1.42 mmol) in 5.7 mL of dried DMF was introduced in a dried round bottom flask and flushed with argon. The solution was cooled down to 0°C. Sodium hydride (68 mg, 2.84 mmol) was added to the medium portion wise. After 30 min of stirring at 0°C, methyl iodide (177 μL , 2.84 mmol) was added. The medium was heated to room temperature and stirred overnight. The conversion of the reaction was checked by TLC (1/1 cyclohexane/ethyl acetate). Deionised water was added drop by drop on the medium cooled to 0 °C until no more gas formation could be observed. An orange precipitate appeared. The heterogeneous solution was extracted with ethyl acetate three times. The organic phase was dried with MgSO_4 and evaporated under vacuum. Flash chromatography on silica gel (100% cyclohexane to 50/50 mixture of cyclohexane/ethyl acetate) afforded 4-((3-iodo-4-methoxyphenyl)(methyl)amino)quinoline-2-carbonitrile (350 mg, yield 57%). Orange solid. mp: 175 – 180 °C. IR (film): 1571, 1562, 1482, 1430, 1279, 1109, 808, 766, 713, 603 cm^{-1} . ^1H NMR (300 MHz, CDCl_3) δ : 8.08 – 7.99 (m, 1H), 7.63 (ddd, J = 8.4, 6.8, 1.4 Hz, 1H), 7.59 – 7.50 (m, 2H), 7.37 – 7.27 (m, 1H), 7.21 (s, 1H), 6.91 (dd, J = 8.8, 2.7 Hz, 1H), 6.71 (d, J = 8.8 Hz, 1H), 3.84 (s, 3H), 3.44 (s, 3H). ^{13}C NMR (75 MHz, CDCl_3) δ : 155.6 (C), 154.3 (C), 149.9 (C), 144.1 (C), 134.3 (CH), 130.6 (CH), 130.4 (CH), 127.5 (CH), 125.2 (CH), 124.4 (2 CH), 123.2 (C), 118.0 (C), 112.5 (CH), 111.5 (CH), 86.7 (C), 56.8 (CH_3), 43.7 (CH_3). HRMS (ESI $^+$) ($\text{M} + \text{H}$) $^+$: m/z calcd for $\text{C}_{18}\text{H}_{15}\text{N}_3\text{OI}$ 416.0260, found 416.0267.

4.7.3. N-(3-iodo-4-methoxyphenyl)-N,2-dimethylquinolin-4-amine (10b). A solution of 4-chloro-2-methylquinoline (471 mg, 2.65 mmol, 1 eq) in 1,4-dioxane (20 mL) was introduced in a dried sealed tube flushed with argon. Then 3-iodo-4-methoxyaniline (660 mg, 2.65 mmol, 1 eq) was added along with a dozen drops of concentrated HCl. The reaction was stirred at 140 °C overnight. The completion was monitored by TLC (1/1 cyclohexane/ethyl acetate). The medium was diluted with a solution of NaOH (0.5 M) until pH = 7 – 8. Then, it was extracted by ethyl acetate three times. The organic phase was dried with MgSO_4 and evaporated under a vacuum. The crude product (535 mg, 1.37 mmol, 1 eq) was then dissolved in 5.5 mL of DMF and introduced in a dried round bottom flask. The solution was cooled to 0 °C, and sodium hydride (66 mg, 2.74 mmol, 2 eq) was added to the medium portion-wise. After 30 min of stirring at 0°C, methyl iodide (0.171 mL, 2.74 mmol, 2 eq) was added. The medium was allowed to stir at room temperature overnight. The conversion of the reaction was checked by TLC (9/1 ethyl acetate/methanol). Deionized water was added drop by drop on the medium cooled to 0°C. A precipitate appeared, and the product was extracted by ethyl acetate. The organic layers were dried with MgSO_4 and evaporated under a vacuum. The crude solid was then purified by flash column chromatography (100/0 to 93/7 dichloromethane/methanol), and the pure product was obtained as a solid (423 mg, 64%). m.p. 171-173 °C. IR (neat) 1731, 1588, 1562, 1486, 1280, 1244, 1047, 1014, 764, 671 cm^{-1} . ^1H NMR (300 MHz, CDCl_3) δ : 8.05 (d, J = 8.3 Hz, 1H), 7.61 (t, J = 9.3 Hz, 2H), 7.46 (d, J = 2.7 Hz, 1H), 7.25 (d, J = 7.8 Hz, 1H), 6.94 (s, 1H), 6.83 (dd, J = 8.8, 2.7 Hz, 1H), 6.70 (d, J = 8.8 Hz, 1H), 3.85 (s, 3H), 3.43 (s, 3H), 2.75 (s, 3H). ^{13}C NMR (75 MHz, CDCl_3) δ : 159.3 (C), 154.0 (C), 153.8 (C), 144.8 (C), 131.8 (CH), 129.4 (CH),

128.6 (CH), 124.8 (CH), 124.5 (CH), 122.0 (CH), 113.8 (C), 113.0 (CH), 111.4 (CH), 56.7 (OCH₃), 42.7 (CH₃), 25.2 (CH₃). HRMS (ESI⁺) for C₁₈H₁₈NO₂I [M + H]⁺: *m/z* calcd 405.0464, found 405.0461.

4.7.4. 4-((3-iodo-4-methoxyphenyl)(methyl)amino)quinazoline-2-carbonitrile (10c). In a dried sealed tube under argon, 4-chloroquinazoline-2-carbonitrile (103 mg, 0.53 mmol) was dissolved in dry 1,4-dioxane (5 mL/mmol). 3-iodo-4-methoxyaniline (135 mg, 0.53 mmol) and concentrated HCl (5 μ L) were added. The reaction was stirred at 140 °C overnight. The solvent was evaporated. The intermediate (80 mg, 0.12 mmol) was dissolved in DMF (1 mL) and cooled at 0 °C with an ice bath. NaH (16 mg, 0.4 mmol) was added by portion and the reaction was stirred at 0 °C for 30 min. Methyl iodide (23 μ L, 0.35 mmol) was added drop by drop and the reaction was stirred at 0 °C for 1 hour. Deionized water was added slowly, and the mixture was extracted with EtOAc. The organic layer was dried with MgSO₄, filtered, and concentrated in vacuum. Purification by column chromatography on silica gel (EtOAc/cyclohexane, 0/10 to 5/5) afforded **10c** (yield 61%). Colorless oil. ¹H NMR (300 MHz, DMSO-*d*₆) δ 7.93 – 7.71 (m, 3H), 7.47 – 7.27 (m, 2H), 7.08 (d, *J* = 8.8 Hz, 1H), 6.99 (d, *J* = 8.6 Hz, 1H), 3.87 (s, 3H), 3.54 (s, 3H). ¹³C NMR (75 MHz, DMSO-*d*₆) δ 160.9 (C), 157.1 (C), 150.4 (C), 140.5 (C), 139.4 (C), 136.3 (CH), 133.4 (CH), 128.4 (CH), 127.6 (CH), 127.5 (CH), 125.8 (CH), 116.8 (C), 116.2 (C), 112.2 (CH), 86.8 (C), 56.7 (OCH₃), 42.9 (CH₃). HRMS (ESI⁺) (M + H)⁺: *m/z* calcd for C₁₇H₁₄IN₄O 417.0212, found 417.0208.

4.7.5. 4-chloro-2-methylquinazoline.[58] A mixture of 2-methylquinazolin-4(3H)-one **1** (2 g, 12.5 mmol) in 41 mL of anhydrous toluene and DIPEA (3.4 mL, 19.98 mmol) in a 250 mL round-bottomed flask equipped with a condenser was refluxed for 1 h. To this warm solution was added phosphorus oxychloride (1.85 mL, 19.35 mmol), and the mixture was heated at 80 °C for 2 h and cooled to room temperature. The mixture was diluted with 100 mL of ethyl acetate, washed 40 mL of ice-cold water, 400 mL of NaHCO₃, 40 mL of water, 2 x 40 mL of HCl 1M, 40 mL of saturated NaCl. The organic layer was dried with MgSO₄, filtered, and concentrated in a vacuum. Flash chromatography on silica gel (EtOAc/Cyclohexane 1/9) afforded the desired compound (1.63 g, yield 72%). White powder. ¹H NMR (300 MHz, CDCl₃) δ 8.31 – 8.16 (m, 1H), 8.08 – 7.86 (m, 2H), 7.66 (ddd, *J* = 8.2, 6.6, and 1.6 Hz, 1H), 2.86 (s, 3H).

4.7.6. N-(3-iodo-4-methoxyphenyl)-2-methylquinazolin-4-amine. In a dried sealed tube under argon, 4-chloro-2-methylquinazoline **2** (178 mg, 1 mmol) was dissolved in anhydrous 1,4-dioxane (5 mL/mmol). 3-iodo-4-methoxyaniline (250 mg, 1 mmol) and concentrated HCl (10 μ L) were added. The reaction was stirred at 140 °C overnight. NaHCO₃ (2M) solution was added, followed by extraction with EtOAc. The organic layer was dried with MgSO₄, filtered, and concentrated in a vacuum. Flash chromatography on silica gel (EtOAc/Cyclohexane/TEA 49/50/1) afforded the desired compound (387 mg, yield 99%). White powder. ¹H NMR (300 MHz, CDCl₃) δ 8.17 (d, *J* = 2.5 Hz, 1H), 7.91 – 7.70 (m, 4H), 7.48 (t, *J* = 7.6 Hz, 1H), 6.87 (d, *J* = 8.9 Hz, 1H), 3.90 (s, 3H), 2.69 (s, 3H).

4.7.7. N-(3-iodo-4-methoxyphenyl)-N,2-dimethylquinazolin-4-amine (10d). N-(3-iodo-4-methoxyphenyl)-2-methylquinazolin-4-amine (1.17 g, 2.99 mmol) was dissolved in DMF (25 mL) and cooled at 0 °C with an ice bath. NaH (400 mg, 9.87 mmol) was added by portion and the reaction was stirred at 0 °C for 30 min. Methyl iodide (200 μ L, 8.97 mmol) was added drop by drop and the reaction was stirred at 0 °C for 1 hour. Deionized water was added slowly, and the mixture was extracted with EtOAc. The organic layer was dried with MgSO₄, filtered, and concentrated in vacuum. Chromatography on silica gel (EtOAc/Cyclohexane 0% to 50%) afforded **10d** (740 mg, yield 61%). White powder. ¹H NMR (300 MHz, CDCl₃) δ 7.82 (d, *J* = 8.3 Hz, 1H), 7.67 (d, *J* = 2.5 Hz, 1H), 7.57 (m, 1H), 7.13 – 6.96

(m, 3H), 6.77 (d, $J = 8.8$ Hz, 1H), 3.90 (s, 3H), 3.58 (s, 3H), 2.74 (s, 3H). ^{13}C NMR (75 MHz, CDCl_3) δ 137.0, 132.3, 127.1, 126.1, 124.6, 111.4, 56.8, 42.9, 26.3.

4.7.8. *N*-((tetrahydro-2H-pyran-2-yl)oxy)acrylamide. A solution of acrylic acid (532 μL , 7.8 mmol) and *O*-(tetrahydro-2H-pyran-2-yl)hydroxylamine (1 g, 8.5 mmol) in dried dichloromethane (20 mL) was introduced in a dried round bottom flask flushed with argon. The solution was cooled to 0 $^\circ\text{C}$, then DCC was added (1.76 g, 8.5 mmol) portion-wise. The reaction was stirred at room temperature overnight. A white precipitate appeared. The medium was filtered on celite and evaporated under a vacuum to give a white solid. The crude solid was purified by flash column chromatography (100% ethyl acetate) to give *N*-((tetrahydro-2H-pyran-2-yl)oxy)acrylamide as a colorless oil (855 mg, 64%). ^1H NMR (200 MHz, CDCl_3) δ : 9.41 (br s, 1H), 6.39 (d, $J = 16.9$ Hz, 1H), 6.30-6.05 (m, 1H), 5.68 (d, $J = 10.6$ Hz, 1H), 4.96 (s, 1H), 3.95 (t, $J = 8.2$ Hz, 1H), 3.80 – 3.52 (m, 1H), 1.79 (m, 3H), 1.57 (m, 3H).

4.7.9. (*E*)-3-(5-((2-cyanoquinolin-4-yl)(methyl)amino)-2-methoxyphenyl)-*N*-((tetrahydro-2H-pyran-2-yl)oxy)acrylamide (**11a**). A solution of 4-((3-iodo-4-methoxyphenyl)(methyl)amino)quinoline-2-carbonitrile (575 mg, 1.39 mmol) in dried DMF (19 mL) was introduced in a dried sealed tube flushed with argon. Then *N*-((tetrahydro-2H-pyran-2-yl)oxy)acrylamide (650 mg, 3.8 mmol), triethylamine (1.4 mL, 9.9 mmol), $\text{P}(o\text{-Tolyl})_3$ (138 mg, 0.45 mmol) and palladium acetate (115 mg, 0.51 mmol) were added to the medium. The reaction is stirred at 100 $^\circ\text{C}$ overnight. The completion of the reaction was monitored by TLC (1/1 cyclohexane/ethyl acetate). The medium was evaporated under vacuum and directly purified by flash column chromatography (100/0 cyclohexane/ethyl acetate to 50/50 then ethyl acetate/MeOH 95/5) to give (*E*)-3-(5-((2-cyanoquinolin-4-yl)(methyl)amino)-2-methoxyphenyl)-*N*-((tetrahydro-2H-pyran-2-yl)oxy)acrylamide as an orange solid (503 mg, 79%). ^1H NMR (300 MHz, CDCl_3) δ : 8.80 (s, 1H), 8.01 (d, $J = 8.6$ Hz, 1H), 7.84 (d, $J = 15.9$ Hz, 1H), 7.67 – 7.48 (m, 2H), 7.32 – 7.13 (m, 3H), 7.04-6.90 (m, 1H), 6.88 – 6.78 (m, 1H), 4.96 (s, 1H), 4.02-3.87 (m, 2H), 3.84 (s, 3H), 3.70 – 3.54 (m, 2H), 3.45 (s, 3H), 1.87-1.71 (m, 2H), 1.66-1.46 (m, 2H). ^{13}C NMR (75 MHz, CDCl_3) δ 155.7 (C), 154.4 (C), 149.8 (C), 143.0 (C), 134.1 (C), 130.5 (CH), 130.3 (CH), 127.3 (CH), 126.1 (CH), 125.3 (CH), 125.2 (C), 124.2 (CH), 123.0 (C), 118.7 (CH), 118.0 (C), 112.6 (2CH), 112.0 (2CH), 102.9 (CH), 62.7 (CH₂), 55.9 (CH₃), 43.8 (CH₃), 28.2 (CH₂), 25.1 (CH₂), 18.8 (CH₂). HRMS (ESI⁺) calcd for $\text{C}_{26}\text{H}_{27}\text{N}_4\text{O}_4$ [$\text{M} + \text{H}$]⁺ 459.2032, found 459.2030.

4.7.10. (*E*)-3-(2-methoxy-5-(methyl(2-methylquinolin-4-yl)amino)phenyl)-*N*-((tetrahydro-2H-pyran-2-yl)oxy)acrylamide (**11b**). A solution of *N*-(3-iodo-4-methoxyphenyl)-*N*,2-dimethylquinolin-4-amine (117 mg, 0.289 mmol, 1 eq) in dry DMF (4 mL) was introduced in a dried sealed tube flushed with argon. Then *N*-((tetrahydro-2H-pyran-2-yl)oxy)acrylamide (133 mg, 0.777 mmol, 2.7 eq), triethylamine (0.283 mL, 2.030 mmol, 7 eq), $\text{P}(o\text{-Tolyl})_3$ (27 mg, 0.089 mmol, 0.3 eq) and palladium acetate (27 mg, 0.120 mmol, 0.4 eq) were added to the medium. The reaction was stirred at 100 $^\circ\text{C}$ overnight. The completion of the reaction was monitored by TLC (9/1 DCM/MeOH). The medium was evaporated under vacuum and directly purified by flash chromatography (10/0 to 9/1 DCM/MeOH) to obtain the pure product as an orange solid (84 mg, 65%). m.p 79-81 $^\circ\text{C}$. IR (neat) 2962, 2943, 1669, 1630, 1493, 1423, 1257, 1129, 1035, 895, 766 cm^{-1} . ^1H NMR (300 MHz, CDCl_3) δ 8.42 (d, $J = 8.5$ Hz, 1H), 7.87 (d, $J = 15.8$ Hz, 1H), 7.55 (t, $J = 7.7$ Hz, 1H), 7.42 – 7.30 (m, 2H), 7.22 – 7.05 (m, 2H), 6.93 (d, $J = 8.9$ Hz, 1H), 6.84 (s, 1H), 6.66 (d, $J = 15.8$ Hz, 1H), 4.99 (s, 1H), 4.00-3.94 (m, 1H), 3.91 (s, 3H), 3.65-3.52 (m, 4H), 2.93 (s, 3H), 1.79 (m, 4H), 1.57 (m, 4H). ^{13}C NMR (75 MHz, CDCl_3) δ 167.3 (C), 156.3 (C), 155.8 (C), 141.6 (C), 131.4 (CH), 126.4 (CH), 125.6 (CH), 125.5 (CH), 124.4 (CH), 119.3 (C), 112.7 (2CH), 108.2 (CH), 106.0 (C), 102.5 (CH), 62.5 (CH₂), 56.0 (OCH₃),

44.6 (CH₃), 28.0 (CH₂), 25.0 (CH₂), 22.0 (CH₃), 18.6 (CH₂). HRMS (ESI⁺) for C₂₆H₃₀N₃O₄ [M + H]⁺: *m/z* calcd 448.2236, found 448.2228.

4.8.1. (*E*)-3-(5-((2-cyanoquinolin-4-yl)(methyl)amino)-2-methoxyphenyl)-*N*-hydroxyacrylamide (**12a**). A solution of (*E*)-3-(5-((2-cyanoquinolin-4-yl)(methyl)amino)-2-methoxyphenyl)-*N*-((tetrahydro-2H-pyran-2-yl)oxy)acrylamide (100 mg, 0.22 mmol) in a 1/1 mixture of 1,4-dioxane (2 mL) and methanol (2 mL) was introduced in a round bottom flask under argon. A solution of HCl 4N in dioxane (65 μ L, 0.26 mmol) was added drop by drop to the medium. The reaction was stirred at room temperature for 30 min. The completion of the reaction was monitored by TLC (1/1 cyclohexane/ethyl acetate). The solvent was evaporated under vacuum and the crude solid was purified by flash chromatography (50/50 to 0/100 cyclohexane/ethyl acetate) yielding to (*E*)-3-(5-((2-cyanoquinolin-4-yl)(methyl)amino)-2-methoxyphenyl)-*N*-hydroxyacrylamide (69 mg, 85%). Yellow solid. mp: 177 – 182 °C. IR (film): 2947, 1641, 1569, 1491, 1235, 1031, 970, 758 cm⁻¹. ¹H NMR (200 MHz, MeOD) δ 7.87 (d, *J* = 3.8 Hz, 2H), 7.73 (d, *J* = 15.5 Hz, 2H), 7.55 (s, 1H), 7.51 – 7.33 (m, 3H), 7.20 (d, *J* = 8.8 Hz, 1H), 6.56 (d, *J* = 15.5 Hz, 1H), 3.99 (s, 3H), 3.79 (s, 3H). ¹³C NMR (75 MHz, DMSO) δ 162.8 (C), 154.8 (C), 154.1 (C), 148.5 (C), 142.8 (C), 132.9 (C), 132.5 (CH), 130.4 (CH), 129.3 (CH), 127.1 (CH), 126.2 (CH), 125.1 (CH), 124.4 (C), 123.3 (CH), 122.0 (C), 120.5 (CH), 117.7 (C), 113.0 (CH), 111.9 (CH), 55.9 (CH₃), 43.8 (CH₃). HRMS (ESI⁺) calcd for C₂₁H₁₉N₄O₃ [M + H]⁺ 375.1457, found 375.1456.

4.8.2. (*E*)-*N*-hydroxy-3-(2-methoxy-5-(methyl(2-methylquinolin-4-yl)amino)phenyl)acrylamide (**12b**)

A solution of (*E*)-3-(2-methoxy-5-(methyl(2-methylquinolin-4-yl)amino)phenyl)-*N*-((tetrahydro-2H-pyran-2-yl)oxy)acrylamide (140 mg, 0.313 mmol, 1 eq) in a 1/1 mixture of 1,4-dioxane (1.5 mL) and methanol (1.5 mL) was introduced in a round bottom flask under argon. A solution of HCl 4N in dioxane (0.093 mL, 0.376 mmol, 1.2eq) was added drop by drop to the medium until the mixture become red. The reaction was stirred at room temperature for 30 min and the completion was monitored by TLC (9/1 dichloromethane/methanol). The solvents were evaporated under vacuum and the crude solid was purified by flash chromatography to obtain an orange solid (110 mg, 96%). m.p. 133°C. IR (neat) 2963, 2926, 1658, 1632, 1594, 1494, 1468, 1444, 1258, 1022, 758, 733 cm⁻¹. ¹H NMR (300 MHz, DMSO-*d*₆) δ 14.67 (s, 1H), 10.62 (s, 1H), 8.03 (d, *J* = 8.4 Hz, 1H), 7.83 – 7.74 (m, 1H), 7.66 – 7.48 (m, 2H), 7.33 (dd, 3H), 7.25 – 7.11 (m, 2H), 6.51 (d, 1H), 3.91 (s, 3H), 3.63 (s, 3H), 2.80 (s, 3H). ¹³C NMR (75 MHz, DMSO- *d*₆) δ 157.0 (C), 156.3 (C), 154.1 (C), 140.8 (2C), 139.2 (C), 132.5 (CH), 132.3 (CH), 127.6 (CH), 126.1 (CH), 125.5 (CH), 125.3 (CH), 124.9 (C), 121.2 (CH), 120.0 (CH), 117.5 (C), 113.3 (CH), 106.6 (CH), 56.1 (OCH₃), 45.1 (CH₃), 19.9 (CH₃). HRMS (ESI⁺) for C₂₁H₂₂N₃O₃ [M + H]⁺: *m/z* calcd 364.1661, found 364.1661. HPLC: *t*_R = 8.58 min, purity : 97%.

4.8.3. (*E*)-3-(5-((2-cyanoquinazolin-4-yl)(methyl)amino)-2-methoxyphenyl)-*N*-hydroxyacrylamide (**12c**). In a sealed tube under argon, the compound **10c** (40 mg, 0.09 mmol) was dissolved in dry DMF (2mL). *N*-((tetrahydro-2H-pyran-2-yl)oxy)acrylamide (45 mg, 0.26mmol), triethylamine (0.1 mL, 0.63 mmol), P(*o*-Tolyl)₃ (8.7mg, 0.3 mmol), Pd(OAc)₂ (8.6mg, 0.4mmol) were added. The reaction was stirred at 100°C overnight. The solvent was evaporated. The mixture was filtered on celite, and the solvent evaporated. The intermediate (35 mg) was dissolved in a 1:1 solution of 1,4-dioxane (0.5 mL) and MeOH (0.5 mL). A solution of HCl 4N in dioxane (25 μ L) was added and the reaction was stirred at room temperature for 1 hour. The solvents were evaporated under vacuum. Purification by

preparative HPLC afforded **12c** (yield 30% over two steps). Colorless oil. ¹H NMR (300 MHz, DMSO-*d*₆) δ 7.79 (m, 2H), 7.64 – 7.55 (m, 2H), 7.42 – 7.25 (m, 2H), 7.17 (d, *J* = 8.7 Hz, 1H), 7.00 (d, *J* = 8.4 Hz, 1H), 6.51 (d, *J* = 15.8 Hz, 1H), 3.91 (s, 3H), 3.56 (s, 3H). ¹³C NMR (75 MHz, DMSO-*d*₆) δ 162.7 (C), 160.9 (C), 156.5 (C), 150.4 (C), 139.5 (2C), 133.4 (CH), 132.3 (CH), 128.4 (2CH), 127.7 (CH), 126.0 (CH), 125.8 (CH), 124.9 (C), 121.1 (CH), 116.9 (C), 116.2 (C), 113.3 (CH), 56.1 (OCH₃), 42.9 (CH₃). HRMS (ESI⁺) (*M* + *H*)⁺: *m/z* calcd for C₂₀H₁₈N₅O₃ 376.1410, found 376.1393. HPLC: 100 %.

4.8.4. (E)-N-hydroxy-3-(2-methoxy-5-(methyl(2-methylquinazolin-4-yl)amino)phenyl)acrylamide (12d). In a sealed tube under argon, the compound **10d** (252 mg, 0.62 mmol) was dissolved in dry DMF (8.5 mL). *N*-((tetrahydro-2H-pyran-2-yl)oxy)acrylamide (286 mg, 1.68 mmol), triethylamine (0.6 mL, 4.34 mmol), Pd(OAc)₂ (56 mg, 0.24 mmol), P(*o*-Tolyl)₃ (60 mg, 0.19 mmol), were added. The reaction was stirred at 100 °C overnight. The solvent was evaporated. DMF was coevaporated in the presence of toluene. Chromatography on silica (Cyclohexane 100%, EtOAc/Cyclohexane 5/5, EtOAc/MeOH 95/5) afforded (*E*)-3-(2-methoxy-5-(methyl(2-methylquinazolin-4-yl)amino)phenyl)-*N*-((tetrahydro-2H-pyran-2-yl)oxy)acrylamide (264 mg, yield 95 %).

To a solution under argon and cooled at 0 °C with an ice bath of (*E*)-3-(2-methoxy-5-(methyl(2-methylquinazolin-4-yl)amino)phenyl)-*N*-((tetrahydro-2H-pyran-2-yl)oxy)acrylamide (204 mg; 0.45 mmol; 1 equiv.) in a mixture of methanol and dioxane (10 mL, 1/1) was slowly added a solution of HCl at 1N (137 μL; 0.55 mmol; 1.1 equiv.). The mixture was stirred at room temperature for 1h and a solution of HCl at 4N in dioxane (137 μL; 0.55 mmol; 1.1 equiv.) was slowly added at 0 °C. The mixture was stirred at room temperature for 1h at room temperature and the solvent was evaporated under reduced pressure. The crude was purified by preparative TLC (DCM/MeOH 9/1) to give **12d**. Orange solid (45 mg; 0.12 mmol; 27 %); m.p.: 181-183 °C; IR (neat): 2957, 2925, 2874, 2837, 2235, 1723, 1568, 1497, 1455, 1380, 1204, 1109, 1031, 968, 878, 787, 762, 732 cm⁻¹; ¹H NMR (300 MHz, MeOD) δ : 7.77 (m, 3H), 7.62 (s, 1H), 7.43 (d, *J* = 8.3 Hz, 3H), 7.22 (m, 2H), 7.00 (d, *J* = 8.5 Hz, 1H), 6.59 (d, *J* = 15.9 Hz, 1H), 4.01 (s, 3H), 3.81 (s, 3H), 2.78 (s, 3H). ¹³C NMR (75 MHz, MeOD) δ : 166.1 (C), 162.6 (C), 162.2 (C), 159.5 (C), 144.3 (C), 139.7 (C), 135.8 (CH), 135.3 (CH), 129.7 (CH), 128.4 (CH), 127.4 (CH), 127.3 (CH), 127.1 (C), 121.7 (CH), 121.0 (CH), 114.4 (CH), 113.9 (C), 56.7 (CH₃), 44.4 (CH₃), 23.3 (CH₃). HRMS (ESI⁺) *m/z*; [*M* + *H*]⁺ Calcd. for C₂₀H₂₁N₄O₃ 365.1608; found 365.1615.

4.8.5. N-((tetrahydro-2H-pyran-2-yl)oxy)pent-4-ynamide. A solution of pent-4-ynoic acid (764 mg, 7.8 mmol) and *O*-(tetrahydro-2H-pyran-2-yl)hydroxylamine (1 g, 8.5 mmol) in dried dichloromethane (20 mL) was introduced in a dried round bottom flask flushed with argon. The solution was cooled to 0 °C, then DCC was added (1.76 g, 8.5 mmol) portion wise. The reaction was stirred at room temperature overnight. A white precipitated appeared. The medium was filtered on celite and evaporated under vacuum to give a white solid. The crude solid was purified by flash column chromatography (100% ethyl acetate) to give *N*-((tetrahydro-2H-pyran-2-yl)oxy)pent-4-ynamide as a colourless oil (1.2 g, 76%). ¹H RMN (300 MHz, DMSO-*d*₆) δ: 11.04 (s, 1H), 4.80 (s, 1H), 3.91 (s, 1H), 3.50 (d, *J* = 11.6 Hz, 1H), 2.80 (s, 1H), 2.35 (d, *J* = 6.2 Hz, 2H), 2.18 (t, *J* = 7.0 Hz, 2H), 1.58 (m, 6H).

4.8.6. 5-(5-((2-cyanoquinolin-4-yl)(methyl)amino)-2-methoxyphenyl)-N-hydroxypent-4-ynamide (13a). In a sealed tube and purged with argon, are added 4-((3-iodo-4-methoxyphenyl)(methyl)amino)quinoline-2-carbonitrile (30.0 mg, 0.072 mmoles), *N*-((tetrahydro-2H-pyran-2-yl)oxy)pent-4-ynamide (28.0 mg, 0.144 mmol), PdCl₂P(Ph)₃ (12 mg, 0.017 mmol), CuI (7 mg, 0.036 mmol), Et₃N (21.0 mg, 0.22 mmol) and DMF (1mL). The mixture is degassed

and stirred overnight at room temperature. The reaction mixture is diluted with DCM and then filtered through Celite; the filtrate is evaporated. The formation of the intermediate compound is confirmed by LC / MS, the compound is used in the next step without purification.

A solution of the intermediate compound (29.0 mg, 0.06 mmol) in anhydrous dioxane (1 mL) is added a solution of HCl in 4N dioxane (0.5 mL). The mixture is stirred for 30 minutes at room temperature, then evaporated at room temperature and purified by HPLC using a gradient of acetonitrile in water. After lyophilization, the compound 5-(5-((2-cyanoquinolin-4-yl)(methyl) amino)-2-methoxyphenyl)-*N*-hydroxypent-4-ynamide is obtained in the form of a yellow solid with a yield of 35%. mp: 170 – 175 °C. IR (film): 2987, 1644, 1496, 1066, 766 cm⁻¹. ¹H RMN (400 MHz, DMSO-*d*₆) δ: 10.48 (br. s, 1H), 8.44 (s, 1H), 7.93 (d, *J* = 8.3 Hz, 1H), 7.65 (t, *J* = 7.5 Hz, 1H), 7.53 (s, 1H), 7.42 (d, *J* = 8.5 Hz, 1H), 7.34 (t, *J* = 7.6 Hz, 1H), 7.06 (d, *J* = 2.5 Hz, 1H), 7.02 – 6.84 (m, 2H), 3.73 (s, 3H), 2.55 (t, *J* = 7.4 Hz, 2H), 2.16 (t, *J* = 7.3 Hz, 2H). ¹³C RMN (101 MHz, DMSO-*d*₆) δ: 167.2, 156.8, 153.9, 149.1, 142.7, 133.7, 130.3, 129.9, 128.3, 127.2, 125.1, 125.1, 122.3, 118.1, 113.2, 112.4, 112.1, 94.1, 76.6, 55.8, 43.7, 40.2, 31.5, 15.4. HRMS (ESI⁺) calcd for C₂₃H₂₁N₄O₃ [M + H]⁺ 401.1614, found 401.1621.

4.8.7. 3-((5-((2-cyanoquinolin-4-yl)(methyl)amino)-2-methoxyphenyl)thio)-*N*-hydroxypropanamide (**14a**). 4-((3-iodo-4-methoxyphenyl)(methyl)amino)quinoline-2-carbonitrile (**10a**) (40 mg, 0.096 mmol), 3-mercapto-*N*-((tetrahydro-2H-pyran-2-yl)oxy)propenamide (24 mg, 0.116 mmol), PdG3-Xantphos (7 mg, 6 mol%), Et₃N (50 μL, 0.356 mmol), and dioxane (1.0 mL) were stirred at r.t. for 2 h. The medium was filtered on celite and evaporated under vacuum to give a white solid. To the crude solid in dioxane was added dropwise HCl in dioxane 4M (0.6 mL) and the mixture stirred for 30 minutes at r.t. the solvent was removed under vacuum. the product was purified by HPLC (water/ACN) to yield a yellow oil (81%).

¹H NMR (300 MHz, DMSO-*d*₆) δ 10.35 (s, 1H), 8.71 (s, 1H), 7.89 (d, *J* = 8.4 Hz, 1H), 7.71 – 7.54 (m, 1H), 7.50 (s, 1H), 7.45 – 7.25 (m, 2H), 7.04 (d, *J* = 2.6 Hz, 1H), 6.80 (d, *J* = 8.7 Hz, 1H), 6.69 (dd, *J* = 8.7, 2.6 Hz, 1H), 3.70 (s, 3H), 3.40 (s, 3H), 2.93 (t, *J* = 7.1 Hz, 2H), 2.12 (t, *J* = 7.1 Hz, 2H). ¹³C NMR (75 MHz, DMSO-*d*₆) δ 153.8, 149.0, 143.4, 133.6, 130.1, 129.8, 127.0, 125.1, 122.7, 122.2, 121.9, 121.6, 118.1, 115.8, 114.4, 111.7, 111.5, 56.1, 43.7, 31.6, 26.2. HRMS (ESI⁺) : *m/z* C₂₁H₂₁N₄O₃S [M + H]⁺ : calcd 409.1334, found 409,1330. HPLC: 100 %.

4.8.8. (*E*)-5-(5-((2-cyanoquinolin-4-yl)(methyl)amino)-2-methoxyphenyl)-*N*-hydroxypent-4-enamide (**15a**). In a sealed tube purged with argon, are added 4-((3-iodo-4-methoxyphenyl) (methyl) amino) quinoline-2-carbonitrile (**10a**) (30,0 mg, 0.072 mmol), *N*-((tetrahydro-2H-pyran-2-yl) oxy) pent-4-enamide (42.0 mg, 0.20 mmol), P(*o*-Tolyl)₃ (7.20 mg, 0.023 mmol), Pd (OAc)₂ (6.0 mg, 0.026 mmol), EtN₃ (49.0 mg, 0.48 mmol) and DMF (1 mL), the mixture is degassed and heated overnight at 100 ° C. The reaction medium is brought to room temperature, diluted with DCM, and then filtered through Celite. The filtrate is evaporated. LC/MS confirms the formation of the intermediate compound. The compound is used in the next step without purification. To a solution of this intermediate compound in anhydrous dioxane (1 mL), is added a solution of HCl in 4N dioxane (0.5 mL). The mixture is stirred for 30 minutes at room temperature, then evaporated at room temperature and purified by HPLC using a gradient of acetonitrile in water. After lyophilization, the compound (*E*)-5-(5-((2-cyanoquinolin-4-yl) (methyl) amino)-2-methoxyphenyl)-*N*-hydroxypent-4-enamide (**15a**) is obtained in the form of a solid yellow with a yield of 50% over two steps. m.p = 177 – 182 °C. IR (neat): 2947, 1641, 1569, 1491,1235, 1031, 970, 758 cm⁻¹. ¹H RMN (400 MHz, MeOD) δ : 7.87 (dd, *J*

= 8.6, 3.7 Hz, 1H), 7.59 (t, J = 7.5 Hz, 1H), 7.48 (dd, J = 17.2, 8.6 Hz, 1H), 7.32 (d, J = 6.9 Hz, 1H), 7.22 (d, J = 6.9 Hz, 2H), 6.86 (s, 2H), 6.65 (d, J = 15.8 Hz, 1H), 6.20 – 5.99 (m, 1H), 4.85 (s, 3H), 3.79 (s, 3H), 3.46 (d, J = 4.6 Hz, 3H), 3.31 (q, J = 1.7 Hz, 1H), 2.44 (q, J = 7.1 Hz, 1H), 2.30 – 2.14 (m, 1H). ^{13}C NMR (101 MHz, MeOD) δ : 172.0, 156.1, 155.7, 150.6, 144.4, 134.9, 131.3, 131.2, 130.3, 129.2, 127.7, 126.9, 125.3, 123.7, 118.9, 113.2, 111.7, 56.3, 44.5, 33.5, 30.3. HRMS (ESI⁺): m/z $\text{C}_{23}\text{H}_{23}\text{N}_4\text{O}_3$ [M + H]⁺: calcd 403.1770, found 403.1768. HPLC: 100 %.

4.8.9. (*E*)-*N'*-(1-(4-methoxy-3-(methoxymethoxy)phenyl)ethylidene)-4-methylbenzenesulfonohydrazide. To a mixture of 1-(4-methoxy-3-(methoxymethoxy)phenyl)ethan-1-one (500 mg, 2.38 mmol, 1 eq) in 20 mL of ethanol, were added *p*-toluenesulfonohydrazide (488 mg, 2.62 mmol, 1.1 eq) and MgSO_4 (291 mg, 2.42 mmol, 1 eq). The reaction was stirred and heated at 80 °C overnight. The reaction was monitored by TLC (1/1 cyclohexane/ethyl acetate). The mixture was hot-filtered, and the filtrate was allowed to cool at 0°C. The precipitate was filtered to afford the product as a white solid (427 mg, 47%). m.p : 166-169°C. IR (neat) 3194, 2840, 1511, 1273, 1251, 1166, 1076, 920, 813, 715, 663 cm^{-1} . ^1H NMR (300 MHz, Acetone- d_6) δ 9.14 (s, 1H), 7.89 (d, J = 8.3 Hz, 2H), 7.58 (d, J = 2.3 Hz, 1H), 7.40 (d, J = 8.0 Hz, 2H), 7.33 (dd, J = 8.5, 2.3 Hz, 1H), 6.97 (d, J = 8.5 Hz, 1H), 5.20 (s, 2H), 3.86 (s, 3H), 3.51 (s, 3H), 2.42 (s, 3H), 2.20 (s, 3H). ^{13}C NMR (75 MHz, Acetone- d_6) δ 152.8 (C), 144.4 (C), 131.4 (C), 130.1 (2CH), 129.0 (2CH), 128.8 (C), 125.2 (C), 122.0 (CH), 117.3 (C), 115.9 (CH), 112.4 (CH), 96.4 (CH₂), 56.3 (OCH₃), 56.2 (OCH₃), 21.4 (CH₃), 13.7 (OCH₃). HRMS (ESI⁺) for $\text{C}_{18}\text{H}_{23}\text{N}_2\text{O}_5\text{S}$ [M + H]⁺: m/z calcd 379.1328, found 379.1329.

4.8.10. 4-(1-(4-methoxy-3-(methoxymethoxy)phenyl)vinyl)-2-methylquinoline.

A microwave tube was charged with 4-chloro-2-methylquinoline (141 mg, 0.794 mmol, 1 eq), (*E*)-*N'*-(1-(4-methoxy-3-(methoxymethoxy)phenyl)ethylidene)-4-methylbenzenesulfonohydrazide (300 mg, 0.794 mmol, 1 eq), $\text{Pd}_2(\text{dba})_3 \cdot \text{CHCl}_3$ (23 mg, 2.5 mol%), Xphos (40 mg, 10 mol%) and LiOrBu (161 mg, 2.01 mmol, 2.5 eq). The tube was capped and purged with argon three times, and then distilled dioxane (4 mL) was added via syringe. It allowed to heat at 100°C for 3h. The reaction mixture was allowed to cool to room temperature and ethyl acetate was added to the mixture which was filtered through Celite. The solvents were evaporated under reduce pressure and the crude residue was purified by flash chromatography on silica gel to obtain a yellow oil (198 mg, 74%). IR (neat) 2999, 2901, 2837, 1593, 1511, 1442, 1377, 1267, 1155, 1138, 1077, 982, 923, 814, 766 cm^{-1} . ^1H NMR (300 MHz, CDCl_3) δ 8.05 (d, J = 8.4 Hz, 1H), 7.75 (d, J = 8.4 Hz, 1H), 7.65 (ddd, J = 8.4, 6.9, 1.5 Hz, 1H), 7.35 (ddd, J = 8.2, 6.9, 1.3 Hz, 1H), 7.26 (d, J = 10.1 Hz, 2H), 6.79 – 6.68 (m, 2H), 6.05 – 5.80 (m, 1H), 5.45 – 5.29 (m, 1H), 5.19 (s, 2H), 3.86 (s, 3H), 3.48 (s, 3H), 2.78 (s, 3H). ^{13}C NMR (75 MHz, CDCl_3) δ 158.8 (C), 151.2 (C), 148.3 (C), 147.4 (C), 144.1 (C), 138.8 (C), 133.09 (C), 129.5 (CH), 129.1 (CH), 127.5 (CH), 125.8 (CH), 125.6 (CH), 125.0 (CH₂), 122.4 (CH), 120.8 (C), 120.4 (CH), 116.9 (CH₂), 113.0 (CH), 56.2 (2OCH₃), 25.3 (CH₃). HRMS (ESI⁺) for $\text{C}_{21}\text{H}_{22}\text{NO}_3$ [M + H]⁺: m/z calcd 336.1600, found 336.1605.

4.8.11. 2-methoxy-5-(1-(2-methylquinolin-4-yl)vinyl)phenyl trifluoromethanesulfonate (16a**).**

To a solution of 4-(1-(4-methoxy-3-(methoxymethoxy)phenyl)vinyl)-2-methylquinoline (178 mg, 0.53 mmol, 1 eq) in methanol (15mL), was added 275 mg of *p*-toluenesulfonic acid (1.59 mmol, 3 eq) and the solution was stirred and heated at 60°C for 8h. The mixture was quenched with distilled water and the aqueous layer was extracted with ethyl acetate. The organic layer was dried over MgSO_4 and concentrated under reduced pressure. The residue was dissolved

in dry DCM and pyridine was added (0.180 mL, 2.4 mmol, 4 eq). The solution was cooled to 0°C and a solution of trifluoromethanesulfonic anhydride (0.200 mL, 1.2 mmol, 2 eq) was added dropwise. The reaction was stirred and monitored by TLC (7/3 cyclohexane/ethyl acetate). After 5h, the mixture was quenched with a solution of HCl (10%) and extraction with DCM. The organic layer was washed with saturated solutions of NaHCO₃ and NaCl and dried over MgSO₄. The solvents were evaporated under reduced pressure, and the crude residue was purified by flash chromatography on silica gel (cyclohexane/ethyl acetate 10/0 to 7/3) to afford an orange solid (136 mg, 61%). m.p. 111-112°C. IR (neat) 2845, 2359, 1514, 1423, 1205, 1141, 936, 824, 768 cm⁻¹. ¹H NMR (300 MHz, CDCl₃) δ 8.08 (d, *J* = 8.8 Hz, 1H), 7.71 – 7.62 (m, 2H), 7.38 (t, *J* = 7.6 Hz, 1H), 7.27 (d, *J* = 2.2 Hz, 1H), 7.23 (s, 1H), 7.15-7.07 (m, 1H), 6.92 (d, *J* = 8.6 Hz, 1H), 5.97 (s, 1H), 5.43 (s, 1H), 3.91 (s, 3H), 2.79 (s, 3H). ¹³C NMR (75 MHz, CDCl₃) δ 158.8 (C), 151.2 (2C), 148.3 (C), 147.4 (C), 145.9 (C), 144.1 (C), 138.8 (C), 133.1 (C), 129.5 (CH), 129.1 (CH), 127.5 (CH), 125.8 (CH), 125.6 (CH), 122.4 (CH), 120.4 (CH), 116.9 (CH₂), 113.0 (CH), 56.3 (OCH₃), 25.3 (CH₃). ¹⁹F NMR (188 MHz, CDCl₃) δ -73.81. HRMS (ESI⁺) for C₂₀H₁₇F₃NO₄S [M + H]⁺: *m/z* calcd 424.0830, found 424.0825.

4.8.12. Ethyl (E)-3-(2-methoxy-5-(1-(2-methylquinolin-4-yl)vinyl)phenyl)acrylate. A microwave tube was charged with 2-methoxy-5-(1-(2-methylquinolin-4-yl)vinyl)phenyl trifluoromethanesulfonate (100 mg, 0.236 mmol, 1 eq), ethyl acrylate (0.128 mL, 1.18 mmol, 5 eq), PdCl₂(PPh₃)₂ (8.5 mg, 5 mol%), dppp (5 mg, 5 mol%) and NaHCO₃ (139 mg, 1.65 mmol, 7 eq). The tube was capped and purged with argon three times, and then DMF (3 mL) was added via syringe. The mixture was heated at 150 °C for 6h and after completion, the reaction mixture was allowed to cool to room temperature and ethyl acetate was added. The solvents were evaporated under reduce pressure and the crude residue was purified by flash chromatography on silica gel (cyclohexane/ethyl acetate 10/0 to 7/3) to obtain a colorless solid (50 mg, 57%). m.p. 122-123 °C. IR (neat) 2979, 2839, 1704, 1632, 1602, 1561, 1273, 1176, 1026, 797 cm⁻¹. ¹H NMR (300 MHz, CDCl₃) δ 8.06 (d, *J* = 8.4 Hz, 1H), 7.89 (d, *J* = 16.2 Hz, 1H), 7.76 – 7.59 (m, 2H), 7.50 (d, *J* = 2.3 Hz, 1H), 7.39 – 7.30 (m, 1H), 7.19 (dd, *J* = 8.6, 2.3 Hz, 1H), 6.81 (d, *J* = 8.6 Hz, 1H), 6.46 (d, *J* = 16.2 Hz, 1H), 5.94 (s, 1H), 5.36 (s, 1H), 5.29 (s, 1H), 4.25 (q, *J* = 7.1 Hz, 2H), 3.87 (s, 3H), 2.79 (s, 3H), 1.32 (t, *J* = 7.1 Hz, 3H). ¹³C NMR (75 MHz, CDCl₃) δ 167.3 (C), 158.8 (C), 158.3 (C), 148.3 (C), 148.2 (C), 145.2 (C), 139.7 (CH), 132.6 (C), 129.7 (CH), 129.3 (CH), 129.0 (CH), 127.1 (CH), 125.8 (CH), 125.7 (CH), 125.2 (C), 123.5 (C), 122.4 (CH), 119.5 (CH), 115.9 (CH₂), 111.1 (CH), 60.4 (CH₂), 55.6 (OCH₃), 25.4 (CH₃), 14.3 (CH₃). HRMS (ESI⁺) for C₂₄H₂₄NO₃ [M + H]⁺: *m/z* calcd 374.1756, found 374.1757.

4.8.13. (E)-N-hydroxy-3-(2-methoxy-5-(1-(2-methylquinolin-4-yl)vinyl)phenyl)acrylamide (17a). A solution of KOH (11.2 g, 199.6 mmol) in methanol (28 mL) was added to a stirred solution of hydroxylamine hydrochloride (9.34 g, 134.4 mmol) in methanol (48 mL) at 0 °C. The reaction mixture was stirred at 0°C for 30 min. The resultant precipitate was removed by filtration. The filtrate was collected to provide free hydroxylamine solution which was stored in a refrigerator before use.

Ethyl (E)-3-(2-methoxy-5-(1-(2-methylquinolin-4-yl)vinyl)phenyl)acrylate (40 mg, 0.107 mmol, 1 eq) was added to the above freshly hydroxylamine solution (0.563 mL) at 0 °C. The reaction mixture was warmed to room temperature and stirred at 25 °C for 3 h until the reaction was complete (progress was monitored by TLC). The solvent was removed under vacuum and the crude residue was purified by flash chromatography on silica gel (cyclohexane/ethyl acetate 10/0 to 7/3) to obtain a yellow oil (18 mg, 46%). IR (neat) 2360, 1594, 1495, 1461, 1408, 1262, 1183, 1097, 1049, 819, 733, 701 cm⁻¹. ¹H NMR (300 MHz, DMSO-*d*₆) δ 10.71 (s, 1H), 8.99 (s, 1H), 7.97 (d, *J* = 8.5 Hz, 1H), 7.63 (dq,

$J = 16.0$, 7.6 Hz, 3H), 7.51 (s, 1H), 7.40 (t, $J = 7.6$ Hz, 1H), 7.35 (s, 1H), 7.16 (d, $J = 8.5$ Hz, 1H), 7.01 (d, $J = 8.5$ Hz, 1H), 6.43 (d, $J = 16.0$ Hz, 1H), 6.06 (s, 1H), 5.36 (s, 1H), 3.85 (s, 3H), 2.51 (s, 3H). ^{13}C NMR (75 MHz, DMSO- d_6) δ 169.3 (C), 162.8 (C), 158.7 (C), 157.5 (C), 147.7 (C), 147.6 (C), 147.4 (C), 144.6 (C), 132.0 (C), 129.2 (CH), 128.9 (CH), 128.7 (CH), 125.7 (CH), 125.6 (CH), 125.4 (CH), 122.2 (CH), 116.3 (CH₂), 111.9 (CH), 55.7 (OCH₃), 24.8 (CH₃). HRMS (ESI⁺) for C₂₂H₂₁N₂O₃ [M + H]⁺: m/z calcd 361.1552, found 361.1554.

4.9. In vitro metabolism assay in hepatic microsomes

4.9.1. High performance liquid chromatography-tandem mass spectrometry (HPLC-MS/MS)

Isocratic elution was achieved with a flow rate of 200 $\mu\text{L}/\text{min}$ of the mobile phase, acetonitrile/water (60:40, v/v) with 0.2% formic acid using a HPLC system (Ultimate 3000, Dionex, USA) fitted with a Hypersil[®] C18 column (2.1 \times 100 mm, 5 μm). HPLC-MS/MS analyses were performed using the LTQ-Orbitrap[™] Velos Pro mass spectrometer (Thermo Fischer Scientific Inc, Waltham, MA, USA) operating in positive electrospray ionization. Run time was 5.0 min. Quantification of compounds was performed by multiple reaction monitoring (MRM) with the following ion transitions: m/z 375.2 \rightarrow 357.1 for **12a**, m/z 365.2 \rightarrow 347.1 for **12d**, m/z 386.2 \rightarrow 353.1 for **isoCA4-HDi**, m/z 317.2 \rightarrow 302.1 for **isoCA-4** and m/z 342.2 \rightarrow 324.2 for propafenone (PPF) with a collision energy of 25%. Using Xcalibur[®] software, calibration curves were fitted with $1/c$ weighted least-squares regression by plotting the peak area ratio of each analyte to IS against its concentration.

4.9.2. Incubation of compounds in hepatic microsomes

Working solutions of compounds **12a**, **12d**, **isoCA4-HDi**, **isoCA-4** and **PPF** were prepared at 200 $\mu\text{g}/\text{mL}$ in methanol. Pooled rat (RLM) and human liver microsomes (HLM) were provided by ThermoFischer Scientific, France. Incubations of each compound were performed with a protein concentration of 1 mg/mL in buffer at pH 7.4. PPF was used as a positive control in the liver microsomes test. After pre-warming for 5 min at 37°C, in the presence of 1 mM NADPH, 6.4 mM glucose-6-phosphate and 2 U/mL glucose-6-phosphate dehydrogenase, the incubation started at 37°C after addition of the substrate at 10 μM . After 0, 0.5, 1, 3, and 6h, 50 μL aliquots (in triplicate) were drawn in tubes containing 100 μL of IS solution ($c=1000$ ng/mL acetonitrile) and mixed with 1 mL ethyl acetate to stop the reaction. After centrifugation and vacuum evaporation, the residue was dissolved in 0.1 mL acetonitrile and analyzed by HPLC-MS/MS (MRM). Control incubations without NADPH were performed at 3h. After quantification of the ratio (%) of the remaining concentration to its initial value, half-life time (min) was calculated from the relationship: $t_{1/2} = 0.693/k$, where k is the slope of the \ln concentration ratio (%) vs. time. The intrinsic clearance was calculated as: $\text{CL}_{\text{int}} = (0.693 \times \text{incubation volume}) / (t_{1/2} \times \text{microsomal protein})$ given in $\mu\text{L}/\text{min}/\text{mg}$ protein.

4.10. Biology

4.10.1. Cell Culture and Proliferation Assay

Cell culture and proliferation assay. Cancer cell lines were obtained from the American type Culture Collection (Rockville, USA) and were cultured according to the supplier's instructions. K562R (doxorubicin-resistant) leukemia cells were a generous gift from JP Marie (France). MiaPaca2 and HT-29 cells were grown in Dulbecco minimal essential medium (DMEM) containing 4.5 g/L glucose supplemented with 10% FCS and 1% glutamine. Human K562

and K562R, HCT116, A549, MCF7, and MDA-MB231 cells were grown in RPMI 1640 containing 10% FCS and 1% glutamine. All cell lines were maintained at 37 °C in a humidified atmosphere containing 5% CO₂. Cell viability was determined by a luminescent assay according to the manufacturer's instructions (Promega, Madison, WI, USA). For IC₅₀ determination, the cells were seeded in 96-well plates (3 × 10³ cells/well) containing 90 µL of growth medium. After 24 h of culture, the cells were treated with the tested compounds at 10 different final concentrations. Each concentration was obtained from serial dilutions in the culture medium starting from the stock solution. Control cells were treated with the vehicle.

Experiments were performed in triplicate. After 72 h of incubation, 100 µL of CellTiter Glo Reagent was added for 15 min before recording luminescence with a spectrophotometric plate reader PolarStar Omega (BMG LabTech). The dose-response curves were plotted with Graph Prism software, and the IC₅₀ values were calculated using the Graph Prism software from polynomial curves (four or five-parameter logistic equations).

4.10.2. Cell Cycle Analysis.

Exponentially growing cancer HT-29 cells were incubated with compounds **12a** and **12d** at 0.1, 0.5, 1, and 2 nM in DMSO for 24 h. Cell-cycle profiles were determined by flow cytometry on a FC500 flow cytometer (Beckman-Coulter, France) as described previously.[59]

4.10.3. Mitochondrial membrane potential assay

One of the hallmarks of apoptosis is the loss of mitochondrial membrane potential (DJm). The changes in the mitochondrial potential were detected by 5,5',6,6'-tetrachloro-1,1',3,3'-tetraethylbenzimidazolylcarbocyanine iodide/chloride (JC-1), a cationic dye that exhibits potential-dependent accumulation in mitochondria, indicated by fluorescence emission shift from red (590 nm) to green (525 nm). In brief, HT-29 cells were treated with different concentrations of compound **12a** for 24 h. After treatment, cells were re-suspended in 1 ml of PBS containing 2 µM final concentration JC-1 probe and incubated at 37 °C for 15 min. Analysis of cells was performed on a FC500 flow cytometer (Beckman Coulter, France).

4.10.4. HDAC inhibition in vitro pharmacology.

50% is the most common cut-off value for further investigation (determination of IC₅₀ or EC₅₀ values from concentration-response curves) that we would recommend. Results showing an inhibition (or stimulation) between 25% and 50% are indicative of weak to moderate effects (in most assays, they should be confirmed by further testing as they are within a range where more inter-experimental variability can occur). Results showing an inhibition (or stimulation) lower than 25% are not considered significant and are mainly attributable to the variability of the signal around the control level. Low to moderate negative values have no real meaning and are attributable to the variability of the signal around the control level. High negative values (≥ 50%) that are sometimes obtained with high concentrations of test compounds are generally attributable to non-specific effects of the test compounds in the assays. On a rare occasion, they could suggest an allosteric effect of the test compound.

4.10.5. In vitro microtubule assembly assay

Pure tubulin (40 µM, Cytoskeleton Inc, USA) was equilibrated in 80 mM PIPES, pH 6.9, 2 mM MgCl₂, 0.5 mM EGTA, 5% Glycerol, 1mM GTP at 4°C in a 96well-microplate (half area, Greiner ref 675096). The samples were

supplemented with the desired drug (or the vehicle, i.e., DMSO). Microplates were then transferred to a thermostatically controlled reader (37°C, BMG FLUOstar OPTIMA). Assembly kinetics was followed by measuring the absorbance of the samples at 350 nm.

4.10.6. Cell-based assay for the quantification of the effect of drugs on microtubules

7,500 HeLa cells were seeded in 96-well microplates (Greiner #655083) in 100 μ L of complete medium per well and then incubated at 37 °C in 5% CO₂. 24 hours after seeding, cells were treated with compounds (1 concentration per column, 1 plate per molecule) at different concentrations or DMSO at 0.1%, which was used as a positive control, and further incubated for 30 min at 37 °C in 5% CO₂. At the end of the incubation, the medium was aspirate. Cells were permeabilized for 10 minutes at 37°C using 100 μ L per well of OPT buffer (80 mM Pipes, 1 mM EGTA, 1 mM MgCl₂, 0.5% Triton X-100, and 10% glycerol, pH 6.8) pre-warmed to 37°C. This buffer allows cell permeabilization and elimination of free tubulin, while preserving intact microtubules. After buffer aspiration, cells were fixed overnight at room temperature using 100 μ L per well of 4% formaldehyde in PBS pH 7.2. Cells were washed 3 times in PBS pH 7.2, 0.1% Tween-20 (150 μ L per well). Then 50 μ l of α 3A1 anti-tubulin antibody[60] (1/5,000 in PBS pH 7.4, 0.3% BSA, 0.03% NaN₃) were added for 45 minutes. After washing of cells as described above, 50 μ l of anti-mouse antibody coupled to HRP (1/2,000 in PBS pH 7.4, 0.3% BSA, 0.03% NaN₃) were added for 45 minutes. Then cells were rewashed. The microplate was placed into the BMG FLUOstar OPTIMA Microplate Reader, and 100 μ l of ECL Western blotting substrate (Biorad Clarity) were injected into each well. The luminescent signal was read immediately after injection.

For the Fig. 10, HeLa cells (a gift from P. Chavrier, Institut Curie, Paris, France; ATCC CCL-2), MDA-MB-231 cells (a gift from D. Drubin, University of California-Berkeley, California, USA) were grown in DMEM Glutamax supplemented with 10% fetal calf serum at 37 °C in 5% CO₂. All cell lines were periodically screened for mycoplasma contaminations.

50.000 HeLa cells or MDA-MB-231 were seeded on 12 mm glass coverslips (MGF cat. Nr. 65.300.21). 24h later, cells were fixed with ice cold methanol for 3 min and processed for immunofluorescence. Anti-Alpha-Tubulin antibody (Cat. Nr. ab18251) and Goat Anti-Rabbit IgG H&L, Alexa Fluor® 568 (Cat. Nr. ab175471) were purchased from Abcam. Donkey anti-Rabbit IgG Highly Cross-Adsorbed, Alexa Fluor 647 (Cat. Nr. A31573) was purchased from Invitrogen. Primary antibodies were incubated on the coverslips for 1h at 37°C in a humidified chamber at dilution 1:200 in PBS-BSA 1%-Tx-100 0.3%. Secondary antibodies were incubated on the coverslips for 1h at RT at dilution 1:200 in PBS-BSA 0.3%. Coverslips were mounted with DAPI-Fluoromount-G (Cat. Nr. 0100-20 – Southern Biotech).

4.10.7. Immunofluorescence

Cells were fixed and processed for immunofluorescence analysis of the MT network as previously described,[61] using anti- α -tubulin clone α 3A1,[60] as primary antibody and a secondary antibody coupled to Alexa 488 (Jackson Immuno-Research Laboratories, 115-545-003). DNA was stained with 20 μ M Hoechst 33342 (Sigma, #23491-52-3). Images were captured with a Zeiss AxioimagerM2 microscope equipped with the acquisition software AxioVision.

For figure 10, Immunofluorescence images were acquired on a Leica Thunder epifluorescence microscope (Leica Microsystems Ltd., Wetzlar, Germany) using a 63x objective (N.A. 1.40). LasX software® was used for image

deconvolution with the Leica proprietary algorithm “small volume computational clearing”. Further image analysis was performed using the open-source software FIJI. Graphics were generated using the open-source software Instant Clue.[62]

4.10.8. Western blot

Cells were seeded in 6-well plates (3×10^5 cells/well). After one day, they were treated with or without compounds **12a**. Then, cells were harvested, and protein extracts were prepared in RIPA buffer (50mM Tris pH 8, 400mM NaCl, 1% Triton-X-100, 0.5% sodium deoxycholate, 0.1% SDS) supplemented with EDTA-free protease inhibitor cocktail (Roche). Protein extracts were sonicated. Proteins extracts (10 μ g) were run in 4-20% Mini-PROTEAN® TGX™ Precast Protein Gels (Biorad, France), transferred onto a PVDF membrane, and probed with anti-phospho-histone H2AX (anti- γ H2AX (ser 139) ab2893.abcam), anti-H2AX ab11175.abcam), anti-acetylated (Lys105/106) SMC3 (MABE1073, Millipore), or anti- β actin (mouse mAb, A5441, Sigma) antibodies, followed by HRP-conjugated secondary antibody. Immunoreactivity was revealed using an enhanced chemiluminescence detection kit (ECL, Biorad) and visualized by Image Lab BIORAD imaging system.

4.11. Molecular Modeling

Molecular Modeling. X-ray structures of five different tubulin cocrystals were retrieved from the PDB40 (accession codes 6H9B and 2V5X, respectively) and prepared using the Protein Preparation Wizard from the Schrödinger suite, including optimization of the hydrogen bond network and a short minimization with position restraints on heavy atoms using the OPLS_2005 force field. Coordinates for compound **12a** were generated using CORINA v3.44 software. Molecules were then docked in the colchicine binding site between chains C and D from PDB structure of tubulin (6H9B) and in the SAHA binding site of HDAC8 (2V5X), using GOLD v5.1 software. Default parameters of GOLD and CHEMPLP function were used for docking calculations with tubulin.

For docking calculations with HDAC8, the zinc ion was set as a bipyramidal trigonal geometry atom, with ChemScore function. Default GOLD parameters were used for the remaining variables.

Structures of complexes were finally exported for further examination and depiction with Pymol (including hydrogen bonds and hydrophobic interactions).

4.12. Animal tumor models and treatment

4.12.1. Cells

MCA205 mouse fibrosarcoma cell line was purchased from Merck (SCC173) and maintained in RPMI media supplemented with 1% L-glutamine, 10% SVF, 1% Penicillin Streptomycin antibiotic, 1% sodium pyruvate and 1% of non-essential amino acids and cultured at 37°C / 5% CO₂. Cells were washed two times and resuspended in PBS before mice inoculation.

4.12.2. Mice treatments

0.15×10^6 MCA205 cells were injected subcutaneously in mice right flank. 7 days after injection, mice were randomly divided into groups for control and treatments. **12a** was diluted in PEG vehicle (60% PEG400, 10% EtOH, 30% H₂O). Mice were intra-tumoral or intraperitoneally treated with PEG vehicle or **12a** at indicated doses (0.1, 0.25, 0.5 mg/kg

or 1 mg/kg) at day 7, 9, 11, 14, 16 and 18 post MCA205 tumorous cell inoculation. Body weight and tumor size measurements were monitored as indicated time points.

4.12.3. Ethical statements

C57BL/6 female mice were purchased from Envigo laboratory. All mice were housed in the PFEP (Institut Gustave Roussy, France) animal facility. For experiments, adult mice (7 weeks) were kept in ventilated cages. All animal experiments followed the French government's ethical and animal experiment regulations and were approved by the Ethics Committee for Animal Experimentation under number 2016_064_5677.

4.12.4. In vivo statistical analysis

Data were analyzed with Prism software (version 8; GraphPad Software, San Diego, Calif). The nonparametric Kruskal-Wallis test or a mixed-effects analysis were performed as indicated in figures. Values are expressed as means \pm SEM. Statistical significance was defined at P values of less than 0.05.

Declaration of competing interest

The authors declare that they have no known competing financial interests or personal relationships that could have appeared to influence the work reported in this paper.

Acknowledgments

The authors gratefully acknowledge support of this project from CNRS, Université Paris-Saclay, and La Ligue Nationale Contre le Cancer through an Equipe Labellisée 2014 grant.

Appendix A. Supplementary data

Supplementary data to this article can be found online at

Abbreviations

clogP calculated logarithm distribution between octanol and water; 2-Dicyclohexylphosphino-2',4',6'-triisopropylbiphenyl (Xphos); 1-Ethyl-3-(3-dimethylaminopropyl)carbodiimide (EDCI); HDACi Histone deacetylase inhibitor; Human liver microsomes (HLM); Hydroxybenzotriazole (HoBt); *iso*CA-4 *isocombretastatin* A-4; *iso*CA-4HDi *isocombretastatin* 4-HDACi; Structure activity relationships (SAR); *p*-Toluenesulfonic acid (*p*TSA); TPI tubulin polymerization inhibitor; TLC, thin layer chromatography. Rat liver microsomes (RLM); 3,4,5-trimethoxyphenyl-A ring (TMP); Trichostatin A (TSA); Tris(dibenzylideneacetone)dipalladium(0)-chloroform adduct (Pd₂dba₃.CHCl₃).

References

- [1] R.R. Ramsay, M.R. Popovic-Nikolic, K. Nikolic, E. Uliassi, M.L. Bolognesi, A perspective on multi-target drug discovery and design for complex diseases, *Clin. Transl. Med.*, 7 (2018) e3.
- [2] A. Anighoro, J. Bajorath, G. Rastelli, Polypharmacology: Challenges and Opportunities in Drug Discovery, *J. Med. Chem.*, 57 (2014) 7874-7887.

- [3] T. Korcsmáros, M.S. Szalay, C. Böde, I.A. Kovács, P. Csermely, How to design multi-target drugs, *Expert Opin. Drug Discov.*, 2 (2007) 799-808.
- [4] G.R. Zimmermann, J. Lehár, C.T. Keith, Multi-target therapeutics: when the whole is greater than the sum of the parts, *Drug Discov. Today*, 12 (2007) 34-42.
- [5] R. Morphy, Z. Rankovic, Designed Multiple Ligands. An Emerging Drug Discovery Paradigm, *J. Med. Chem.*, 48 (2005) 6523-6543.
- [6] M.L. Bolognesi, A. Cavalli, Multitarget Drug Discovery and Polypharmacology, *ChemMedChem*, 11 (2016) 1190-1192.
- [7] D. Sunil, P.R. Kamath, Indole based Tubulin Polymerization Inhibitors: An Update on Recent Developments, *Mini Rev. Med. Chem.*, 16 (2016) 1470-1499.
- [8] S. Iyer, D.J. Chaplin, D.S. Rosenthal, A.H. Boulares, L.-Y. Li, M.E. Smulson, Induction of Apoptosis in Proliferating Human Endothelial Cells by the Tumor-specific Antiangiogenesis Agent Combretastatin A-4, *Cancer Res.*, 58 (1998) 4510-4514.
- [9] K. Grosios, S.E. Holwell, A.T. McGown, G.R. Pettit, M.C. Bibby, In vivo and in vitro evaluation of combretastatin A-4 and its sodium phosphate prodrug, *Br. J. Cancer*, 81 (1999) 1318-1327.
- [10] J. Griggs, J.C. Metcalfe, R. Hesketh, Targeting tumour vasculature: the development of combretastatin A4, *Lancet Oncol.*, 2 (2001) 82-87.
- [11] G.M. Cragg, D.J. Newman, D.G.I. Kingston, 2.02 - Terrestrial Plants as a Source of Novel Pharmaceutical Agents, in: H.-W. Liu, L. Mander (Eds.) *Comprehensive Natural Products II*, Elsevier, Oxford, 2010, pp. 5-39.
- [12] G.R. Pettit, M.R. Rhodes, D.L. Herald, E. Hamel, J.M. Schmidt, R.K. Pettit, Antineoplastic Agents. 445. Synthesis and Evaluation of Structural Modifications of (Z)- and (E)-Combretastatin A-4, *J. Med. Chem.*, 48 (2005) 4087-4099.
- [13] K. Ohsumi, T. Hatanaka, K. Fujita, R. Nakagawa, Y. Fukuda, Y. Nihei, Y. Suga, Y. Morinaga, Y. Akiyama, T. Tsuji, Syntheses and antitumor activity of cis-restricted combretastatins: 5-Membered heterocyclic analogues, *Bioorg. Med. Chem. Lett.*, 8 (1998) 3153-3158.
- [14] A.A. Bekhit, H.M.A. Ashour, Y.S. Abdel Ghany, A.E.-D.A. Bekhit, A. Baraka, Synthesis and biological evaluation of some thiazolyl and thiadiazolyl derivatives of 1H-pyrazole as anti-inflammatory antimicrobial agents, *Eur. J. Med. Chem.*, 43 (2008) 456-463.
- [15] S. Messaoudi, B. Treguier, A. Hamze, O. Provot, J.-F. Peyrat, J.R. De Losada, J.-M. Liu, J. Bignon, J. Wdziejczak-Bakala, S. Thoret, J. Dubois, J.-D. Brion, M. Alami, IsoCombretastatins A versus Combretastatins A: The Forgotten isoCA-4 Isomer as a Highly Promising Cytotoxic and Antitubulin Agent, *J. Med. Chem.*, 52 (2009) 4538-4542.
- [16] A. Hamze, A. Giraud, S. Messaoudi, O. Provot, J.-F. Peyrat, J. Bignon, J.-M. Liu, J. Wdziejczak-Bakala, S. Thoret, J. Dubois, J.-D. Brion, M. Alami, Synthesis, biological evaluation of 1,1-diarylethylenes as a novel class of antimitotic agents, *ChemMedChem*, 4 (2009) 1912-1924.
- [17] A. Maksimenko, M. Alami, F. Zouhiri, J.D. Brion, A. Pruvost, J. Mougin, A. Hamze, T. Boissenot, O. Provot, D. Desmaele, P. Couvreur, Therapeutic modalities of squalenoyl nanocomposites in colon cancer: An ongoing search for improved efficacy, *ACS Nano*, 8 (2014) 2018-2032.
- [18] O. Provot, A. Hamze, J.-F. Peyrat, J.-D. Brion, M. Alami, Discovery and Hit to Lead Optimization of Novel Combretastatin A-4 Analogues: Dependence of C-Linker Length and Hybridization, *Anti-Cancer Agents Med. Chem.*, 13 (2013) 1614-1635.
- [19] S. Messaoudi, A. Hamze, O. Provot, B. Tréguier, J. Rodrigo De Losada, J. Bignon, J.-M. Liu, J. Wdziejczak-Bakala, S. Thoret, J. Dubois, J.-D. Brion, M. Alami, Discovery of Isoerianin Analogues as Promising Anticancer Agents, *ChemMedChem*, 6 (2011) 488-497.
- [20] M.A. Soussi, O. Provot, G. Bernadat, J. Bignon, J. Wdziejczak-Bakala, D. Desravines, J. Dubois, J.-D. Brion, S. Messaoudi, M. Alami, Discovery of azaisoerianin derivatives as potential antitumors agents, *Eur. J. Med. Chem.*, 78 (2014) 178-189.
- [21] A. Hamze, M. Alami, O. Provot, Developments of isoCombretastatin A-4 derivatives as highly cytotoxic agents, *Eur. J. Med. Chem.*, 190 (2020) 112110.
- [22] I. Khelifi, T. Naret, A. Hamze, J. Bignon, H. Levaique, M.C. Garcia Alvarez, J. Dubois, O. Provot, M. Alami, N,N-bis-heteroaryl methylamines: Potent anti-mitotic and highly cytotoxic agents, *Eur. J. Med. Chem.*, 168 (2019) 176-188.
- [23] M.A. Soussi, O. Provot, G. Bernadat, J. Bignon, D. Desravines, J. Dubois, J.-D. Brion, S. Messaoudi, M. Alami, IsoCombretastatin Quinazolines: Potent Cytotoxic Agents with Antitubulin Activity, *ChemMedChem*, 10 (2015) 1392-1402.
- [24] I. Khelifi, T. Naret, D. Renko, A. Hamze, G. Bernadat, J. Bignon, C. Lenoir, J. Dubois, J.-D. Brion, O. Provot, M. Alami, Design, synthesis and anticancer properties of IsoCombretastatin Quinolines as potent tubulin assembly inhibitors, *Eur. J. Med. Chem.*, 127 (2017) 1025-1034.

- [25] T. Naret, I. Khelifi, O. Provot, J. Bignon, H. Levaique, J. Dubois, M. Souce, A. Kasselouri, A. Deroussent, A. Paci, P.F. Varela, B. Gigant, M. Alami, A. Hamze, 1,1-Diheterocyclic Ethylenes Derived from Quinaldine and Carbazole as New Tubulin-Polymerization Inhibitors: Synthesis, Metabolism, and Biological Evaluation, *J. Med. Chem.*, 62 (2019) 1902-1916.
- [26] J.E. Bolden, M.J. Peart, R.W. Johnstone, Anticancer activities of histone deacetylase inhibitors, *Nat. Rev. Drug Discov.*, 5 (2006) 769-784.
- [27] P.A. Marks, V.M. Richon, T. Miller, W.K. Kelly, Histone Deacetylase Inhibitors, in: *Advances in Cancer Research*, Academic Press, 2004, pp. 137-168.
- [28] P.A. Marks, W.S. Xu, Histone deacetylase inhibitors: Potential in cancer therapy, *J. Cell. Biochem.*, 107 (2009) 600-608.
- [29] M. Phimmachanh, J.Z.R. Han, Y.E.I. O'Donnell, S.L. Latham, D.R. Croucher, Histone Deacetylases and Histone Deacetylase Inhibitors in Neuroblastoma, *Front. Cell Dev. Biol.*, 8 (2020).
- [30] A. Hamze, How do we improve histone deacetylase inhibitor drug discovery?, *Expert Opin. Drug Discov.*, 15 (2020) 527-529.
- [31] Z. Huang, W. Zhou, Y. Li, M. Cao, T. Wang, Y. Ma, Q. Guo, X. Wang, C. Zhang, C. Zhang, W. Shen, Y. Liu, Y. Chen, J. Zheng, S. Yang, Y. Fan, R. Xiang, Novel hybrid molecule overcomes the limited response of solid tumours to HDAC inhibitors via suppressing JAK1-STAT3-BCL2 signalling, *Theranostics*, 8 (2018) 4995-5011.
- [32] D. Lamaa, H.P. Lin, L. Zig, C. Bauvais, G. Bollot, J. Bignon, H. Levaique, O. Pamlard, J. Dubois, M. Ouassiss, M. Souce, A. Kasselouri, F. Saller, D. Borgel, C. Jayat-Vignoles, H. Al-Mouhammad, J. Feuillard, K. Benihoud, M. Alami, A. Hamze, Design and Synthesis of Tubulin and Histone Deacetylase Inhibitor Based on iso-Combretastatin A-4, *J. Med. Chem.*, 61 (2018) 6574-6591.
- [33] B. Wang, X. Chen, J. Gao, L. Su, L. Zhang, H. Xu, Y. Luan, Anti-tumor activity evaluation of novel tubulin and HDAC dual-targeting inhibitors, *Bioorg. Med. Chem. Lett.*, 29 (2019) 2638-2645.
- [34] M.-W. Chao, M.-J. Lai, J.-P. Liou, Y.-L. Chang, J.-C. Wang, S.-L. Pan, C.-M. Teng, The synergic effect of vincristine and vorinostat in leukemia in vitro and in vivo, *J. Hematol. Oncol.*, 8 (2015) 82.
- [35] M. Sun, J. Qin, Y. Kang, Y. Zhang, M. Ba, H. Yang, Y. Duan, Y. Yao, 2-Methoxydiol derivatives as new tubulin and HDAC dual-targeting inhibitors, displaying antitumor and antiangiogenic response, *Bioorg. Chem.*, 120 (2022) 105625.
- [36] Y. Wang, M. Sun, Y. Wang, J. Qin, Y. Zhang, Y. Pang, Y. Yao, H. Yang, Y. Duan, Discovery of novel tubulin/HDAC dual-targeting inhibitors with strong antitumor and antiangiogenic potency, *Eur. J. Med. Chem.*, 225 (2021) 113790.
- [37] X. Peng, J. Chen, L. Li, Z. Sun, J. Liu, Y. Ren, J. Huang, J. Chen, Efficient Synthesis and Bioevaluation of Novel Dual Tubulin/Histone Deacetylase 3 Inhibitors as Potential Anticancer Agents, *J. Med. Chem.*, 64 (2021) 8447-8473.
- [38] A. Bruneau, M. Roche, A. Hamze, J.-D. Brion, M. Alami, S. Messaoudi, Stereo-retentive Palladium-Catalyzed Arylation, Alkenylation, and Alkynylation of 1-Thiosugars and Thiols Using Aminobiphenyl Palladacycle Precatalyst at Room Temperature, *Chem. Eur. J.*, 21 (2015) 8375-8379.
- [39] M. Roche, G. Frison, J.-D. Brion, O. Provot, A. Hamze, M. Alami, Csp²-N Bond formation via ligand-free Pd-catalyzed oxidative coupling reaction of N-tosylhydrazones and indole derivatives, *J. Org. Chem.*, 78 (2013) 8485-8495.
- [40] M. Roche, J. Bignon, J.-D. Brion, A. Hamze, M. Alami, Tandem One-Pot Palladium-Catalyzed Coupling of Hydrazones, Haloindoles, and Amines: Synthesis of Amino-N-vinylindoles and Their Effect on Human Colon Carcinoma Cells, *J. Org. Chem.*, 79 (2014) 7583-7592.
- [41] A. Giraud, O. Provot, A. Hamze, J.-D. Brion, M. Alami, One-pot hydrosilylation-protodesilylation of functionalized diarylalkynes: a highly selective access to Z-stilbenes. Application to the synthesis of combretastatin A-4, *Tetrahedron Lett.*, 49 (2008) 1107-1110.
- [42] For a review on Zinc binding groups for histone deacetylase inhibitors, see: L. Zhang, J. Zhang, Q. Jiang, L. Zhang, W. Song, Zinc binding groups for histone deacetylase inhibitors, *J. Enzyme Inhib. Med. Chem.*, 33 (2018) 714-721.
- [43] A. Hamze, E. Rasolofonjatovo, O. Provot, C. Mousset, D. Veau, J. Rodrigo, J. Bignon, J.-M. Liu, J. Wdzieczak-Bakala, S. Thoret, J. Dubois, J.-D. Brion, M. Alami, B-Ring-Modified isoCombretastatin A-4 Analogues Endowed with Interesting Anticancer Activities, *ChemMedChem*, 6 (2011) 2179-2191.
- [44] R. Schobert, K. Effenberger-Neidnicht, B. Biersack, Stable combretastatin A-4 analogues with sub-nanomolar efficacy against chemoresistant HT-29 cells, *Int. J. Clin. Pharmacol. Ther.*, 49 (2011) 71-72.
- [45] H. Vakifahmetoglu-Norberg, A.T. Ouchida, E. Norberg, The role of mitochondria in metabolism and cell death, *Biochem. Biophys. Res. Commun.*, 482 (2017) 426-431.
- [46] J.B. Spinelli, M.C. Haigis, The multifaceted contributions of mitochondria to cellular metabolism, *Nat. Cell Biol.*, 20 (2018) 745-754.

- [47] A. Mathur, Y. Hong, B.K. Kemp, A.A. Barrientos, J.D. Erusalimsky, Evaluation of fluorescent dyes for the detection of mitochondrial membrane potential changes in cultured cardiomyocytes, *Cardiovasc. Res.*, 46 (2000) 126-138.
- [48] S. Bouchet, C. Linot, D. Ruzic, D. Agbaba, B. Fouchaq, J. Roche, K. Nikolic, C. Blanquart, P. Bertrand, Extending Cross Metathesis To Identify Selective HDAC Inhibitors: Synthesis, Biological Activities, and Modeling, *ACS Med. Chem. Lett.*, 10 (2019) 863-868.
- [49] S. Petersen, R. Casellas, B. Reina-San-Martin, H.T. Chen, M.J. Difilippantonio, P.C. Wilson, L. Hanitsch, A. Celeste, M. Muramatsu, D.R. Pilch, C. Redon, T. Ried, W.M. Bonner, T. Honjo, M.C. Nussenzweig, A. Nussenzweig, AID is required to initiate Nbs1/ γ -H2AX focus formation and mutations at sites of class switching, *Nature*, 414 (2001) 660-665.
- [50] E.P. Rogakou, D.R. Pilch, A.H. Orr, V.S. Ivanova, W.M. Bonner, DNA Double-stranded Breaks Induce Histone H2AX Phosphorylation on Serine 139, *J. Biol. Chem.*, 273 (1998) 5858-5868.
- [51] A. Munshi, J.F. Kurland, T. Nishikawa, T. Tanaka, M.L. Hobbs, S.L. Tucker, S. Ismail, C. Stevens, R.E. Meyn, Histone Deacetylase Inhibitors Radiosensitize Human Melanoma Cells by Suppressing DNA Repair Activity, *Clin. Cancer Res.*, 11 (2005) 4912-4922.
- [52] K. Camphausen, W. Burgan, M. Cerra, K.A. Oswald, J.B. Trepel, M.-J. Lee, P.J. Tofilon, Enhanced Radiation-Induced Cell Killing and Prolongation of γ H2AX Foci Expression by the Histone Deacetylase Inhibitor MS-275, *Cancer Res.*, 64 (2004) 316-321.
- [53] S. Ramirez-Rios, S. Michallet, L. Peris, C. Barette, C. Rabat, Y. Feng, M.-O. Fauvarque, A. Andrieux, K. Sadoul, L. Lafanechère, A New Quantitative Cell-Based Assay Reveals Unexpected Microtubule Stabilizing Activity of Certain Kinase Inhibitors, Clinically Approved or in the Process of Approval, *Front. Pharmacol.*, 11, 543, 10.3389/fphar.2020.00543(2020).
- [54] S. Pecnard, O. Provot, H. Levaique, J. Bignon, L. Askenatzis, F. Saller, D. Borgel, S. Michallet, M.-C. Laisne, L. Lafanechère, M. Alami, A. Hamze, Cyclic bridged analogs of isoCA-4: Design, synthesis and biological evaluation, *Eur. J. Med. Chem.*, 209 (2021) 112873.
- [55] A. Marabelle, L. Tselikas, T. de Baere, R. Houot, Intratumoral immunotherapy: using the tumor as the remedy, *Ann. Oncol.*, 28 (2017) xii33-xii43.
- [56] P.A. Ascierto, M. Del Vecchio, C. Robert, A. Mackiewicz, V. Chiarion-Sileni, A. Arance, C. Lebbé, L. Bastholt, O. Hamid, P. Rutkowski, C. McNeil, C. Garbe, C. Loquai, B. Dreno, L. Thomas, J.J. Grob, G. Liskay, M. Nyakas, R. Gutzmer, J. Pikiel, F. Grange, C. Hoeller, V. Ferraresi, M. Smylie, D. Schadendorf, L. Mortier, I.M. Svane, D. Hennenken, A. Qureshi, M. Maio, Ipilimumab 10 mg/kg versus ipilimumab 3 mg/kg in patients with unresectable or metastatic melanoma: a randomised, double-blind, multicentre, phase 3 trial, *Lancet Oncol.*, 18 (2017) 611-622.
- [57] R. Darrigrand, A. Pierson, M. Rouillon, D. Renko, M. Boulpicante, D. Bouyssié, E. Mouton-Barbosa, J. Marcoux, C. Garcia, M. Ghosh, M. Alami, S. Apcher, Isoginkgetin derivative IP2 enhances the adaptive immune response against tumor antigens, *Commun. Biol.*, 4 (2021) 269.
- [58] N. Sirisoma, A. Pervin, H. Zhang, S. Jiang, J.A. Willardsen, M.B. Anderson, G. Mather, C.M. Pleiman, S. Kasibhatla, B. Tseng, J. Drewe, S.X. Cai, Discovery of N-(4-Methoxyphenyl)-N,2-dimethylquinazolin-4-amine, a Potent Apoptosis Inducer and Efficacious Anticancer Agent with High Blood Brain Barrier Penetration, *J. Med. Chem.*, 52 (2009) 2341-2351.
- [59] C. Venot, M. Maratrat, C. Dureuil, E. Conseiller, L. Bracco, L. Debussche, The requirement for the p53 proline-rich functional domain for mediation of apoptosis is correlated with specific PIG3 gene transactivation and with transcriptional repression, *The EMBO Journal*, 17 (1998) 4668-4679.
- [60] L. Peris, M. Thery, J. Fauré, Y. Saoudi, L. Lafanechère, J.K. Chilton, P. Gordon-Weeks, N. Galjart, M. Bornens, L. Wordeman, J. Wehland, A. Andrieux, D. Job, Tubulin tyrosination is a major factor affecting the recruitment of CAP-Gly proteins at microtubule plus ends, *J. Cell Biol.*, 174 (2006) 839-849.
- [61] K.C. Pereira, A.L. Porter, S. Potavathi, A.P. LeBris, B. DeBoef, Insight into the palladium-catalyzed oxidative arylation of benzofuran: heteropoly acid oxidants evoke a Pd(II)/Pd(IV) mechanism, *Tetrahedron*, 69 (2013) 4429-4435.
- [62] H. Nolte, T.D. MacVicar, F. Tellkamp, M. Krüger, Instant Clue: A Software Suite for Interactive Data Visualization and Analysis, *Sci. Rep.*, 8 (2018) 12648.